TRANSPORT AND RETENTION OF SILVER

NANOPARTICLES IN WATER SATURATED POROUS MEDIA

A thesis
Presented to
the faculty of the School of Engineering and Applied Science
University of Virginia

By

Dianjun Ren

In Partial Fulfillment
of the requirements for the degree of
Doctor of Philosophy in Civil and Environmental Engineering
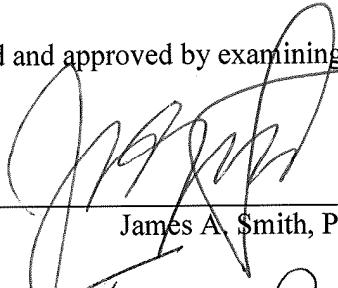
University of Virginia
Nov.2013

APPROVAL SHEET

The dissertation is submitted in partial fulfillment of the
Requirements for the degree of

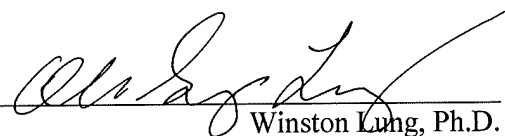Doctor of Philosophy in Civil and Environmental Engineering

_____
Dianjun Ren (Author)

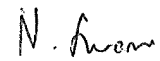This dissertation has been read and approved by examining committee:

_____
James A. Smith, Ph.D. (Thesis Advisor)

_____
Teresa B. Culver, Ph.D. (Committee Chair)

_____
Lisa M. Colosi, Ph.D.

_____
Winston Lung, Ph.D.

_____
Nathan Swami, Ph.D. (External Member)

Accepted for the School of Engineering and Applied Science

_____
Dean, School of Engineering and Applied Science

November 2013

2

To my dad and mom

谨以此献给我的父亲母亲

ACKNOWLEDGEMENTS

The day when I first arrived on campus of University of Virginia still seems fresh. It was a sunny day in the summer of 2008. It was a long day filled with sunshine. While the daylight allowed me to tour around, the night would give me a time to rest. My feeling was mixed, which is how I feel about the journey of PhD program.

First and foremost, I want to express my sincere appreciation to my advisor Dr. James A Smith, for his continuous guidance, unparalleled caring, and dedicated support throughout my past four years in University of Virginia. Without any of these, I would never be able to walk this far. His positive attitude and unwavering belief in me made the work with him a true rewarding experience. Every time after my meeting with him, I was filled with encouragement and well ready to tackle every obstacles on the road, however insurmountable it seems to be beforehand.

My thesis proposal committee members, Dr. Teresa Culver, Dr. Nathan Swami, and Dr. Lisa Colosi have been providing most constructive feedbacks on the proposal and thesis. I also had the great honor to work closely with Dr. Colosi on the life cycle analysis research. That she was being so energetic and dedicated to the work set an unmatched role model for me not only in the academic but also the life ahead.

I want to thank Dr. Joanne B Dugan too. She kindly supported and guided me out of the most difficult period of time in my graduate program. Without her I would have been totally lost somewhere! I could not fully express my appreciation to her by any words.

I got lots of my inspirations and momentum from my best friends in University of Virginia. Sharing the joy when I was up and cheering me up when I was down, each of you have made a difference in my life in Charlottesville. Some are still studying, while some are working elsewhere. I will see each of you again and many times in the future, to cherish those good old days in Jefferson's academic village we have shared together!

My work could not be completed without the help from my dearest colleagues. From designing the experiments to analyzing the sample, they contributed in very bit to the completion of the work. Han, Karl, Carly, Lydia, Jon, Emma, Daniel and many others, the thanks go to you all.

In the later period of my graduate program, I was fortunate enough to be chosen as an EREF (Environmental Research and Education Foundation) fellow and was funded by them. I am truly grateful to Dr. Bryan Staley, Ms. Stephanie Hollomon and other kind people from this foundation for generous help of all sorts. I was able to concentrate on the research through their financial support.

My final deepest thanks and appreciation go to my family. Without their constant, unconditional love and support, I could not imagine I could ever undertake this path. None of them could speak English, but their words are so caring and full of wisdom that they always can speak the most truth of the life in States. I am deeply loved and blessed by my mom and dad. And in no way I can repay all the debt I owe them. I love you so much!

TABLE OF CONTENTS

ABSTRACT

Silver nanoparticles have unique physic-chemical properties that make them useful for a variety of commercial applications. By contrast, silver nanoparticles can negatively impact natural ecosystems. For the last 20 years, the widespread manufacturing, use, and subsequent disposal of silver nanoparticles has led to the ever-increasing exposure of environmental systems to the risk of silver nanoparticles. It is thus crucial to understand the fate and transport behavior of silver nanoparticles through natural ecosystems.

A well-defined water-saturated Ottawa sand filled column was used first to study the transport behavior of silver nanoparticles. The column transport experiments were performed to investigate the impact of solution ionic strength as well as the sand grain size on the transport behavior of proteinate-capped silver nanoparticles. Results showed that the AgNP retention in the columns increased with the solution ionic strength and reduction in mean sand particle diameter, with the influence from ionic strength having the more significant effect on the retention. The increased nanoparticle-sand interaction instead of aggregation of nanoparticles contributed to the increased retention of nanoparticles. In almost all cases, significant amounts of silver nanoparticles exited the columns, suggesting the silver nanoparticles are relatively mobile in sand porous media.

The transport of silver nanoparticles was subsequently evaluated through a porous ceramic medium which has the same characteristics as a point-of-use ceramic filter for drinking water treatment. Two types of experiments were performed: i) pulse injection of silver nanoparticle suspensions at different ionic strengths; effluent samples were

collected over time and analyzed for silver concentration; ii) immobilization of silver nanoparticles on ceramic disk using a paint-on, dipping, or fire-in method; a synthetic, moderately hard water sample with both monovalent and divalent inorganic ions was used as an influent solution, and the effluent was collected and analyzed for silver over time. For the first investigation, the retention of silver nanoparticles ranged from 10% to 13% depending on specific conditions. The mobility decreased with increasing ionic strength and to a less extent with increasing nanoparticle diameter. Citrate-capped particles were found to be slightly less mobile than proteinate-capped particles. In the second part, the fire-in-treated disks had a significant lower release rate of silver nanoparticles compared to ceramic disks treated with either paint-on or dipping method, suggesting that the fire-in method is a superior method with respect to silver retention in the ceramic filter media.

The last porous medium investigated was manufactured geosynthetic clay liners. The transport behavior was evaluated under different ionic strengths and with two types of electrolytes. In general, at least 30% of silver nanoparticles breakthrough the geosynthetic clay liner in all scenarios, except with the high ionic strength water (100 mM), where full retention was achieved. The retention rate was found to increase with the ionic strength. The electrolyte type (monovalent or divalent) had a lesser impact on the total retention of silver nanoparticles relative to ionic strength. The retained silver nanoparticles under high ionic strength can be released by introducing that with low ionic strength. This observation suggested the existence of both primary and secondary energy minimum in nanoparticle-surface interaction profile. Overall, the results indicate that a

geosynthetic clay liner does not effectively retain silver nanoparticles in under certain water chemistry conditions.

In the last part of this dissertation, silver-impregnated ceramic water filters were closely evaluated from the perspective of social, economic and environmental sustainability. By defining a functional unit as the total volume of water consumed by a typical household over ten years (37,960 L), a side-by-side comparison was performed between a centralized water system and the ceramic filters. From a case study in South Africa, it showed that ceramic filters are generally 3-6 times more cost-effective than the centralized system in term of the reduction of waterborne diarrheal disease. The ceramic filters also scored higher in the following four categories (out of five categories investigated): energy use, water use, global warming potential, and particulate matter emissions (PM10). This triple-bottom-line-based assessment offers strong evidence that ceramic filters are a more sustainable choice for drinking water treatment in developing countries than the centralized water system.

LIST OF FIGURES

LIST OF TABLES

production.

CHAPTER 1: INTRODUCTION & OBJECTIVES

1.1 Introduction

From early times, silver has been considered an effective anti-microbial agent in preserving food and drink (Russell & Russell, 1995). In the last decade, the rapid development of nanotechnology has advanced the anti-microbial abilities of silver through introduction of the "nano" form of silver. With at least one of three dimensions smaller than 100 nm, silver nanoparticles have greater surface area, higher reactivity, and tunable electronics and optical properties relative to bulk silver. Various nanotechnologies have been used widely in textiles, medications, disinfection sprays, water filters, and many other types of consumer products. As of 2008, silver nanotechnology has become the most prevalent type of nanotechnology in consumer products, accounting for more than 20% of all nanoparticle-related consumer products (Woodrow Wilson International Center for Scholars, 2008).

Despite the fact that the superb anti-microbial performance of silver nanoparticles significantly improves the quality of life for human beings, the widespread use of silver nanoparticles carries certain risks, especially to the environment. Because the application of silver nanoparticles has seen continuous commercial success over the past decade (Maynard et al. 2006), an increasing amount of silver nanoparticles have been introduced into the environment in various ways. For example, silver nanoparticles may leak from underground storage tanks or accidental spills during transportation, and thus enter groundwater systems through surface runoff and seepage. The particles may also be introduced into the environment from consumer products containing silver nanoparticles, such as silver nanoparticles washed off from socks in washing machines. This pathway

has been experimentally confirmed by Benn and Westerhoff (2008) . Most nanoparticles released into the environment will eventually be transported through groundwater, wastewater treatment plants, and water supply systems, and ultimately end up in the aquatic system.

Efforts have been made to predict and estimate the concentration of silver nanoparticles in the environment through a probabilistic mass flow analysis of silver nanoparticle products. Multiple studies have predicted environmentally-relevant silver nanoparticles' concentrations in environmental systems based on probabilistic materials flow models; these studies all confirmed that the level of silver nanoparticles poses a threat to aquatic organisms (Gottschalk, Sonderer, Scholz, & Nowack, 2009; Mueller & Nowack, 2008). However, the specific transport behavior of silver nanoparticles in environmentally relevant conditions is still unclear. The transport mechanisms of silver nanoparticles in various conditions are critical to assess and understand, since silver nanoparticles discharged into the natural environment contain a significant potential risk to the environment. Thus, this study addresses the transport of silver nanoparticles through media and the relevant human and environmental impacts of the use of silver nanoparticles.

1.2   Objectives

This dissertation primarily focuses on the transport and retention mechanisms of silver nanoparticles through three different porous media: Ottawa sand, porous ceramic, and a geosynthetic clay liner. This dissertation also addresses the transport and retention mechanisms of silver nanoparticles through porous medium in an applied setting, through the evaluation of a silver-impregnated ceramic filter used in rural areas in South Africa.

This component evaluates these filters from the perspectives of environmental burden, economic cost, and health benefits.

The first component of this dissertation is addressed in chapters 2 to 5. Chapter 2 provides a brief background of silver nanoparticles' unique properties, previous research on transport behavior of silver nanoparticles in porous media, and underlying theories relevant to transport mechanisms. Chapters 3 to 5 assess transport behaviors through porous media, with one chapter dedicated to each medium in the order of complexity of the transport mechanisms: from the Ottawa sand, to ceramic disks, and eventually to synthetic clay liners. Specifically, Chapter 3 describes the transport experiments of silver nanoparticles through columns filled with Ottawa sand. The effects of sand grain size on transport behavior, and electrolyte type - as well as electrolyte concentration - are investigated and discussed.

Chapter 4 presents the investigations of transport behavior through a ceramic disk, a type of material used extensively in ceramic point-of-use drinking water filters. The effects of coating and the size of nanoparticles are considered, given a distribution of nanoparticles coated with two different chemicals (citrate and proteinate) and at three different sizes (10 nm, 50 nm and 100 nm). The impacts that are studied include: Ionic strength, nanoparticle size and coating. Experiments are conducted to determine the best techniques to embed silver nanoparticles for the purpose of disinfection. For this, three different silver immobilization techniques (painting, dipping and firing-in) were evaluated. For the purpose of better filter usage in the field, scenarios with physical characteristics similar to the case study site were used to set up these experiments, and results were interpreted with emphasis on usage in the case study area.

Chapter 5 explores interactions between silver nanoparticles and geosynthetic clay liners, a type of material designed to stop leachate from migrating into the groundwater possibility of silver nanoparticles "breaking through" geosynthetic clay liners. Since these liners are used extensively in landfill design, breakthrough of silver nanoparticles would cause due concern. The testing environments were carefully chosen to better recreate the physical and chemical system from waste disposal facilities. Specifically, this chapter explores the environment of a landfill. With the observation of breakthrough of silver nanoparticles in some specific conditions, conclusions are drawn in terms of impact of various factors, such as electrolyte type and concentration.

The second component of this study is addressed in Chapter 6, which investigates the social, economic and environmental sustainability of ceramic filters impregnated with silver nanoparticles within the framework of the "triple bottom line". A site in South Africa - where silver nanoparticle-impregnated point-of-use ceramic water filters are being tested – is the case study site. For the case study, a functional unit was selected as a fair starting point for comparison between the centralized water treatment system and use of the point-of-use ceramic filters. The comparison was extensively carried out given three different perspectives: social sustainability, economic sustainability and environmental sustainability.

Reference

Benn, T. M., & Westerhoff, P. (2008). Nanoparticle Silver Released into Water from Commercially Available Sock Fabrics. *Environmental Science & Technology, 42*, 4133-4139

Gottschalk, F., Sonderer, T., Scholz, R. W., & Nowack, B. (2009). Modeled

Environmental Concentrations of Engineered Nanomaterials (Tio2, Zno, Ag, Cnt,

Fullerenes) for Different Regions. *Environmental Science & Technology, 43*(24),

9216-9222

Mueller, N. C., & Nowack, B. (2008). Exposure Modeling of Engineered Nanoparticles

in the Environment. *Environmental Science & Technology, 42*(12), 4447-4453

Russell, A. D., & Russell, N. J. (1995). Biocides: Activity, Action and Resistance, Fifty

Years of Antimicrobials: Past Perspectives and Future Trends. In P. A. Hunter, G.

K. Darby & N. J. Russell (Eds.). Cambridge: Cambridge University Press.

Woodrow Wilson International Center for Scholars. (2008). The Project on Emerging

Nanotechnologies.

CHAPTER 2: BACKGROUND

2.1   Availability and toxicity of silver

2.1.1   Applications of silver nanoparticles

Silver nanoparticles show commercial promise because of their outstanding broad-spectrum biocidal effects. The Woodrow Wilson Institute compiled an inventory of nanotechnology consumer products and noted that the number of products that use silver nanoparticles increased from 67 products in April, 2007 to 93 products in May, 2007 (Woodrow Wilson International Center for Scholars, 2008).

The antibacterial, antifungal, antibiotic and (partially) antiviral properties make silver nanoparticles popular in a wide variety of products: cosmetics, disinfection sprays, odor-free textiles, wound dressings, food containers, personal hygiene products, and paints, to name a few. Silver is also a promising antibacterial agent for hospital use, as it will not cause bacterial resistance because of its broad-spectrum antibiotic capabilities. Additionally, it was also found to be effective in inhibiting the HIV virus, as silver nanoparticles bind to host cells with particle sizes ranging from 1 nm to 10 nm and inhibit the ability of the HIV virus to corrupt those cells (Elechiguerra et al., 2005).

2.1.2   Prevalence of silver nanoparticles in environment

To assess the risk posed to living organisms by silver nanoparticles, it is important to understand the prevalence of silver nanoparticles in the natural environment. Unfortunately, because of the complexity of environmental sampling, the relatively low

concentrations of nanoparticles, and lack of an effective detection method, it is not easy to isolate and quantify nanoparticles in environmental samples.

Therefore, instead of direct monitoring, researchers have typically predicted the concentrations of silver nanoparticles in the natural environment based on mass flow balances using life cycle assessments of silver nanoparticles from manufacture to end-of-life. Blaser et al. (Blaser, Scheringer, MacLeod, & Hungerbuhler, 2008) estimated that 15% of the total silver in European aquatic systems comes from consumer products containing silver nanoparticles. Inevitably, silver released from consumer products accumulate in wastewater, which is either treated in wastewater treatment plants or directly discharged into the aquatic system without proper treatment (Benn & Westerhoff, 2008). The portion of silver treated in a wastewater treatment plant is likely to mix with sewage sludge; this sludge is either buried in a landfill, incinerated in a thermal treatment plant, or applied in agricultural fields as fertilizer. While incineration leaves only trace amounts of silver in the environment, both landfill deposition and fertilizer application allow the silver to further migrate into - and thus contaminate groundwater. In addition, the silver that is left untreated will ultimately enter the ecosystem. Despite a significant fraction of silver nanoparticles that agglomerate and settle within sediments near the point of their introduction into the environment, there is still another fraction of silver nanoparticles that are transported into estuarine waters, posing great danger to individual aquatic organisms, and ecosystems as a whole (Chinnapongse, MacCuspie, & Hackley, 2011).

2.2   Fate of silver nanoparticles in different porous media

2.2.1   Sandy column

Compared to extensive studies in the literature on the toxicity of silver nanoparticles, there were only two studies on the transport and retention behavior of silver nanoparticles in a sand porous medium (Sagee, Dror, & Berkowitz, 2012; Tian, Gao, Silvera-Batista, & Ziegler, 2010). When it comes to other porous medium, such as ceramic disks and geosynthetic clay liners, this author has not found any existing studies.

Traditionally, column experiments have been used to study the transport mechanisms. Tian (Tian et al., 2010) investigated the transport behavior of silver nanoparticles in a column filled with well-defined quartz sand. The sand was sieved into a grain distribution of 0.35 mm to 0.6 mm. The surface treatments yielded two kinds of sand: one was free of organic matter, and the other was free of both organic matter and metal oxides. Aqueous suspensions of surfactant-coated silver nanoparticles were introduced into to the column and breakthrough curves were recorded and analyzed. The results showed that the breakthrough curves were similar for the two kinds of sand. Also, the use of sieved sand with a narrow size distribution failed to capture the wide range of size distribution found in natural sand.

To interpret the observations, the DLVO theory and the classical colloidal filtration theory were used. Sagee et al. (Sagee et al., 2012) did a series of transport experiments on a column filled with natural soil. Silver nanoparticles of a single size (30 nm) with a more common coating – citrate – were used in this study. In that study, the roles of humic acid, sand grain size, and flow rate on transport mechanisms were studied. The results showed that the retention of silver nanoparticles decreases with the humic acid concentration, and the flow rate but with the increase of sand grain size.

In addition to the silver nanoparticle studies, there have been other studies conducted on the transport behavior of other types of engineered nanoparticles, such as C_{60}, carbon nanotubes (single wall and multiple wall), and iron nanoparticles (Jaisi & Elimelech, 2009; Kanel & Al-Abed, 2011; Li, Wang, Pennell, & Abriola, 2008; Pelley & Tufenkji, 2008; Tian et al., 2010; Wang et al., 2008). The similarity between the different nanoparticles can shed some light on the research on transport of silver nanoparticles.

Additionally, the transport and retention of colloid particles (e.g. latex microspheres) has been studied in detail in the past. Many classical theories such as clean bed filtration theory and physical-chemical filtration were developed for colloid particles. However, it is dubious to apply the theories developed from colloid particles directly to silver nanoparticles, as the retention behavior is likely to change due to the extremely small size of nanoparticles (nm) compared to that of colloid particles (μm). Therefore conclusions drawn from colloid transport may not readily apply to silver nanoparticles.

Earlier studies collectively showed that the transport mechanisms of silver nanoparticles (and other nanoparticles as well) are mainly affected by the electrolytes, flow rate, ionic strength, humic acid, sand grain size, and pH. However, the knowledge of transport mechanisms is far from complete, especially related to other porous media such as ceramic disks and geosynthetic clay liners.

2.2.2 *Ceramic disks*

Ceramic disks were studied as a surrogate to a ceramic filter, which has been widely used as a point-of-use intervention device for communities in developing countries without access to clean drinking water. Gaining popularity over the last decade because of its low cost and high performance, silver nanoparticles were creatively applied

to ceramic filters in order to further enhance the disinfection capability. However, some preliminary studies showed that silver sometimes leached out of these filters and entered the potable drinking water supply. In a report submitted to "Potters for Peace" (a non-governmental organization promoting silver-impregnated ceramic filters), the investigator noted that it is not recommended to drink the water that first passes through a new filter, because a significant amount of silver leaches out in the first run (D.S.Lantagne, 2001). There was still a detectable amount of silver present in the filtered water after being used for six months (D.S.Lantagne, 2001). The fact is concerning for two reasons: 1) people directly intake silver nanoparticles from the drinking water which is supposed to be clean and safe, and 2) the ceramic filter progressively loses its disinfection capability due to the loss of silver. The understanding of transport/release mechanisms of silver nanoparticles through ceramic filters (disks) will directly benefit the promotion of ceramic filter technology by reducing the risks and increasing the life span.

2.2.3   Geosynthetic clay liner

Geosynthetic clay liners, which are often abbreviated as GCL, are mainly used in waste disposal facilities as barriers to contain the migration of leachate from contaminating the ground water system. The low permeability ($<10^{-7}$ cm/s) is an ideal characteristic to effectively prevent the downward flow of leachate.

With the increasing usage of silver nanoparticles in commercial products, it is expected that more silver nanoparticle products end up in a waste disposal facility in the future. Whether a GCL can properly stop the transport of nanoparticles is of interest in assessing the risk to the groundwater system.

As of today, no scientific research has been reported to investigate the transport of silver nanoparticles through a geosynthetic clay liner. Thus, a knowledge gap has been identified. The risk of groundwater being exposed to silver nanoparticles and the increasing amount of silver nanoparticle products makes addressing this gap even more important.

Reference

Benn, T. M., & Westerhoff, P. (2008). Nanoparticle Silver Released into Water from Commercially Available Sock Fabrics. *Environmental Science & Technology, 42*, 4133-4139

Blaser, S. A., Scheringer, M., MacLeod, M., & Hungerbuhler, K. (2008). Estimation of Cumulative Aquatic Exposure and Risk Due to Silver: Contribution of Nano-Functionalized Plastics and Textiles. *Science of the Total Environment, 390*(2-3), 396-409

Chinnapongse, S. L., MacCuspie, R. I., & Hackley, V. A. (2011). Persistence of Singly Dispersed Silver Nanoparticles in Natural Freshwaters, Synthetic Seawater, and Simulated Estuarine Waters. *Science of the Total Environment, 409*(12), 2443-2450

D.S.Lantagne. (2001). Investigation of the Potters for Peace Colloidal Silver Impregnated Ceramic Filter - Report 1: Intrinsic Effectiveness. Alston, MA: Alethia Environmental.

Elechiguerra, J. L., Burt, J. L., Morones, J. R., Camacho-Bragado, A., Gao, X., Lara, H. H., & Yacaman, M. J. (2005). Interaction of Silver Nanoparticles with Hiv-I. *Journal of Nanobiotechnology, 3*(6), 1-10

Jaisi, D. P., & Elimelech, M. (2009). Single-Walled Carbon Nanotubes Exhibit Limited Transport in Soil Columns. *Environmental Science Technology, 43*(24), 9161-9166

Kanel, S. R., & Al-Abed, S. R. (2011). Influence of Ph on the Transport of Nanoscale Zinc Oxide in Saturated Porous Media. *Journal of Nanoparticle Research, 13*(9), 4035-4047

Li, Y., Wang, Y., Pennell, K. D., & Abriola, L. M. (2008). Investigation of the Transport and Deposition of Fullerene (C60) Nanoparticles in Quartz Sands under Varying Flow Conditions. *Environmental Science Technology, 42*(19), 7174-7180

Pelley, A. J., & Tufenkji, N. (2008). Effect of Particle Size and Natural Organic Matter on the Migration of Nano- and Microscale Latex Particles in Saturated Porous Media. *Journal of Colloid and Interface Science, 321*(1), 74-83

Sagee, O., Dror, I., & Berkowitz, B. (2012). Transport of Silver Nanoparticles (Agnps) in Soil. *Chemosphere, 88*(5), 670-675

Tian, Y., Gao, B., Silvera-Batista, C., & Ziegler, K. J. (2010). Transport of Engineered Nanoparticles in Saturated Porous Media. *Journal of Nanoparticle Research, 12*(7), 2371-2380

Wang, Y., Li, Y., Fortner, J. D., Hughes, J. B., Abriola, L. M., & Pennell, K. D. (2008). Transport and Retention of Nanoscale C 60aggregates in Water-Saturated Porous Media. *Environmental Science Technology, 42*(10), 3588-3594

Woodrow Wilson International Center for Scholars. (2008). The Project on Emerging

Nanotechnologies.

CHAPTER 3: TRANSPORT THROUGH OTTAWA SAND

3.1   Introduction

Silver and its compounds have been used since the age of the ancient Egyptians, when silver vessels were used to preserve water and wine (Russell & Russell, 1995). Before the emergence of antibiotics, silver compounds were widely used during World War I to prevent wound infection. Metallic silver was used to treat surgical prostheses and splints and to serve as a fungicide. Soluble silver compounds were used to treat a range of diseases from mental illness to gonorrhea (Drake & Hazelwood, 2005). Even today, silver sulfadiazine is the standard antibacterial treatment for serious burn wounds (Chen & Schluesener, 2008). Recent advances in nanotechnology have demonstrated that nano-size particles of metallic silver have strong antimicrobial properties.

Silver nanoparticles (AgNPs) have large surface areas and high reactivity compared with the bulk solid; thus, they exhibit remarkable physical, chemical, and biological properties, such as an increased catalytic activity because of their highly reactive facets (Elechiguerra et al., 2005). In addition, there is increasing interest in using AgNPs as a special class of biocidal agents (Kallman, Oyanedel-Craver, & Smith, 2011; V. A. Oyanedel-Craver & J. A. Smith, 2008; Zhang, Smith, & Oyanedel-Craver, 2012).

In April 2005, a partnership between the Woodrow Wilson International Center

for Scholars and the Pew Charitable Trusts established The Project on Emerging Nanotechnologies. The project maintains an extensive consumer product inventory with more than 800 products, produced by 420 companies, located in 21 countries. AgNPs, the active component of more than 20% of the nano-products currently available on the market, are the most commonly cited nanomaterial (Fauss, 2008). Approximately 88% of these products have some form of antibacterial or antimicrobial activity (Fauss, 2008).

AgNPs are fine particles of metallic (zero-valent) silver, which have at least one dimension lower than 100 nm. AgNPs exhibit physical properties that are different from both the ion and the bulk material. Because of their strong antibacterial properties, several studies have shown the potential use of AgNPs in biomedical and environmental applications, such as the treatment of wounds and burns (Chen & Schluesener, 2008; Furno et al., 2004; Maneerung, Tokura, & Rujiravanit, 2007) and water disinfection (Jain & Pradeep, 2005; LePape et al., 2002). As noted in several recent publications (Badawy, Luxton, & Silva, 2010; Benn & Westerhoff, 2008; Choi & Hu, 2008, 2009), AgNPs used in commercial products likely enter conventional liquid- and solid-waste streams (e.g. wastewater treatment plants and sanitary landfills). Little is known about the fate and transport of AgNPs in aquatic systems or about their effects on ecosystems.

Several recent studies have investigated the fate and transport of nanoparticles (e.g. carbon nanotubes, latex nanoparticles, silver nanoparticles, zinc oxide and fullerenes) in saturated porous media (Jaisi & Elimelech, 2009; Kanel & Al-Abed, 2011; Li, Wang, Pennell, & Abriola, 2008; Pelley & Tufenkji, 2008; Tian, Gao, Silvera-Batista, & Ziegler, 2010; Y. Wang et al., 2008). To our knowledge, only a few studies have explicitly addressed transport of AgNPs. Tian et al. (Tian et al., 2010) studied AgNPs

transport through two sands with similar particle size distributions but having different surface zeta potentials. The effluent AgNPs breakthrough was nearly identical for both sands, indicating that the surface zeta potential of the sand particles does not have a significant impact on AgNPs transport. Thio et al. (Thio et al., 2011) investigated the mobility of silver nanoparticles with two different coatings (citrate and PVP) under different water chemistry conditions . They concluded that AgNPs could be very mobile in environmentally relevant conditions.

For the work presented herein, the effects of porous media particle size and water chemistry on AgNP transport are investigated by batch experiments and sand column experiments. A well-characterized commercially available AgNP, silver proteinate, is used in our study. To our knowledge, this is the first study to examine the transport of this nanoparticle in a porous media. Silver proteinate is commonly used in ceramic water filters endorsed by Potters for Peace (Vinka A Oyanedel-Craver & James A Smith, 2008) and other commercial applications. The proteinate capping agent improves the particle stability in aquatic systems and may therefore improve its mobility when released to the environment. Herein, the transport behavior is experimentally studied using Ottawa sands having three distinct mean particle sizes and under three different electrolyte concentrations. The sorption of AgNPs to the sands is also quantified using a batch equilibrium sorption methodology. These data are combined to study the relative effects of particle aggregation/filtration and nanoparticle-sand-surface interactions on nanoparticle retention in the column. Column experiments are quantitatively analyzed using a mathematical model that incorporates nanoparticle attachment/detachment kinetics and maximum retention capacities.

3.2   Materials and methods

3.2.1   Materials

Proteinate-capped AgNPs were obtained from Argenol Laboratories, Spain and used as received (Vinka A Oyanedel-Craver & James A Smith, 2008). Reagent-grade electrolytes ($MgSO_4$ and KNO_3) from Sigma-Aldrich were used to prepare divalent and monovalent electrolyte stock solutions. They were mixed with silver nanoparticle solutions to achieve different ionic strengths. US Silica Inc. (Berkeley, WV) provided three kinds of Ottawa sand with median grain diameters (d_{50}) determined through sieve tests as follows: 0.55, 0.34 and 0.18 mm (also referred to as coarse, medium and fine sand throughout this paper). Prior to experiments, the sand samples were washed with tap water, a 10% nitric acid solution, and deionized water to remove surface impurities (such as iron hydroxide and organic coatings) that could interfere with deposition of silver nanoparticles during transport experiments. After purifying the sand, it was dried at 105 ºC for 24 h, and then stored in a capped sterile bottle for later use.

3.2.2   Quantification and Characterization of AgNPs

The concentration of AgNPs in solution was determined using a calibrated UV-vis spectrophotometer. Samples were also crosschecked with an AAnalyst 200 atomic absorption spectrometer (AAS) (Perkin-Elmer) for quality assurance. Morphological characteristics were examined through a NiComp Dynamic light scattering (DLS) system and a transmission electron microscope (TEM) (model: JEOL 2000FX). Aqueous AgNPs suspensions were sonicated for 5 min before DLS measurement to ensure the nanoparticles were mono-dispersed. The zeta potential (ζ) of AgNPs was measured by filling liquid samples into the folded capillary cell (DTS 1060, Malvern Instruments) and

quantified with a ZetaSizer Nano Z zeta potential instrument (Malvern Instruments).

Time-resolved hydrodynamic diameter and zeta potential charge were monitored closely

under either monovalent or divalent electrolyte solutions over 12 hours. All

measurements were performed at room temperature (24 ± 1 °C) and at a pH of 7.

3.2.3 Batch Sorption

Batch sorption experiments were performed to independently evaluate the

sorption of AgNPs from water to sand as a function of ionic strength. For these tests, 10

g of sand and 10 mL of a AgNPs aqueous suspension at initial concentrations ranging

from 0 to 50 mg/L were mixed in 15 mL disposable glass centrifuge tubes with Teflon-

lined caps. Ionic strength was adjusted by adding 1M $MgSO_4$ solution. The contents

were mixed on a mechanical shaker for two hours (the time predetermined to reach

equilibrium). The tubes were then centrifuged at 2,000 g for 30 min. This centrifugal

force removed the sand particles from solution but did not remove the AgNPs. The

concentration of AgNPs in the supernatant was quantified and the absorbed concentration

was calculated by difference. Several additional samples were included for quality

control. Controls were properly selected and performed to exclude sorption to vial

surface. AgNP recoveries were consistently greater than 95% and the sorption data were

not adjusted for these relatively small losses.

3.2.4 Packed-bed column tests

A borosilicate glass column (15 cm $\times$ 1 cm I.D.) with Teflon end fittings (Kontes,

Vineland, NJ) was used for porous media transport experiments. Two stainless-steel

mesh screens were placed inside the column at both ends to prevent elution of sand

particles. Each column was dry packed in small increments while the column was

vibrated to minimize air entrapment. Porosity was determined gravimetrically ranging from 0.23 to 0.31. The consistency of packing for different columns was later verified by [^{3}H-H$_2$O] tracer tests.

Upon packing, degassed DI water was used to flush the column for 3 hours (approximately 18 pore volumes) to completely saturate the column at a rate 0.6 mL/min by an Acuflow series IV HPLC pump (Vinka A Oyanedel-Craver & James A Smith, 2008). A pulse injection of conservative tracer [^{3}H]-H$_2$O was injected to evaluate the hydraulic properties of the sand column namely: dispersivity and hydraulic conductivity. Concentrations of tracer in effluent samples were quantified with a calibrated Packard 1900CA liquid scintillation analyzer.

For AgNP transport experiments, two-step procedure was performed. A 50 mg/L AgNP solution at a selected ionic strength was fed into the column at a constant flow rate. Then, a AgNP-free background solution with the same ionic strength as used in previous steps was reintroduced to rinse the column. Effluent samples were collected and prepared accordingly for analysis.

3.2.5   Theoretical development

The following one-dimensional advection-dispersion equation was used to describe the transport of AgNPs in the packed columns:

$$\frac{\partial C}{\partial t} + \frac{\rho_b}{\theta_w}\frac{\partial S}{\partial t} = D\frac{\partial^2 C}{\partial x^2} - q\frac{\partial C}{\partial x} \tag{3-1}$$

$$\frac{\rho_b}{\theta_w}\frac{\partial S}{\partial t} = k_{att}\psi C - k_{det}\rho S \tag{3-2}$$

where C (ML^{-3}) is the concentration of AgNPs, ρ_b (ML^{-3}) is soil bulk density, θ_w (-) is the volumetric water content, t (T) is the time, q (LT^{-1}) is the linear velocity of the water, S (MM^{-1}) is the solid-phase concentration of AgNPs, D (L^{2}T^{-1}) is hydrodynamic dispersion coefficient, x is longitudinal distance, k_{att} (T^{-1}) is the attachment coefficient, k_{det} (T^{-1}) is the detachment coefficient, ψ (-) is the dimensionless blocking coefficient. Adamczyk et al. (Adamczyk, Siwek, Zembala, & Weronski, 1992) gave the relation between ψ and S as follows:

$$\psi = 1 - \frac{S}{S_{max}} \qquad (3\text{-}3)$$

where S_{max} is the maximum retention capability (MM^{-1}). $k_{att}\,\psi$ is the modified attachment coefficient. It accounts for the reduced attachment rate when more AgNPs take up active sites for deposition. When the available sorption sites reach saturation (S/S_{max} close to 1), this modified attachment coefficient is close to zero. A public domain software (Hydrus-1D) was used to fit the breakthrough curves of conservative tracer and the silver nanoparticle, by optimizing D and q for the former case, and k_{att}, k_{det} and S_{max} for the latter case, respectively (Simunek & van Genuchten, 2008).

The surface interaction energy between nanoparticles and collector surface is assumed to be the interaction between the particle and an infinite plate due to the large ratio of collector diameter to particle diameter. A nanoparticle must overcome the energy barrier to deposit on the collector surface. This energy barrier, which is the combined force of van der Waals (VDW) attraction and electrostatic double layer repulsion (EDL), is calculated by classical DLVO theory (Derjaguin, Landau, Verwey and Overbeek). The mathematical procedure has been well documented elsewhere and thus is not included here (Bhattacharjee & Elimelech, 1997; Redman & Walker, 2004).

3.3   Results

3.3.1   *Silver nanoparticle characterization*

The particle size distribution of aqueous silver nanoparticle suspensions were

examined by DLS and the morphology was obtained through TEM, which is included in

the inset in Figure 3-1a. The nanoparticles are mostly spherical. The average

hydrodynamic diameter of AgNPs is approximately 49 nm ± 3.12 nm, and the diameter

from TEM is 14 nm ± Time-resolved DLS measurement are presented in Figure 3-1b as a

function of time in DI water, 10 mM ionic strength as monovalent electrolyte KNO_3, or

10 mM ionic strength as divalent electrolyte $MgSO_4$.
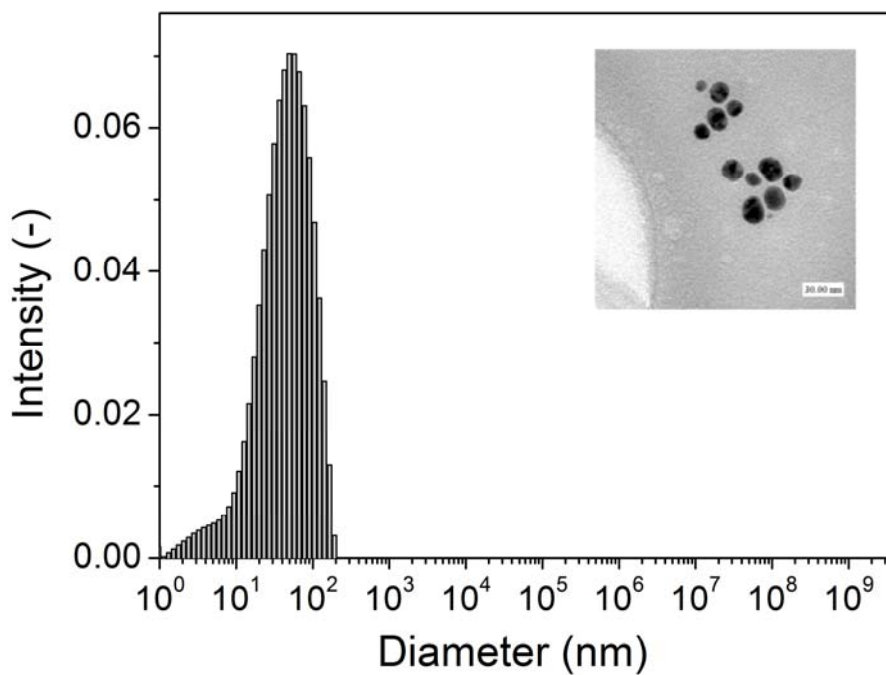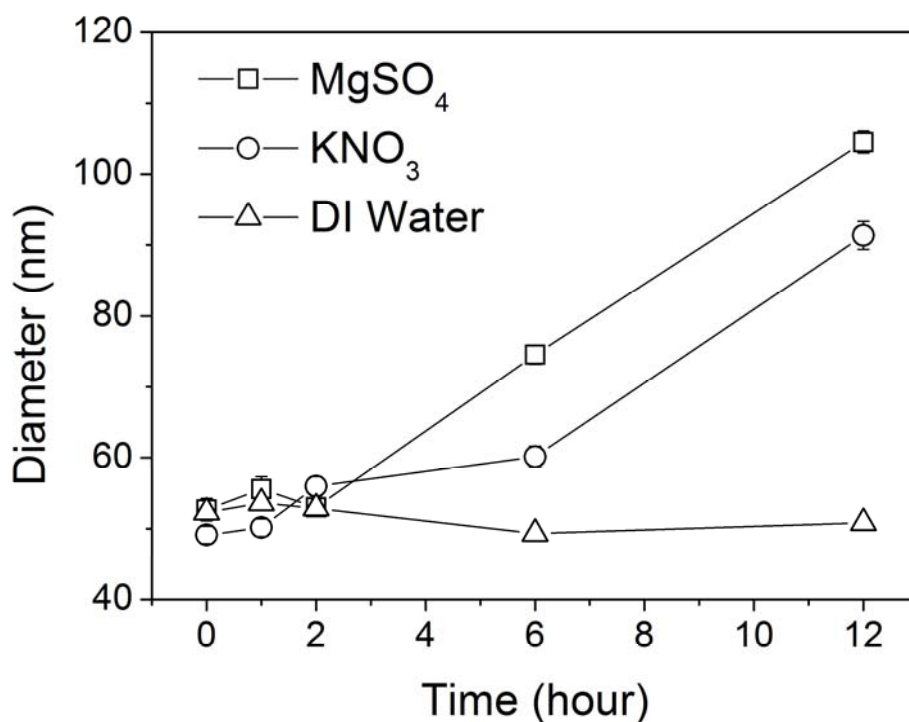
Figure 3-1. (a) The particle-size distribution of proteinate silver nanoparticles as measured by dynamic light scattering (DLS). The inset is a typical transmission electron microscope (TEM). (b) Time-resolved hydrodynamic diameter measurement over a period of 12 hours in 0 mM and 50 mM ionic strength solutions (as either KNO3 or MgSO4)

Figure 3-2 shows the zeta potential of silver nanoparticles in DI water, 10 mM

ionic strength as MgSO$_4$ and 50 mM ionic strength as MgSO$_4$ over a period of 4 hours.

At time zero, the zeta potentials for AgNPs solution under 0 mM, 10 mM and 50 mM

ionic strength were -57.1 mV, -28.4 mV and -22.8 mV, respectively.
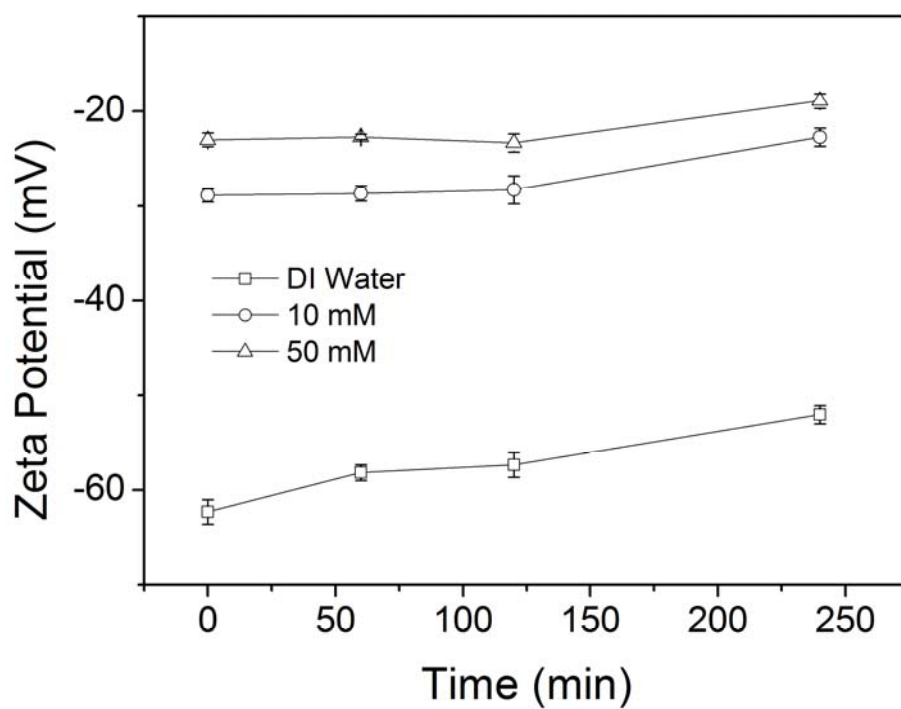
Figure 3-2. Zeta potential of silver nanoparticle solutions in the presence of 0 mM, 10 mM and 50 mM ionic strength as $MgSO_4$, over a time period of 4 hours.
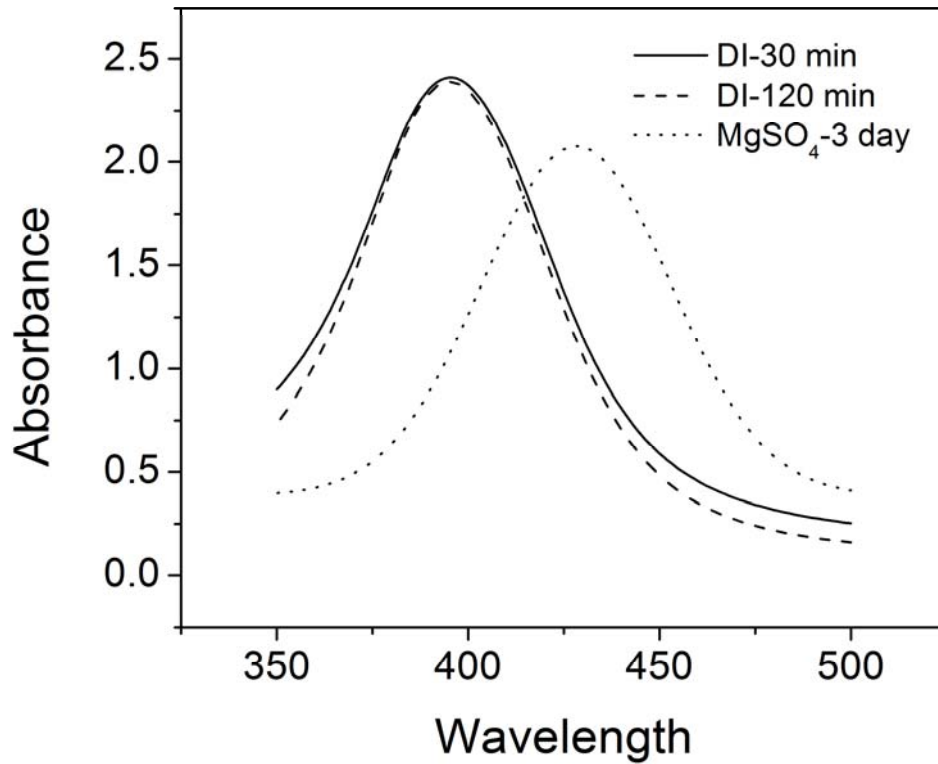
Figure 3-3. UV-vis scan of AgNP suspensions prepared with DI water at 30 min and 120 min after preparation and with MgSO$_4$ (ionic strength 10 mM) 3 days after preparation.

3.3.2   Retention of AgNPs in sand columns

Breakthrough curves of silver nanoparticles for sand columns packed with various Ottawa sands under different ionic strength levels are presented in Figure 3-4, together with fitted model predictions. The concentrations of AgNPs in effluent samples are normalized to the influent concentration, C_0, and plotted as a function of pore volumes of flow passed through the column. Table 3-1 summarizes the properties of all performed column studies as well as fitted parameters for both tracer tests and transport tests. The numerical values of the retained percentage of total injected mass for each experiment are given in Table 3-1.

Table 3-1. Percentage retention of AgNPs in column experiments and associated simulation parameters (S_{max}: maximum attachment capacity; k_{att}: attachment coefficient; k_{det}: detachment coefficient)

Column	Ionic Strength (mM)	Median grain size (mm)	Porosity	Hydraulic Conductivity (cm/min)	Retention (%)	S_{max} (µg/g)	k_{att} (min⁻¹)	k_{det} (min⁻¹)
1	0	0.55	0.312	0.866	24.32	9.2	3.16E-02	3.93E-01
2	10	0.55	0.305	0.533	35.94	11.9	4.26E-01	2.49E-01
3	50	0.55	0.301	0.563	65.03	29.27	6.80E-01	7.45E-04
4	10	0.34	0.289	0.594	38.93	22.36	3.02E-01	1.14E-01
5	50	0.34	0.276	0.618	90.05	43.19	1.05E+00	1.60E-05
6	0	0.18	0.239	0.589	34.49	0.43667	4.30E-02	1.08E-01
7	10	0.18	0.247	0.652	49.47	39.1	3.34E-01	2.74E-05
8	50	0.18	0.259	0.639	100	9.2	1.84E-01	3.93E-01

* NA: there was no detectable AgNPs in effluent, so simulation was not performed.

**Hydraulic conductivity were obtained from modeling fit of tracer breakthrough curves

***S_{max}, K_{att} and K_{det} were obtained from modeling fit of AgNPs breakthrough curves

(a)
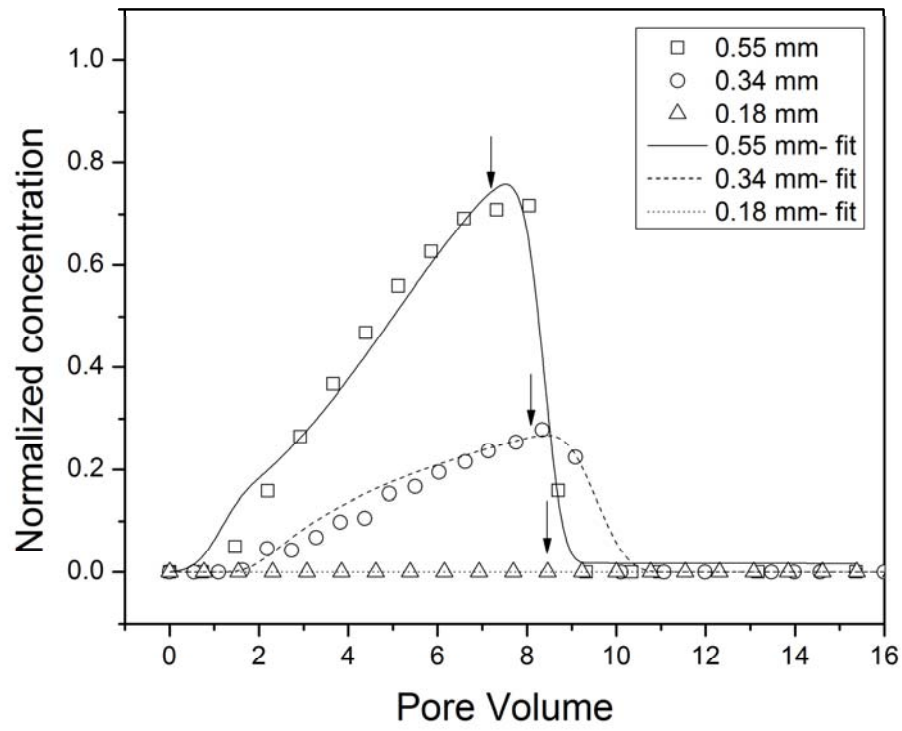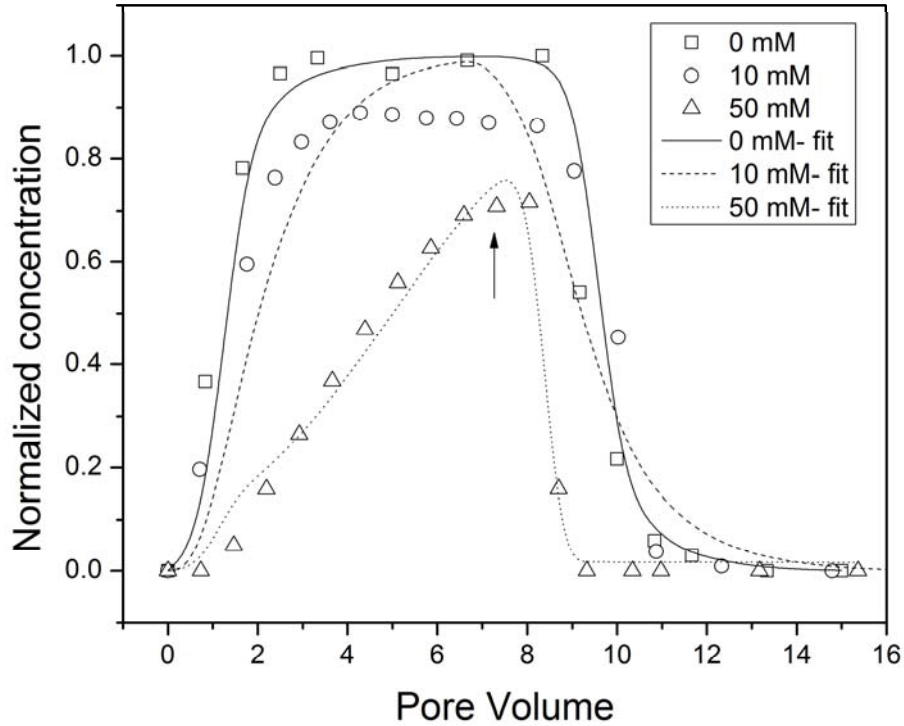
Figure 3-4. Normalized AgNPs breakthrough curves (a) with three sand grain sizes (0.18 to 0.55 mm) and one ionic strength (10 mM) and (b) two different ionic strengths (0 to 50 mM) with one sand grain size (0.55 mm). Arrows indicate the time point where the feed of AgNPs suspension was replaced by AgNP-free background solution.

3.3.3   AgNPs batch adsorption to Ottawa sand

AgNP sorption to Ottawa sand was independently quantified by batch sorption tests. These experiments were performed to quantify nanoparticle-sand interactions exclusive of the influence of pore structure on retention of AgNPs. The upper and lower limits of sand sizes and ionic strengths were investigated and results are reported in Figure 3-5. Sorption isotherm data are well described by a linear sorption model (R^2 are

27

all greater than 0.989). For 0 mM ionic strength, retention of AgNPs was less than 35%

for both sands. The addition of electrolyte significantly increased AgNPs retention.
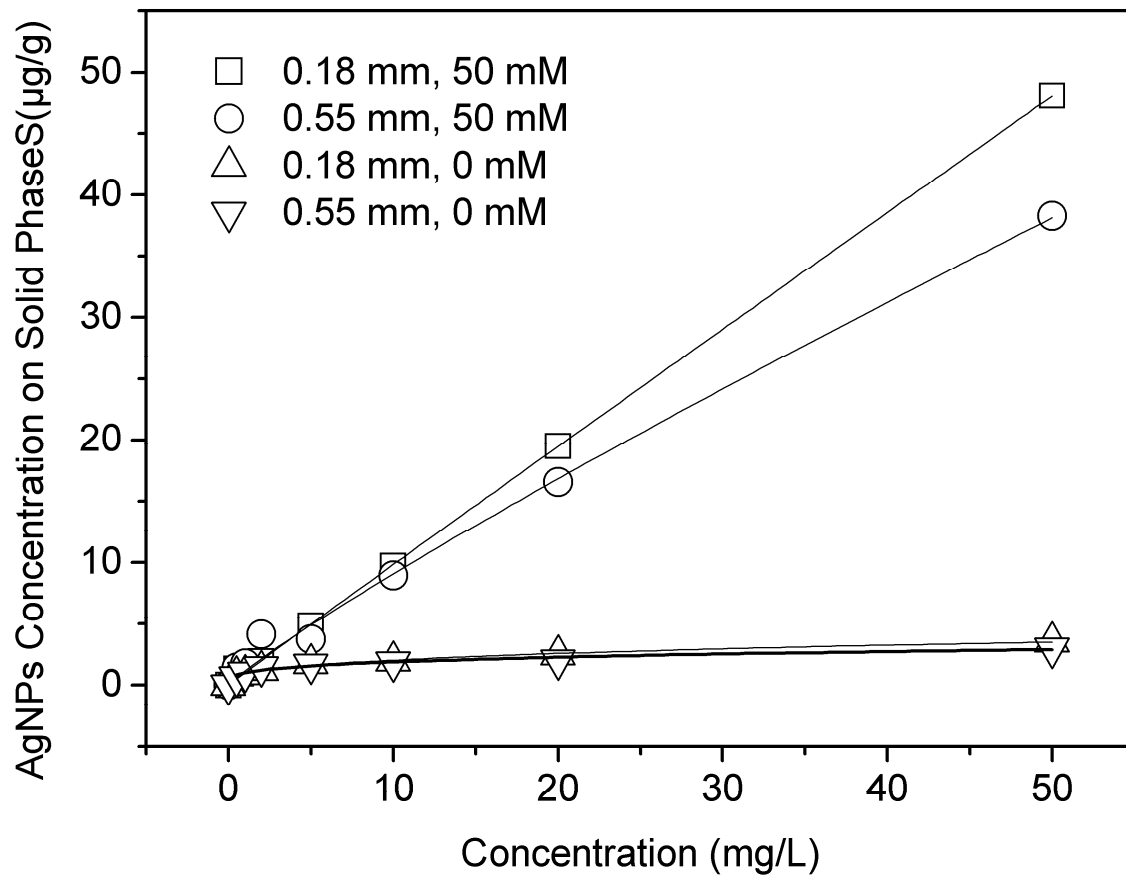
Figure 3-5. Sorption isotherms and linear model fits for AgNPs sorption to two Ottawa sands (0.18 and 0.55 mm) at two ionic strengths (0 and 50 mM).

3.4   Discussion

3.4.1   Properties of proteinate AgNPs

Previous studies have shown that the capping agent influences the fate and

transport of AgNPs in conditions simulating natural environments (Badawy et al., 2010;

Foldbjerg et al., 2009; Huynh & Chen, 2011; Zeng et al., 2010). These studies have

extensively examined both citrate and polyvinylpyrrolidone (PVP), but to date, no study

has include AgNPs capped with proteinate.

The mass percentage of silver in the commercial silver proteinate is 7.66% by weight as determined by atomic absorption spectroscopy and confirmed by the manufacturer's specification. The remainder is the proteinate capping agent (>90%). When dispersed in water, the proteinate coating likely exists as a diffuse hydrated layer on the external AgNP surface. This is confirmed by the relatively large difference in the mean particle diameter as measured by DLS (49 nm) and TEM (15 nm). DLS measures the hydrated particle radius whereas TEM only detects the metallic particle itself (MacCuspie et al., 2011). Proteinate is believed to have a large molecular weight and possibly heterogeneous structure. Similar observations have been reported for AgNPs with PVP coatings, which are similar to proteinate in terms of molecular size. Foldbjery et al. (Foldbjerg et al., 2009) reported a 69 nm particle diameter for PVP-coated AgNPs measured by TEM compared to 118 nm by DLS in DI water. On the contrary, the particle diameters measured by DLS and PVP for citrate-capped AgNPs is small compared to proteinate- and PVP-capped particles (Huynh & Chen, 2011; Jiang, Oberdorster, & Biswas, 2009; P. Wang & Keller, 2009; Zhuang, Qi, & Jin, 2005). This observation is consistent with the relatively small molecular weight of citrate relative to proteinate and PVP. Herein, we reference the hydrodynamic diameter as determined by DLS for the size of our proteinate-capped AgNPs (Bilberg, Malte, Wang, & Baatrup, 2010; Jaisi & Elimelech, 2009; Powers, Slotkin, Seidler, Badireddy, & Padilla, 2011).

The silver proteinate nanoparticles are negatively charged (Figure 3-2), and electrostatic double layer repulsion between AgNPs stabilizes the suspension for a short period of time, as shown by both the hydrodynamic diameters in Figure 3-1b and zeta potentials in Figure 3-2 measured as a function of time. It is also confirmed by the UV-

Vis scan presented in Figure 3-3. Over time, the proteinate capping agent is gradually released into solution. This destabilizes the particles and leads to particle aggregation and larger mean particle diameters in electrolyte solutions (Figure 3-1b). In DI water, the mean particle size decreases. In this case, aggregation is less pronounced in the absence of counter ions and dissolution of the proteinate capping agent result in a net reduction in hydrodynamic particle diameter. Overall, the stabilization effect caused by the proteinate coating appears to be longer lasting than a citrate coating. Huynh et al. (Huynh & Chen, 2011) reported rapid aggregation of citrate-coated AgNPs. The particles grew from 60 nm to 100 nm in 30 min. In the present study, the proteinate-capped AgNPs required almost 12 hr to increase in size from 49 nm to 100 nm.

At 50 mM ionic strength, AgNP aggregation was observed over 12 hours (Figure 3-1b) as evidenced by the increasing hydrodynamic diameters. It is worthy to note that under the same ionic strength, Mg^{2+} as a divalent electrolyte is more effective in inducing aggregation than K^+ as a monovalent electrolyte. This is consistent to the fact that divalent electrolytes compress the electrostatic double layer more effectively than monovalent electrolytes (Elimelech, 1995; Jaisi & Elimelech, 2009). Only $MgSO_4$ was used in the transport experiments to adjust the ionic strength.

Figure 3-2 shows the zeta potential for AgNP suspensions with the same electrolyte but at the different concentrations. The proteinate-capped AgNPs were negatively charged over the examined range of ionic strengths (0 mM to 50 mM). This is consistent with most investigations conducted on AgNPs with other types of capping agents (Badawy et al., 2010; Jaisi & Elimelech, 2009). In general, the absolute value of

the zeta potential decreases with increasing ionic strength, which is a direct result of compression of the diffuse double layer by the electrolyte.

3.4.2   General transport behavior of AgNPs

The normalized breakthrough curves presented in Figure 3-4 lead to several important conclusions regarding AgNPs transport in porous media. First, it is apparent that AgNPs are effectively transported through the sand media under most conditions and are able to exit the columns. The percentages of retained nanoparticle are shown in Table 3-1 for each experiment, ranging from about 24% to 100%, and variations in percent retention are related to the solution ionic strength and mean particle size. Second, solution ionic strength has a strong effect on AgNP transport through the sand porous media. As solution ionic strength increases, AgNP retention increases. Third, as the mean sand particle size is reduced, increased attenuation of AgNPs was observed.

3.4.3   Deposition kinetics of AgNPs with ionic strength

Solution ionic strength has a strong effect on AgNP transport through the sand porous. As solution ionic strength increases, AgNP retention increases, which is evident by inspection of the effluent breakthrough curves in Figure 3-4b. The attachment coefficients (k_{att}) listed in Table 3-1 show a positive dependence on ionic strength for same size of sand. Conversely, detachment coefficients (k_{det}) reduce significantly when increasing ionic strength. This behavior is comparable to previous observations for other types of nanoparticles and colloidal transport behavior (Petosa, Jaisi, Quevedo, Elimelech, & Tufenkji, 2010; Torkzaban, Bradford, van Genuchten, & Walker, 2008; Y. Wang et al., 2008). Two contributing mechanisms may account for the effect of solution ionic strength. First, increasing ionic strength likely compresses the diffuse double layer

surrounding the AgNPs. This in turn allows for enhanced particle-particle interaction

resulting in aggregation and potential for particle settling to the sand surface. The larger

particles are more effectively removed by physical filtration (straining) in a given porous

medium. Yet, our time-resolved DLS measurement suggests this effect is relative minor

(see Figure 3-1b). The aggregation was not observed in the course of the experiments,

which may be a result from the proteinate capping agent.

Secondly, by reducing the thickness of the diffuse double layer surrounding the

AgNPs, sorption of the nanoparticles to the sand particles is expected to increase. This

effect is also supported by the batch sorption data in Figure 3-5. It has shown that silver

nanoparticles and the sand particles both have negatively charged surfaces for the entire

range of ionic strengths we investigated (Figure 3-2). Therefore, the deposition of

AgNPs onto the collector (sand) surface needs to overcome the primary energy barrier

existed between two surfaces. This energy barrier, calculated from DLVO theory, shows

significant decrease from more than 25 k_bT to less than 0.4 k_bT, with the addition of

electrolyte to 50 mM ionic strength (Figure 3-6). The reduction of the energy barrier

effectively changes the deposition to a more favorable condition, and thereby results in

higher retention rates of AgNPs. These calculated values are consistent with our batch

sorption data and our column transport data for AgNPs. A significantly higher percentage

of AgNPs was trapped under high ionic strength conditions relative to low ionic strength

conditions.
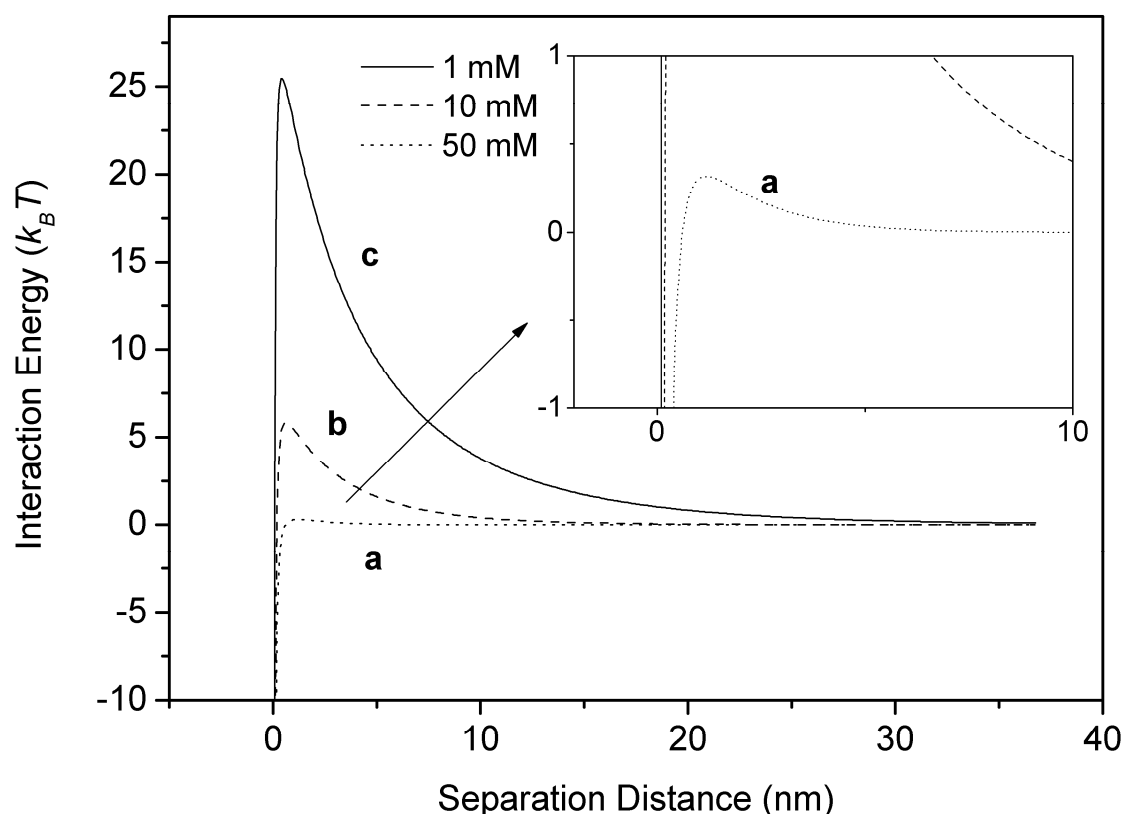
Figure 3-6. Interaction energy profile between particle and collector surface as a function of separation distance. The inset shows the detail for energy profiles close to zero.

3.4.4 The role of sand grain size

The impacts of sand grain size on retention of AgNPs in this study are different depending on ionic strength level. Under low ionic strength ($\leq$10 mM), the energy barrier between particle and collector is sizeable, preventing appreciable deposition of AgNP. Batch experiment results in Figure 3-5 also suggest absorption is a relatively weak effect by itself under low ionic strength. Thus, the observed retentions under low ionic strength in Table 3-1 are less likely to attribute to the adsorption of AgNP. Rather straining effect from sand matrix becomes important, which is defined as the trapping of particles in pores that are too small to allow particle passage. Granted that classical colloid transport theory found straining occurs when the ratio of particle to collector

diameter is greater than 0.05, a study suggests it could occur even when the ratio is as low as 0.003 (Bradford, Torkzaban, & Walker, 2007). More recently, straining is also observed for nanoparticles, where the ratio is as low as 0.0008 for single wall nanotubes. In our case, the ratio of particle of medium sand grain size is 0.0003, 0.0002 and 0.0001 for fine, medium and coarse sands, which is comparable to the lowest reported ratio (0.0008).

It shall be noted that, the Ottawa sand used here is less uniform than the sands used in other studies, most of which used sand with a fraction of size distribution. As shown in Figure 3-7 is the standard sieve test results of three types of sand used in column studies. The uniformity coefficients for examined sands, which is defined as the ratio of grain diameter at 60% passing to that at 10% passing, are 1.8, 2.2 and 1.3 for fine, medium and coarse sand, respectively. Having both large and small sand grain in one column help create small pores and eliminate large pores in sand matrix and thereby enhanced the straining effect towards retention.
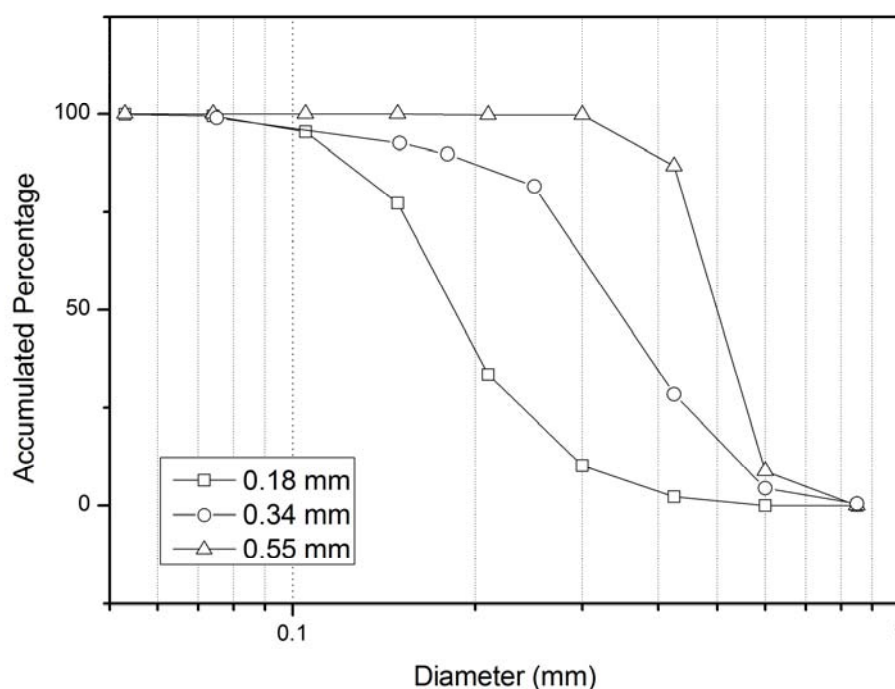
Figure 3-7. Sieve test result of three types of sand used in column experiments.

While with high ionic strength (50 mM), when the electrolyte could effectively reduce the repulsive energy barrier, the absorption of AgNP onto sand surface is dominant. Under such favorable deposition scenario, most of particles colliding with sand surface can be retained providing there are enough absorption sites. Indeed, the total adsorption sites are directly related to the total surface area of sand grains. Larger available sites grant higher deposition percentage. This is confirmed by the sorption isotherms under 50 mM ionic strength in Figure 3-5. For example, when the aqueous phase AgNPs concentration is 50 mg/L, the solid phase concentrations for fine sand and coarse sand are 48.3 and 39.5 µg/g. Additionally, sand matrix consists of fine sand has higher percentage of small pores than that consists of coarse sand.

3.4.5   Implications of transport behavior

The mobility of AgNPs is a key step to perform risk analysis from emerging nanomaterial. This study presented results showing the mobility of AgNPs under a series of environmental relevant conditions. The results showed that the AgNPs could be mobile in environment. Under the ionic strength close to natural ground water (10 mM), we can calculate the maximum travel distance of AgNPs in our uniform porous medium system, using filtration theory. The calculated distances are 7.44, 6.37 and 4.92 m for Ottawa sands with the diameter 0.55, 0.34 and 0.18 mm, respectively (Jaisi & Elimelech, 2009). Furthermore, the transport of AgNPs may be even greater due to the complexity of natural soil system. Heterogeneities, including pore fractures in consolidated sediments could further facilitate the transport of commercial AgNPs discharged into the subsurface environment to a greater distance.

Reference

Adamczyk, Z., Siwek, B., Zembala, M., & Weronski, P. (1992). Kinetics of Localized Adsorption of Colloid Particles. *Langmuir, 8*(11), 2605-2610

Badawy, A., Luxton, T., & Silva, R. (2010). Impact of Environmental Conditions (Ph, Ionic Strength, and Electrolyte Type) on the Surface Charge and Aggregation of Silver Nanoparticles Suspensions. *Environmental Science Technology*

Benn, T. M., & Westerhoff, P. (2008). Nanoparticle Silver Released into Water from Commercially Available Sock Fabrics. *Environmental Science & Technology, 42*, 4133-4139

Bhattacharjee, S., & Elimelech, M. (1997). Surface Element Integration: A Novel

   Technique for Evaluation of Dlvo Interaction between a Particle and a Flat Plate.

   Journal of Colloid and Interface Science, 193(2), 273-285

Bilberg, K., Malte, H., Wang, T., & Baatrup, E. (2010). Silver Nanoparticles and Silver

   Nitrate Cause Respiratory Stress in Eurasian Perch (Perca Fluviatilis). *Aquatic*

   Toxicology, 96(2), 159-165

Bradford, S. A., Torkzaban, S., & Walker, S. L. (2007). Coupling of Physical and

   Chemical Mechanisms of Colloid Straining in Saturated Porous Media. *Water*

   research, 41(13), 3012-3024

Chen, X., & Schluesener, H. J. (2008). Nanosilver: A Nanoproduct in Medical

   Application. *Toxicology Letters, 176*, 1-12

Choi, O., & Hu, Z. (2008). Size Dependent and Reactive Oxygen Species Related

   Nanosilver Toxicity to Nitrifying Bacteria. *Environmental Science & Technology,*

   42, 4583-4588

Choi, O., & Hu, Z. (2009). Role of Reactive Oxygen Species in Determining Nitrification

   Inhibition by Metallic/Oxide Nanoparticles. *Journal of Environmental*

   Engineering, 135(12), 1365-1370

Drake, P. L., & Hazelwood, K. J. (2005). Exposure-Related Health Effects of Silver and

   Silver Compounds: A Review. *Annals of Occupational Hygiene, 49*, 575-585

Elechiguerra, J. L., Burt, J. L., Morones, J. R., Camacho-Bragado, A., Gao, X., Lara, H.

   H., & Yacaman, M. J. (2005). Interaction of Silver Nanoparticles with Hiv-I.

   Journal of Nanobiotechnology, 3(6), 1-10

Elimelech, M. (1995). Particle Deposition and Aggregation: Measurement, Modelling, and Simulation. 441

Fauss, E. (2008). Silver Nanotechnology Commercial Inventory Analysis *Woodrow Wilson International Center for Scholars Project on Emerging Nanotechnologies*. Washington DC.

Foldbjerg, R., Olesen, P., Hougaard, M., Dang, D. A., Hoffmann, H. J., & Autrup, H. (2009). Pvp-Coated Silver Nanoparticles and Silver Ions Induce Reactive Oxygen Species, Apoptosis and Necrosis in Thp-1 Monocytes. *Toxicology Letters, 190*(2), 156-162

Furno, F., Morley, K. S., Wong, B., Sharp, B. L., Arnold, P. L., Howdle, S. M., . . . Reid, H. J. (2004). Silver Nanoparticle and Polymeric Medical Devices: A New Approach to Preventing Infection? *Journal of Antimicrobial Chemotherapy, 54*, 1019-1024

Huynh, K. A., & Chen, K. L. (2011). Aggregation Kinetics of Citrate and Polyvinylpyrrolidone Coated Silver Nanoparticles in Monovalent and Divalent Electrolyte Solutions. *Environmental Science Technology, 45*(13), 5564-5571

Jain, P., & Pradeep, T. (2005). Potential of Silver Nanoparticle-Coated Polyurethane Foam as an Antibacterial Water Filter. *Biotechnology and Bioengineering, 90*(1), 59-63

Jaisi, D. P., & Elimelech, M. (2009). Single-Walled Carbon Nanotubes Exhibit Limited Transport in Soil Columns. *Environmental Science Technology, 43*(24), 9161-9166

Jiang, J., Oberdorster, G., & Biswas, P. (2009). Characterization of Size, Surface Charge, and Agglomeration State of Nanoparticle Dispersions for Toxicological Studies. *Journal of Nanoparticle Research, 11*(1), 77-89

Kallman, E. N., Oyanedel-Craver, V. A., & Smith, J. A. (2011). Ceramic Filters Impregnated with Silver Nanoparticles for Point-of-Use Water Treatment in Rural Guatemala. *Journal of Environmental Engineering-Asce, 137*(6), 407-415

Kanel, S. R., & Al-Abed, S. R. (2011). Influence of Ph on the Transport of Nanoscale Zinc Oxide in Saturated Porous Media. *Journal of Nanoparticle Research, 13*(9), 4035-4047

LePape, H., Solano-Serena, F., Contini, P., Devillers, C., Maftah, A., & Leprat, P. (2002). Evaluation of the Anti-Microbial Properties of an Activated Carbon Fibre Supporting Silver Using a Dynamic Method. *Carbon, 40*, 2947-2954

Li, Y., Wang, Y., Pennell, K. D., & Abriola, L. M. (2008). Investigation of the Transport and Deposition of Fullerene (C60) Nanoparticles in Quartz Sands under Varying Flow Conditions. *Environmental Science Technology, 42*(19), 7174-7180

MacCuspie, R. I., Rogers, K., Patra, M., Suo, Z., Allen, A. J., Martin, M. N., & Hackley, V. A. (2011). Challenges for Physical Characterization of Silver Nanoparticles under Pristine and Environmentally Relevant Conditions. *J. Environ. Monit., 13*, 1212-1226

Maneerung, T., Tokura, S., & Rujiravanit, R. (2007). Impregnation of Silver Nanoparticles into Bacterial Cellulose for Antimicrobial Wound Dressing. *Carbohydrate Polymers, 72*(1), 43-51

Oyanedel-Craver, V. A., & Smith, J. A. (2008). Sustainable Colloidal-Silver-Impregnated Ceramic Filter for Point-of-Use Water Treatment. *Environmental Science & Technology, 42*(3), 927-933

Oyanedel-Craver, V. A., & Smith, J. A. (2008). Sustainable Colloidal-Silver-Impregnated Ceramic Filter for Point-of-Use Water Treatment. *Environmental Science Technology, 42*(3), 927-933

Pelley, A. J., & Tufenkji, N. (2008). Effect of Particle Size and Natural Organic Matter on the Migration of Nano- and Microscale Latex Particles in Saturated Porous Media. *Journal of Colloid and Interface Science, 321*(1), 74-83

Petosa, A. R., Jaisi, D. P., Quevedo, I. R., Elimelech, M., & Tufenkji, N. (2010). Aggregation and Deposition of Engineered Nanomaterials in Aquatic Environments: Role of Physicochemical Interactions. *Environmental Science & Technology, 44*(17), 6532-6549

Powers, C. M., Slotkin, T. A., Seidler, F. J., Badireddy, A. R., & Padilla, S. (2011). Silver Nanoparticles Alter Zebrafish Development and Larval Behavior: Distinct Roles for Particle Size, Coating and Composition. *Neurotoxicology and Teratology, 33*(6), 708-714

Redman, J., & Walker, S. (2004). Bacterial Adhesion and Transport in Porous Media: Role of the Secondary Energy Minimum. *Environmental Science Technology*

Russell, A. D., & Russell, N. J. (1995). Biocides: Activity, Action and Resistance, Fifty Years of Antimicrobials: Past Perspectives and Future Trends. In P. A. Hunter, G. K. Darby & N. J. Russell (Eds.). Cambridge: Cambridge University Press.

Simunek, J., & van Genuchten, M. T. (2008). Modeling Nonequilibrium Flow and
Transport Processes Using Hydrus. *Vadose Zone Journal, 7*(2), 782-797

Thio, B. J. R., Montes, M., Mahmoud, M. A. E. m., Lee, D.-W., Zhou, D., & Keller, A.
A. (2011). Mobility of Capped Silver Nanoparticles under Environmentally
Relevant Conditions. *Environmental Science Technology*

Tian, Y., Gao, B., Silvera-Batista, C., & Ziegler, K. J. (2010). Transport of Engineered
Nanoparticles in Saturated Porous Media. *Journal of Nanoparticle Research,
12*(7), 2371-2380

Torkzaban, S., Bradford, S. A., van Genuchten, M. T., & Walker, S. L. (2008). Colloid
Transport in Unsaturated Porous Media: The Role of Water Content and Ionic
Strength on Particle Straining. *Journal of Contaminant Hydrology, 96*(1-4), 113-
127

Wang, P., & Keller, A. A. (2009). Natural and Engineered Nano and Colloidal Transport:
Role of Zeta Potential in Prediction of Particle Deposition. *Langmuir, 25*(12),
6856-6862

Wang, Y., Li, Y., Fortner, J. D., Hughes, J. B., Abriola, L. M., & Pennell, K. D. (2008).
Transport and Retention of Nanoscale C 60aggregates in Water-Saturated Porous
Media. *Environmental Science Technology, 42*(10), 3588-3594

Zeng, J., Zheng, Y., Rycenga, M., Tao, J., Li, Z.-Y., Zhang, Q., . . . Xia, Y. (2010).
Controlling the Shapes of Silver Nanocrystals with Different Capping Agents.
Journal Of The American Chemical Society, 132(25), 8552-8553

Zhang, H. Y., Smith, J. A., & Oyanedel-Craver, V. (2012). The Effect of Natural Water

    Conditions on the Anti-Bacterial Performance and Stability of Silver

    Nanoparticles Capped with Different Polymers. *Water research, 46*(3), 691-699

Zhuang, J., Qi, J., & Jin, Y. (2005). Retention and Transport of Amphiphilic Colloids

    under Unsaturated Flow Conditions: Effect of Particle Size and Surface Property.

    Environmental Science Technology, 39(20), 7853-7859

CHAPTER 4: TRANSPORT THROUGH POROUS CERAMIC MEDIA

4.1   Introduction

In a recent meta-analysis of water-quality interventions aimed at reducing diarrheal disease in the developing world, Clasen et al.(Thomas Clasen, Schmidt, Rabie, Roberts, & Cairncross, 2007) report that point-of-use (e.g. household-level) water-treatment interventions are more effective in improving water quality than interventions at the source. Household water treatment can be more cost-effective over time compared to centralized water treatment and distribution systems (T. Clasen, Nadakatti, & Menon, 2006).

One of the most promising point-of-use (POU) water-treatment technologies is ceramic water filters manufactured with local labor using clay, water, and a combustible organic material (such as sawdust, flour, or rice husks) (Lantagne, 2001; The Ceramics Manufacturing Working Group, 2011). The clay, combustible material, and water are combined in appropriate proportions and pressed into the shape of a pot and fired in a kiln. During firing, the clay hardens into a ceramic and the sawdust, flour, or rice husk combusts leaving internal porosity for water flow. The pot-shaped filter is placed in a larger, plastic container with a spigot, providing a safe-storage reservoir. An aqueous

colloidal suspension of silver nanoparticles (AgNPs) is typically applied to the filter after firing using a paint brush or submerging the filter in the aqueous AgNP suspension. Presumably, the AgNPs lodge in the pores of the ceramic media and provide disinfection action by the gradual release of ionic silver and reactive oxygen species into solution(Choi & Hu, 2008, 2009a, 2009b; Dankovich & Gray, 2011; Kallman, Oyanedel-Craver, & Smith, 2011; Lok et al., 2007; Morones et al., 2005; Oyanedel-Craver & Smith, 2008).

Two recent studies (Kallman et al., 2011; Oyanedel-Craver & Smith, 2008) have reported that these filters can effectively remove *E. coli* bacteria and turbidity from water along with virus- and protozoan-sized particles(Bielefeldt et al., 2010). It has also been shown in the laboratory that the zero-valent silver nanoparticles (10-100 nm diameter) embedded in the ceramic porous media improve the removal/disinfection of *E. coli* relative to filters without silver (Oyanedel-Craver & Smith, 2008). This POU technology appears to be socially acceptable (Kallman et al., 2011), and there is evidence that the filters can improve human health in the general population (Brown, Sobsey, & Loomis, 2008) and in individuals infected with the human immunodeficiency virus (HIV) (Abebe et al., 2013). Filter factories are gradually spreading throughout the developing world thanks to the efforts of several non-governmental agencies like Potters for Peace, FilterPure, Rural Development Partners International, and PureMadi. Based on a recent survey of global filter factories, Rayner (2009) reports there are 35 established filter factories in 18 countries and filter production at these factories exceeds 40,000 filters per month.

An important consideration in the design and use of ceramic filters is the application of the silver nanoparticles. Although the nanoparticles improve pathogen removal/disinfection in ceramic water filters (Oyanedel-Craver & Smith, 2008), the optimum dose and application method are unknown. Existing filter factories use different types of AgNPs and the mass of silver applied per filter varies at least by an order of magnitude between some factories. Little is known about the retention of the AgNPs in the ceramic filter.

In this work, we present the first study of the transport of silver nanoparticles through ceramic porous media, with a focus on investigating nanoparticle size, capping agent, solution ionic strength, and application method on the release of silver nanoparticles in the filter effluent. More importantly, we quantify silver release from filters fabricated using three different silver application methods: the conventional methods of painting onto the filter an aqueous AgNP suspension (paint-on method) or dipping the filter into a AgNP suspension (dipping method) (Oyanedel-Craver & Smith, 2008), and a new method of adding AgNPs to the clay-combustible mix prior to firing (fire-in method). We hypothesize that AgNPs are relatively mobile in ceramic media; AgNPs applied by conventional methods (e.g. paint-on and dipping) result in significant AgNP release into solution. Furthermore, we hypothesize that application of AgNPs prior to firing the clay-water-sawdust mixture will result in improved AgNP retention relative to conventional application methods.

The experimental results and analyses herein are the first measurements published of AgNP transport through a ceramic porous media and the first experiments to quantify the effects of solution ionic strength, nanoparticle size, and nanoparticle capping agent on

transport of the nanoparticles through ceramic media. It is also the first study to quantify the release of AgNPs into effluent water from ceramic media that has previously been impregnated with AgNPs using the fire-in method, and to compare these results to AgNP release from ceramic media fabricated using conventional methods (paint-on, and dipping). For these experiments, we have used a synthetic, moderately hard water that contains multiple monovalent and divalent inorganic ions to more closely simulate real-world conditions for ceramic filter performance.

4.2   Materials and methods

4.2.1   *Silver Nanoparticles.*

Four kinds of AgNPs were included in this investigation. Silver proteinate (7.66% silver by mass) was obtained from Argenol Laboratories (Spain) and was used as received. This nanoparticle is supplied as a solid powder and has proteinate as a capping agent. This nanoparticle is commonly used in developing-world ceramic water filters and in other commercial applications including as an antiseptic in eyedrops and as an antimicrobial agent in plastics, textiles, cosmetics, and paints (Ren & Smith, 2013). The proteinate capping agent is a bovine serum albumin composed of a single polypeptide chain of 583 amino acid residues (Elechiguerra et al., 2005; Theodore Peters, 1996). Three other types were obtained from NanoComposix (San Diego, USA) and belong to their Nano-Xact series. These particles were chosen to study the effects of nanoparticle size and capping agent on transport. They are shipped in 20 mg/L (as Ag) aqueous suspensions and were used as received; citrate is the capping agent for all three NanoComposix particles.

The mean particle diameter of each type of silver nanoparticle was measured using two methods. The first method employed dynamic light scattering (DLS) with a NiComp 380 DLS submicron particle sizer. DLS measurements were performed following 5-min sample sonication (Branson Ultrasonics Corp., set to 50% power) to insure the aqueous suspension was monodisperse. The second method employed a JEOL 2000FX transmission electron microscope (TEM). Zeta potential was quantified using a Malvern Zetasizer Nano Z. Capping agents used in nanoparticle synthesis were indicated by the manufacturers.

4.2.2 *Ceramic Porous Media*

Ceramic porous media were fabricated in the shape of disks as described by Oyanedel-Craver and Smith (2008). Briefly, 97.6 g of 200-mesh Redart pottery clay (Resco Products, Inc) was mixed homogeneously with 122 g of 48-mesh grog (Resco Products, Inc) and 24.4 g flour (from a local grocery store and used as received). The dry mix (244 g) was combined with 75 mL of deionized, organic-free water (DI water) and again mixed by hand until homogenous. The wet mixture was then divided into 4 equal portions with masses between 79-80 g. Each portion was transferred into a cylindrical plastic mold. A hand-operated press was used to compress the mixture in the mold for 1 min at 1000 psi. The pressed mixture was then removed from the mold and air dried for two days before it was fired in a Rampmaster II electric kiln (Evenheat Kiln, Inc.). The kiln temperature was increased from room temperature to 600 °C at a rate of 150 °C/h, and then to 900 °C at a rate of 300 °C/h. The final temperature (900 °C) was held for another 3 h. The resulting cylindrical ceramic disks produced were 1.2 cm thick and 7.5 cm in diameter with a mass of 56±1 g.

The above-described ceramic disk fabrication method is identical to the method described previously for Redart clay by Oyanedel-Craver and Smith and the pore-size distribution as determined by mercury porosimetry has been previously quantified (Oyanedel-Craver & Smith, 2008). The zeta potential of the ceramic porous media was determined by grinding the ceramic porous media into a powder with a mortar and pestle (Bradford & Kim, 2010) and suspending the particles in aqueous $MgSO_4$ solutions of 1, 10, and 50 mM ionic strength. Each suspension was added to a folded capillary cell (DTS 1060, Malvern Instruments, Worcestershire, UK). Time-resolved hydrodynamic diameter and zeta potential charge were monitored over 12 hr at room temperature (24 ± 1 ˚C) (Ren & Smith, 2013).

Additional ceramic disks were fabricated using the above described procedure but were also treated with AgNPs. Three different methods of AgNP application were studied: the "dipping" method, the "paint-on" method, and the "fire-in" method. The AgNPs used for these treatments were the proteinate-capped AgNPs from Argenol Laboratories and the application amount resulted in either 2.76 mg or 27.6 mg of Ag per disk. The 2.76-mg Ag mass was chosen to approximately correspond to Ag application amounts recommended by Potters for Peace in the production of silver-impregnated ceramic filters. The 27.6 mg mass was chosen to represent the much-higher silver loading being used by some other filter manufacturers.

For the dipping method, each ceramic disk was submerged in a 2000-mg/L silver proteinate suspension (153 mg/L as Ag) for 5 min, air dried for 24 hr, and oven-dried to a constant weight at 80 ºC (approximately 48 hr). The mass of each ceramic disk before and after treatment was recorded. The difference between the two masses equaled the

total weight of silver applied. Multiple disks were treated and measured in the same way. The average mass change was 35.98 mg ± 0.26 mg (n=12, $\alpha = 0.05$), or a mean value of 2.76 mg of Ag per disk.

Based on the dipping method results, an identical mass of silver was chosen for application using the paint-on method. For the paint-on method, a commercial paint brush was used to paint 18 mL of a 2000-mg/L aqueous suspension of silver proteinate (153 mg/L as Ag). 9 mL of this suspension were painted onto each side of the ceramic disk, resulting in a final mass 2.76 mg of Ag per disk.

For the fire-in method, either 143.6 mg of silver proteinate (11.04 mg as Ag) or 1.436 g of silver proteinate (110.4 mg as silver) was added to 75 mL water and sonicated. This aqueous suspension was then combined with clay, grog, and flour as described previously to construct the ceramic disks. In this manner, the silver is added *before* firing the disks, presumably providing a more homogeneous distribution of nanoparticles throughout the porous media while minimizing release of the AgNPs into drinking water during subsequent use of the filter. Each resulting ceramic disk fabricated using the fire-in method contained either 2.76 or 27.6 mg of Ag.

4.2.3 AgNP Transport Experiments

The transport of each type of AgNP was studied using ceramic disks fabricated without any silver addition. Each ceramic disk was placed in a flexible-wall permeameter and a high-performance liquid chromatography (HPLC) pump (Acuflow series IV) was used to inject a $MgSO_4$ solution at a flow rate of 0.6 mL/min through the ceramic disk. This flow rate approximately corresponds to whole-filter flow rates of 2 L/hr (Oyanedel-Craver & Smith, 2008). After 20 pore volumes of flow, the linear

velocity and dispersion coefficient of the porous media was determined with a tracer test using a pulse injection of $[^3H]$-H_2O with subsequent analysis of the tracer breakthrough data using the one-dimensional form of the transient advection-dispersion equation. Additional details are provided in the Supporting Information section. Due to the unique characteristics of fabricated disks, the disk experiments were not performed in duplicates.

Following the tracer test, the influent solution was changed by the addition of a 10 mg/L AgNP suspension for 100 min (approximately 5.8 pore volumes). The inflow solution was then changed back to the original, nanoparticle-free $MgSO_4$ solution until the end of the experiment. Ceramic disk effluent samples were collected over time and analyzed for total silver. The $MgSO_4$ concentration in solutions used in these experiments correspond to ionic strengths of 1, 10, and 50 mM. These values were chosen to represent the ionic strengths of a wide range of natural fresh waters ranging from surface to ground waters. These same ionic-strength levels were used to quantify the zeta potential of the ceramic media as described earlier.

Total Ag concentrations were determined by atomic absorption spectrometry (Perkin Elmer AAnalyst 200) following 10% HNO_3 conditioning. A subset of effluent samples were analyzed for ionic silver (Ag^+) concentrations using a calibrated silver specific-ion electrode (silver/sulfide ion selective electrode, Thermo Scientific, MA, USA). In every case, the Ag^+ concentration was less than 1% of the total silver concentration, suggesting that silver ion release was relatively small over the course of each experiment. This observation is consistent with results reported by Zhang et al. (2012) for aqueous suspensions of AgNPs. Therefore, it was assumed that total silver

concentrations closely estimate the metallic silver (Ag^0) concentrations in effluent samples.

The methods used for mathematical simulation of AgNP effluent concentrations are provided in the Supporting Information section along with a summary of conditions for each experiment and the resulting parameter values (Table 4-S1).

4.2.4   *Silver release from silver-impregnated ceramic disks*

While the above-described AgNP transport experiments provide fundamental information about particle transport, they do not represent the retention and release of silver applied to a ceramic water filter. Therefore, experiments were performed to more closely simulate the performance of ceramic water filters under real-world conditions using the three types of silver-impregnation methods described earlier in this section (paint-on, dipping, and fire-in). In addition, the water chemistry for the solution passed through the filter was chosen to reflect more closely a natural water with multiple monovalent and divalent inorganic ions. Previous research has shown that both the concentration and valence of inorganic ions in solution can affect nanoparticle stability (Chen, Mylon, & Elimelech, 2006; Thio, Lee, Meredith, & Keller, 2010). The solution ionic strength and flow rate were also varied to study the effects of these variables on silver release.

The release of silver over time from disks treated using the paint-on, dipping, and fire-in methods was quantified using methods similar to those described above. Each silver-impregnated ceramic disk was placed in a flexible-wall permeameter. A synthetic, moderately hard water (96 mg/L $NaHCO_3$, 60 mg/L $CaSO_4 \cdot 2H_2O$, 60 mg/L $MgSO_4$, and 4 mg/L KCl) developed by the U.S. Environmental Protection Agency (and denoted as

"EPA water") (U.S. Environmental Protection Agency) was pumped through the disk at a

0.6 mL/min flow rate for 3 hr. The flow rate was then increased to 1.2 mL/min for the

next 3 hr. Effluent samples were collected over time and analyzed for total and ionic

silver concentrations. As noted previously, ionic silver concentrations were consistently

less than one percent of total silver concentrations, indicating that the silver leaving the

ceramic media was in the zero-valent oxidation state. To test the impact of ionic strength

on silver release from the ceramic filters, additional experiments were also performed

wherein DI water was passed through the filter for the first 3 hr and then switched to the

synthetic, moderately hard EPA water for the next 3 hr. A first-order rate model was

used to simulate effluent silver concentrations over time. The model is described in the

Supporting Information section and Table 4-S2.

4.3 Results

4.3.1 *Nanoparticle Characterization*

Table 4-1 summarizes the characteristics of each type of nanoparticle used in this

investigation. The NanoXact particles are marketed as having mean particle diameters of

10, 50, and 100 nm and the measurements made in our laboratory agree well with these

specifications. Mean particle diameters measured by DLS are slightly larger than the

values measured using TEM. This is a typical result of these measurements, as DLS

measurements include water molecules that strongly hydrate the nanoparticles and the

citrate capping agent (MacCuspie et al., 2011). The DLS measurement for silver

proteinate (49.0 nm) is more than three times larger than the TEM measurement (15.8

nm). This is likely caused by a macromolecular proteinate capping agent.   Silver

proteinate diameters measured over time by DLS reveal that the mean diameter decreases

over the course of several hours, presumably as the capping agent is gradually released into solution (Ren & Smith, 2013). Zeta potential values were similar for all the nanoparticles and show a negative particle surface charge.

Table 4-1. Summary data for silver nanoparticles used in this investigation. Data include mean particle diameter as determined by dynamic light scattering (DLS) and transmission electron microscopy (TEM), zeta potential (ζ), and the capping agent used during synthesis.

Name	DLS (nm)	TEM (nm)	ζ *(mv)	Capping Agent
Silver proteinate	49.0	15.8	-57.1	Proteinate
NanoXact-10	13.4	8.2	-56.1	Citrate
NanoXact-50	59.2	49.1	-55.6	Citrate
NanoXact-100	115.1	99.1	-55.4	Citrate

* ζ determined in deionized, organic-free water.

4.3.2   AgNP Transport Experiments

Figures 4-1, 4-S1, 4-2, and 4-3 show effluent concentrations of silver nanoparticles from ceramic disks normalized to the influent AgNP concentration as a function of pore volumes of flow.   Figure 4-1, 4-1S, and 4-3 also have inset bar charts that show the percent of the inflow silver that is retained in the ceramic disk over the course of the experiment. These values were calculated by mass balance from the influent and effluent AgNP concentration data.

Figure 4-1 shows breakthrough curves for 50-nm NanoXact AgNPs for three different ionic strengths (1 mM, 10 mM, and 50 mM). As the ionic strength is increased, the effluent AgNP normalized concentrations plateau at decreasing values. Likewise, the percent silver retained in the ceramic disk increases with increasing ionic strength. Although the relative concentrations are only shown for the 50-nm AgNP, this trend is true for each type of nanoparticle as noted in the inset bar chart.

Figure 4-S1 compares the transport of Argenol silver proteinate and NanoXact-50 nanoparticles through the ceramic disks. Both show similar effluent concentration profiles. Since these particles have similar total particle sizes (including the capping agent and as measured by DLS), the results suggest that changing the capping agent from proteinate to citrate has at best only a small effect on AgNP transport. For each ionic strength, there is a slightly greater retention of the citrate-capped particles (inset in Figure 4-S1).
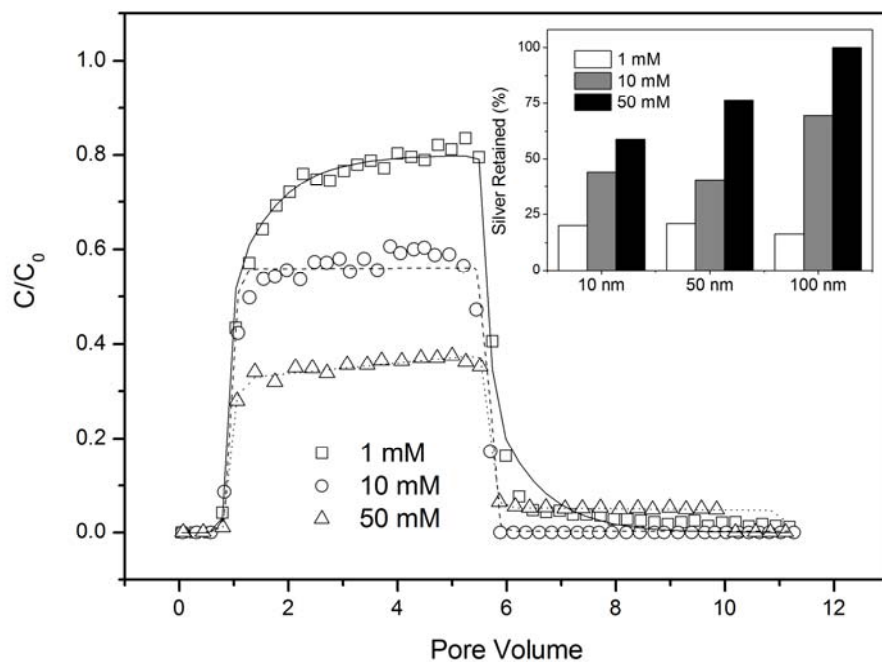
Figure 4-1. Plots of effluent total silver concentration from ceramic disks (C) normalized to the influent total silver concentration (C0) as a function of pore volumes of flow for different ionic strength MgSO4 solutions (1 mM, 10 mM, and 50 mM). Data are for NanoXact 50-nm silver nanoparticles at a flow rate of 0.6 mL/min. Inset: Percent silver retained in the ceramic disk at each ionic strength and for all three mean nanoparticle sizes (10 nm, 50 nm, and 100 nm).

Figure 4-2 presents AgNP transport data for NanoXact-50 at flow rates of 0.2, 0.6, and 3 mL/min. By normalizing the data to pore volumes of flow, the experiments can be directly compared despite the flow rate differences. The data show that there is greater elution of AgNPs from the column as the flow rate is increased.

Figure 4-3 compares AgNP data for the three NanoXact particles. For 10 mM and 50 mM ionic strengths, the nanoparticle retention in the ceramic porous media increases with AgNP size. For 1 mM ionic strength, the AgNP retention does not appear to be affected by particle size.
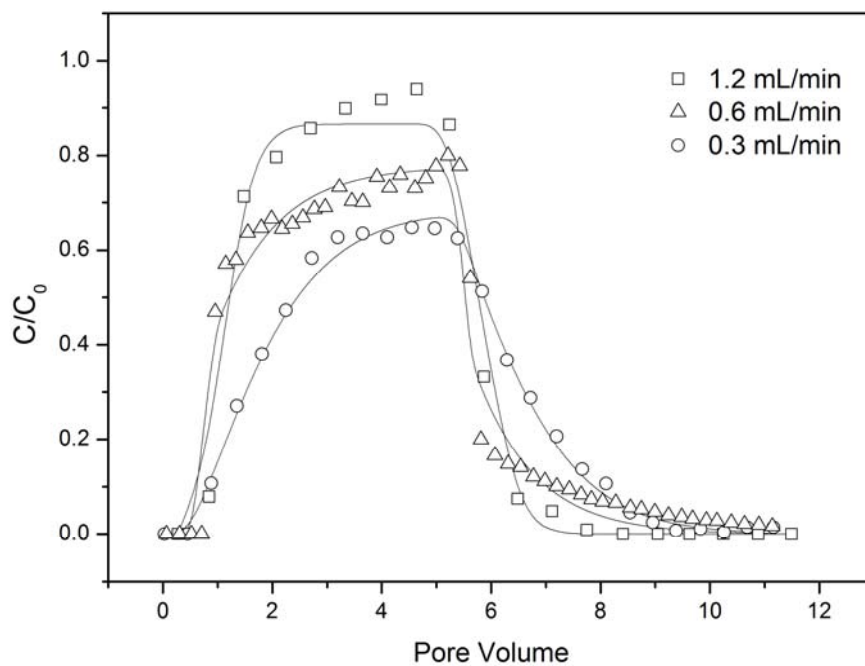
Figure 4-2. Plots of effluent total silver concentration from ceramic disks (C) normalized to the influent total silver concentration (C0) as a function of pore volumes of flow for three different flow rates at a MgSO4 solution ionic strength of 1 mM.
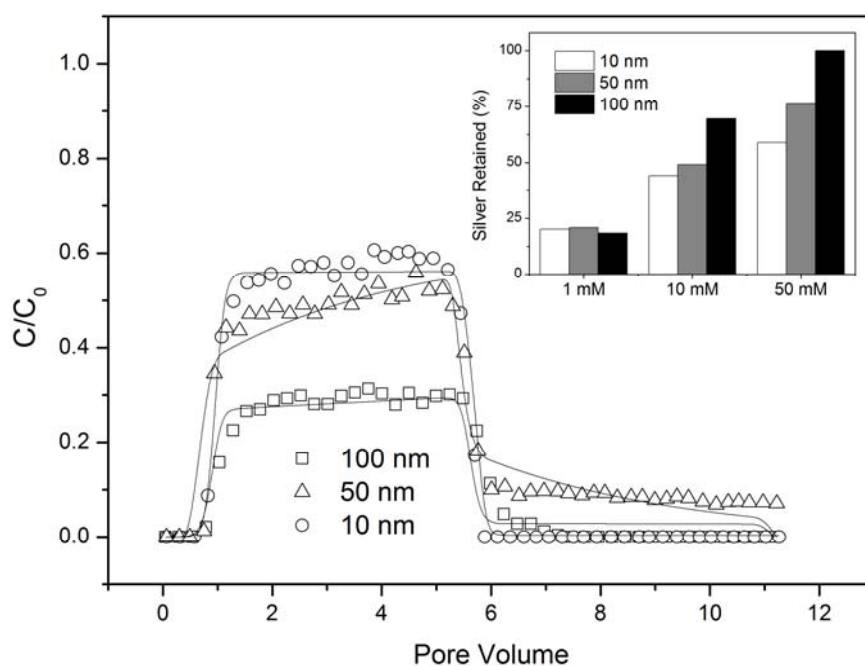
Figure 4-3. Plots of effluent total silver concentration from ceramic disks (*C*) normalized to the influent total silver concentration (*C₀*) as a function of pore volumes of flow for different-sized NanoXact silver nanoparticles. Data are for a flow rate of 0.6 mL/min and a MgSO₄ solution ionic strength of 10 mM. Inset: Percent silver retained in the ceramic disk at each ionic strength and for all three mean nanoparticle sizes.

4.3.3   AgNP Release Experiments

Figures 4-4, 4-5, and 4-6 show results of experiments where AgNPs were applied to filters using the paint-on, dipping, and fire-in methods. For these cases, no AgNPs were present in the inflow water to the ceramic disks, but since AgNPs were embedded into the disk by one of the three application methods, the nanoparticles are released into the effluent water over time. Inflow solutions for these experiments used the synthetic EPA water containing both monovalent and divalent inorganic ions to better represent real-world conditions. Figure 4-4 shows total silver release from ceramic disks that were treated with silver by the conventional paint-on and dipping methods. For each type of disk, the flow rate was maintained at 0.6 mL/min for 180 minutes and then increased to 1.2 mL/min for an additional 180 minutes. Increasing the flow rate at 180 min causes a step increase in effluent silver. During the first 180-min period, total silver released from both types of disks is between 1.1 and 1.3 percent of the silver originally applied to the disk. The paint-on method appears to retain slightly more silver in the disk than the dipping method.
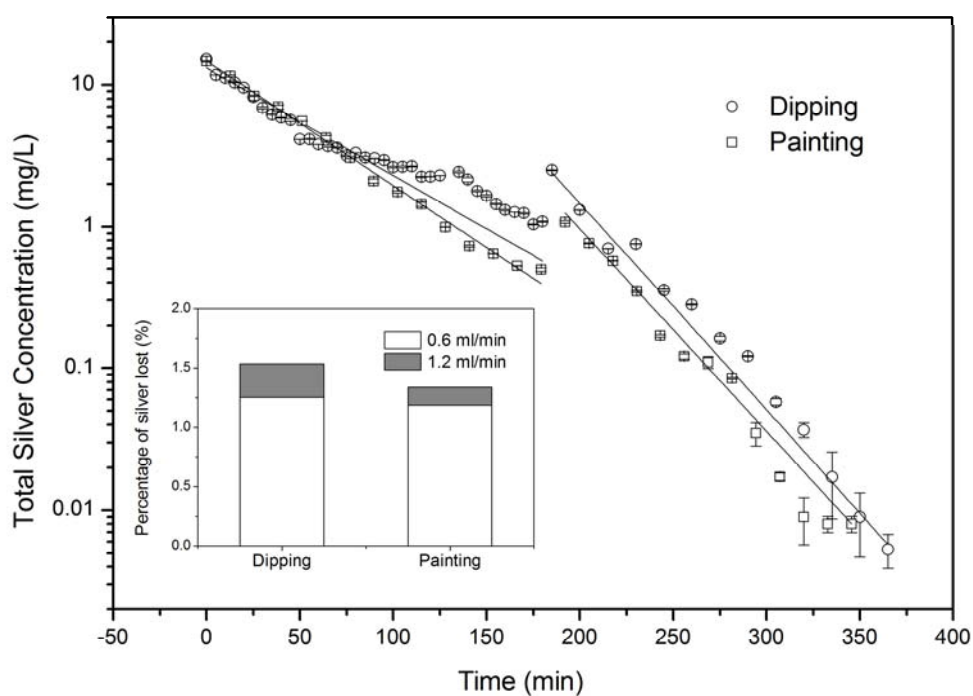
Figure 4-4. Plots of effluent total silver concentration from disks pre-treated with Argenol silver nanoparticles by either painting or dipping methods. The flow rate was 0.6 mL/min from time zero to 180 min. The flow rate increased to 1.2 mL/min from 180 min to the end of the experiment. The inflow solution was a moderately hard synthetic water containing both monovalent and divalent inorganic ions. Inset: Percent of silver released from the disk for each flow rate and for each silver application method.
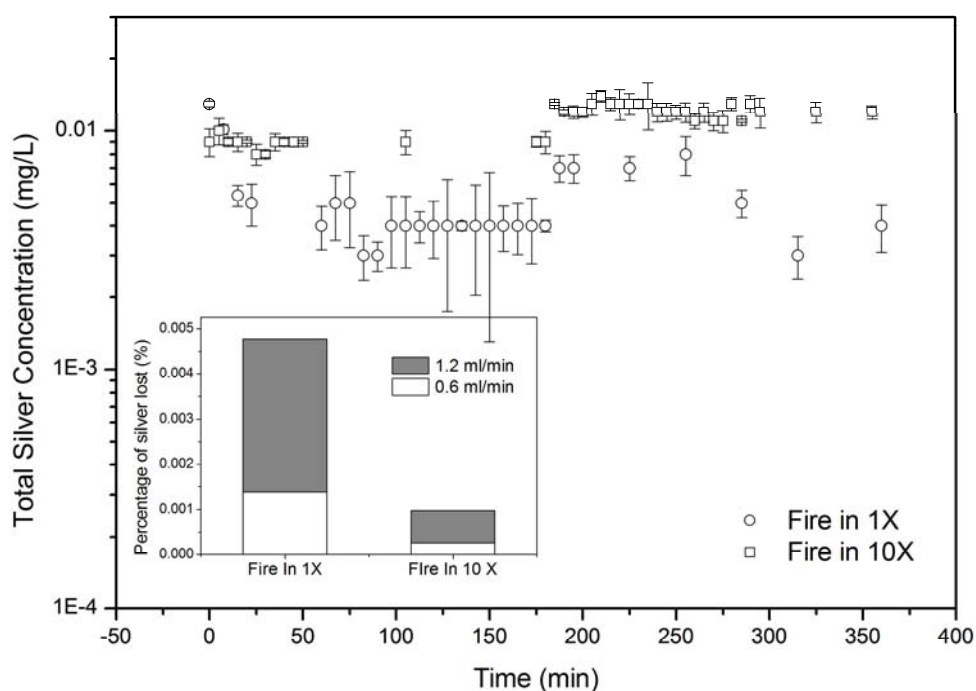
Figure 4-5. Plots of effluent total silver concentration as a function of time for disks fabricated by adding Argenol silver nanoparticles prior to firing the disk. Two different amounts of silver (varying by a factor of 10) were fired into the disks. The flow rate was 0.6 mL/min from time zero to 180 min. The flow rate increased to 1.2 mL/min from 180 min to the end of the experiment. Inset: Percent of silver released from the disk for each flow rate and for each silver application amount.

Figure 4-5 presents data similar to Figure 4-4 for disks manufactured using the fire-in method. Data for two different amounts of silver applied to the disks are included. The "1X" disk contains the same mass of silver as the disks prepared using the paint-on and dipping methods (2.76 mg of Ag per disk). The "10X" disks contain 27.6 mg of Ag per disk. As before, the flow rate through the disks was increased from 0.6 mg/L to 1.2 mg/L after 180 min. Silver concentrations released from the 10X disk are higher than the concentrations released by the 1X disks, but when considered as a percentage of the silver applied to the disks, the 10X release a smaller percentage than the 1X disks.

Doubling the flow rate at 180 min again caused a step increase in effluent silver

concentrations followed by a return to an approximately linear decline with time.

Overall, silver concentrations and percent of total silver released are significantly less

than values observed for disks prepared with the paint-on and dipping methods.
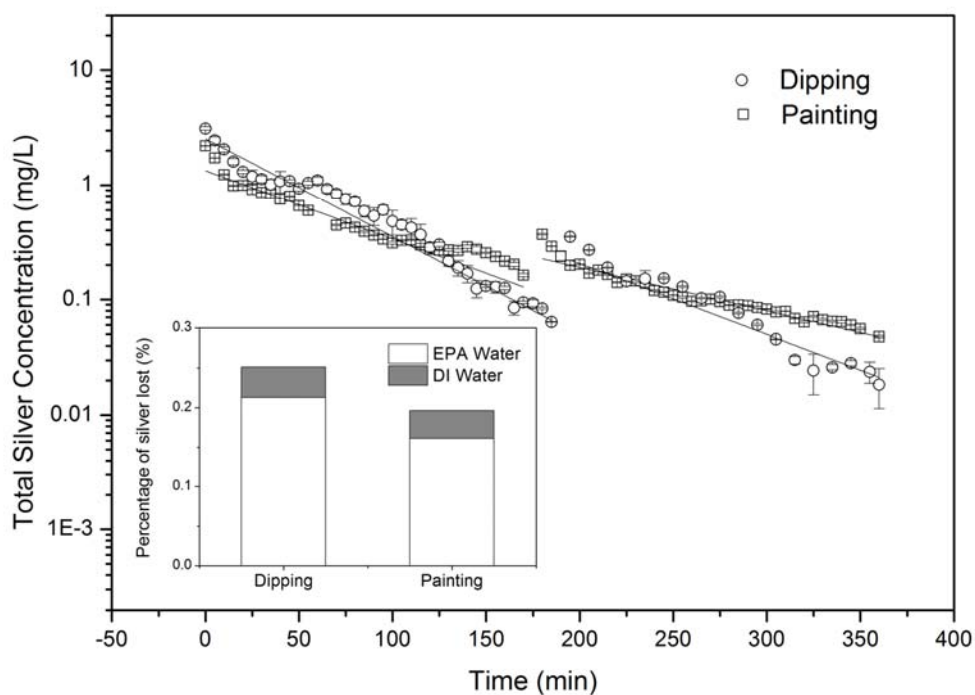
Figure 4-6. Plots of effluent total silver concentration from disks pre-treated with Argenol silver nanoparticles by either painting or dipping methods. The flow rate remained constant at 0.6 mL/min for the duration of the experiment, but the ionic strength of the influent solution was changed from 10 mM (moderately hard synthetic water containing both monovalent and divalent inorganic ions) from time 0 to 180 min to 0 mM ionic strength from time 180 min until the end of the experiment. Inset: Percent of silver released from the disk for each silver application method and for each ionic strength.

Figure 4-6 shows how a change in solution ionic strength will affect silver release for ceramic disks prepared using the paint-on and dipping methods. The synthetic EPA water is used as inflow for the first 180 min. For the subsequent 180 min, DI water is used as influent. The flow rate was maintained at 0.6 mL/min for the duration of this experiment. At 180 min, there is a step increase in effluent silver for both paint-on and dipping disks. Silver concentrations then decrease approximately linearly over time at a slope that is equal to or slightly greater than the slope from the first 180-min period.

4.4   Discussion

4.4.1   *AgNP Transport through Ceramic Porous Media.*

AgNPs are relatively mobile through the ceramic porous media under certain conditions. The extent of mobility depends on both the nanoparticle properties and the water chemistry. Table 4-S1 and the bar charts that are inset in Figures 4-1 and 4-3 show that the percent of silver applied that exits the ceramic disks can be as high as 87%. This is significant given that ceramic water filters are generally believed to retain silver nanoparticles and remove turbidity from inflow water. AgNP mobility is closely related to solution ionic strength, and to a lesser extent, nanoparticle size.

Throughout all the experiments in this study, increased ionic strength correlates to decreases in AgNP mobility (Figures 4-1 and 4-6). This behavior is likely caused by two mechanisms. First, increasing ionic strength can compress the diffuse double layer surrounding the AgNPs. This causes increased particle-particle interaction resulting in aggregation and increased physical filtration (straining) of the nanoparticle clusters (Elimelech, 1995; Jaisi & Elimelech, 2009; Tian, Gao, Silvera-Batista, & Ziegler, 2010; Zhang & Oyanedel-Craver, 2012; H. Y. Zhang et al., 2012). Second, the reduction in the

diffuse double layer surrounding the AgNPs likely reduces the repulsive forces between the nanoparticle and the surface of the ceramic porous media (Elimelech, 1995; Tian et al., 2010). For deposition of AgNPs onto the ceramic surface to occur, the primary energy barrier (according to DLVO theory) must be overcome. For negatively charged particle deposition onto a like-charged surface, the primary energy barrier is reduced with increasing ionic strength. Therefore, the increased retention of the AgNPs with increasing ionic strength may be caused by increased attraction between the nanoparticle and the ceramic porous media surface.

Table 4-2. Peak interaction energies between four types of silver nanoparticles and the ceramic porous medium at three ionic strengths.

Interaction Energy ($k_B T$)	Ionic Strength (mM)		
	1	10	50
Silver proteinate	26.53	6.82	0.75
NanoXact-10	4.38	0.98	0.12
NanoXact-50	24.60	6.32	0.70
NanoXact-100	51.56	13.25	1.47

Based on the zeta potential measurements (Table 4-1) for each type of AgNP used in this investigation and the zeta potential measured for the ceramic media at ionic strengths of 1, 10, and 50 mM, interaction energies between the AgNPs and the ceramic collector surfaces can be quantified using the Derjaguin–Landau–Verwey–Overbeek (DLVO) theory. Details of the calculation method along with plots of interaction energies as a function of separation distance for each nanoparticle and ionic strength are presented in the Supporting Information section (Figures 4-S2 to 4-S5). Peak interaction energies for each ionic strength and AgNP combination are shown in Table 4-2. As expected, interaction energies are significantly reduced as solution ionic strength is

increased. These analyses further support the observed reduced transport of AgNPs through the ceramic porous media with increase ionic strength shown in Figures 4-1 and 4-6. Although this is the first study to present results of AgNP transport through a ceramic porous medium, Ren and Smith (2013) have recently shown that AgNP transport through water-saturated sand porous media also decreases with increasing ionic strength. Although they reported some particle aggregation, they identified increased deposition of nanoparticles on the sand surfaces as the main reason for this behavior. Likewise, several other recent publications have shown that ferrihydrite and fullerene nanoparticle stability and transport is reduced in sand and soil porous media as ionic strength is increased (Tosco, Bosch, Meckenstock, & Sethi, 2012; L. L. Zhang et al., 2012).

These observations have a practical implication. Ceramic filters impregnated with AgNPs may release more silver if the source water is a surface water instead of a ground water. Ground waters typically have higher ionic strengths than surface waters. For a given amount of applied silver, the silver's longevity in the filter may therefore be less for surface water compared to ground water. Additionally, release of silver into the filter effluent and consumption by the user will likely be greater for surface water than ground water.

AgNP size appears to have some effect on transport, but to a less extent than ionic strength. The inset bar chart in Figure 4-3 compares nanoparticle retention in the ceramic porous media for the 10-, 50-, and 100-nm AgNPs for each ionic strength. For 1 and 10 mM ionic strengths, there does not appear to be any discernible effect of particle size on AgNP retention in the porous media. However, for 50 mM ionic strength, AgNP retention increases with particle size.

The effect of particle size on AgNP transport may be influenced by multiple factors (Wang et al., 2012). Consideration of physical filtration alone would suggest that larger particles will be less mobile than smaller particles. Consideration of our DLVO theory energy barriers show that small particles will be retained more than large particles because the peak interaction energy decreases with decreasing particle size (Table 4-2). Zeta potential may also vary with particle size, although for our AgNPs, there was negligible change in zeta potential from our 10-100-nm particles (Table 4-1). A recent study by Wang et al. (2012) studied the effects of silica nanoparticle size on retention in sand porous media. They found that the relative retention of 8-nm particles was slightly greater than for 52-nm particles. They attributed this result to larger deposition rate coefficient (k_d) values for the 8-nm particles relative to the 52-nm particles. For the largest AgNP studied (100 nm), physical filtration may have been significantly more important than particle-collector interaction, and a positive correlation between particle size and particle retention was observed.

4.4.2 AgNP Release from Silver-Impregnated Ceramic Porous Media

Perhaps the most important result of this work pertains to the release of silver nanoparticles that have been previously applied to the ceramic porous media by the paint-on, dipping, or fire-in methods. Figures 4-4 and 4-5 show that while there may not be much difference between the paint-on and dipping methods of silver application, the fire-in method appears to significantly improve nanoparticle retention in the ceramic porous media. In the first 180 minutes of use, ceramic disks treated with silver using the paint-on and dipping methods release slightly more than 1% of the original amount of silver applied and effluent concentrations range between 1 and 10 mg/L. These values are more

than ten times greater than the drinking-water standard for silver of 0.1 mg/L. By contrast, slightly greater than 0.001% of silver was released from ceramic disks with silver fired-in over the first 180 minutes, approximately 1000 times less than the paint-on and dipping methods. Furthermore, the effluent silver concentrations never exceed 0.02 mg/L, which is about one fifth the drinking water standard for silver. Even when the amount of silver applied to the disk is increased by a factor of 10 (e.g. fire-in 10X, Figure 4-5), the effluent concentration never exceeds 0.02 mg/L. These results suggest that for silver retention in the filter, the fire-in method will produce a significant improvement in performance. During the firing process, the AgNPs presumably concentrate in the smallest-diameter pores (as water likely evaporates from the largest pores first) or they may simply exist in pores disconnected with the flow field. Flow field is less likely to be affected because the addition of silver is insignificant amount compared to the base material. Concentration of the silver in the smallest pores likely minimizes their mobilization in the pore water. For the conditions of our work, the maximum firing temperature (900 ˚C) does not exceed the melting point of silver (961 ˚C). The sublimation of silver during the firing is assumed to be minimal.

We should note that although the results in Figure 4-4 show silver levels greater than the drinking water standard for silver, concentrations are declining exponentially with time. Therefore, silver levels in the effluent water likely will fall below drinking water standards within a few hours of use. This result is consistent will silver levels reported by Oyanedel-Craver and Smith (2008) in laboratory studies and by field data in Guatemala reported by Kallman et al. (2011). Nevertheless, the higher rate of silver

release likely renders the filter less effective over time compared to filters fabricated with the fire-in method.

The paint-on method appears to retain slightly more silver than the dipping method (Figure 4-4). This may be caused by capillarity effects. For the dipping method, the aqueous AgNP suspension applied to the ceramic porous media is always at a pressure greater than atmospheric and water and nanoparticles will fill both large and small pores. By contrast, for the paint-on method, the aqueous AgNP suspension is drawn into the ceramic disk by capillary action, with the smallest pores filling first. Therefore, AgNPs are preferentially deposited in the smaller pores relative to larger pores. This likely results in a small increase in retention of the AgNPs because it is more difficult to dislodge AgNPs from small pore spaces relative to larger pore spaces.

Changes in flow rate and solution ionic strength also appear to influence silver release (Figures 4-4, 4-5, and 4-6). Increasing the interstitial water velocity likely dislodges AgNPs that were otherwise immobilized in the ceramic porous media. This result has also been observed for the transport of ferrihydrite nanoparticles in a quartz sand porous medium (Tosco et al., 2012). Likewise, reduction in solution ionic strength reduces particle-particle and particle-surface attractive forces and likely increases AgNP mobility. The results shown in Figures 4-6, the inflow solution was a moderately hard synthetic water containing both monovalent and divalent inorganic ions. It should be noted that natural waters also typically contain mg/L levels of dissolved organic matter (DOM). Prior research has indicated that DOM can increase stability of titanium dioxide nanoparticles with respect to silica surfaces by steric repulsion and repulsive electrostatics even under relatively high ionic strength conditions (Thio, Zhou, & Keller,

2011). Therefore, it is possible that silver nanoparticle mobility could be increased in the presence of DOM.

For the 1X and 10X fire-in methods, we can make very rough estimates of the time until the silver in the filter is depleted. For a flow rate of 0.6 mL/min, the effluent silver concentration maintains a relatively steady value of 0.004 mg/L for the 1X fire-in method (Figure 4-5). These ceramic disks contain 2.76 mg of Ag. Therefore, over a 1-hr flow period, the mass fraction of silver removed from the disk is 5.174×10^{-5}, and it would take about 19,300 hours of flow to deplete all the silver assuming a constant silver release rate and that all the silver can be released from the ceramic porous medium. The 0.6 mL/min flow rate of the ceramic disk corresponds approximately to a 1.5 L/hr flow rate for a whole-pot filter (Oyanedel-Craver & Smith, 2008). If we assume water is being filtered for 24 hours per day, the silver will be depleted in 805 days, or 2.2 years. A similar calculation for the 10X fire-in method (with a relatively constant effluent silver concentration of 0.009 mg/L and a silver mass in the disk of 27.6 mg) results in a predicted silver depletion time of 3,550 days or 9.7 years. Of course in   practice, it is unlikely that water will be filtered 24-hours per day at a 1.5 L/hr flow rate (Schweitzer, Cunningham, & Mihelcic, 2013). It is more difficult to predict the depletion of silver for the paint-on and dipping methods, as the effluent silver concentration generally decreases with time. However, over the course of these experiments, the paint-on and dipping methods release about 1000 times more silver than the fire-in method.

Although the fire-in method appears to be an improved way of applying AgNPs to ceramic water filters due to its increased retention of the silver and the continuous monitoring of silver ions shows the concentration of silver ions, as one effective

disinfectant, was always below the detection limit (0.1 mg/L), no disinfection data has yet

been presented to show that this method results in equal or better disinfection of

pathogens entering the filter. The fire-in method likely results in a more homogeneous

distribution of the silver throughout the porous media (which should improve pathogen

disinfection), it is also possible that some of the silver resides in pores that are

disconnected from continuous flow paths and do not contribute to disinfection. For

fabrication of whole-pot filters, the conventional dipping and paint-on methods are

performed only for filters that have been fired and tested for adequate flow rates. For the

fire-in method, silver is applied prior to firing during the clay-sawdust-water mixing

process. Therefore, the silver applied to filters that break during firing or that do not pass

flow-test requirements is essentially wasted. Successful filter factories typically have

90% or more of their filters pass flow-rate quality assurance tests, so the fire-in method

would increase silver material costs by about 10% relative to the paint-on or dipping

methods. On the other hand, the fire-in method is less labor intensive than the paint-on or

dipping methods and would thereby reduce production costs.

4.5   Supplemental information

4.5.1   *Simulation of tracer and silver nanoparticle transport*

The hydraulic conductivity (K) and coefficient of hydrodynamic dispersion (D)

for each ceramic disk was determined by studying the transport of a conservative tracer

through the porous media. Tracer experiments were conducted by using a pulse injection

of tritiated water ($[^3H]$-H_2O), into the ceramic disk and sequential sampling of the

effluent. The concentrations of the conservative tracer in effluent samples were

quantified with a Packard 1900CA Liquid Scintillation Analyzer.

Effluent tracer and silver concentrations were simulated for parameter identification using the following one-dimensional form of the advection-dispersion-reaction equation as described previously (Bradford, Simunek, Bettahar, Van Genuchten, & Yates, 2003; Schijven, Hassanizadeh, & de Bruin, 2002; Schijven & Simunek, 2002) with the commercial software model Hydrus-1D:

$$\frac{dC}{dt} + \frac{\rho_b}{\theta_w}\left(\frac{dS_1}{dt} + \frac{dS_2}{dt}\right) = D\frac{\partial^2 C}{\partial x^2} - v\frac{dC}{dx} \qquad (4\text{-}1)$$

$$\frac{\rho_b}{\theta_w}\frac{dS_1}{dt} = k_{att1}C - k_{det}\rho_b S_1 \qquad (4\text{-}2)$$

$$\frac{\rho_b}{\theta_w}\frac{dS_2}{dt} = k_{att2}C \qquad (4\text{-}3)$$

where C is the tracer or AgNP concentration (ML^{-3}), ρ_b is the ceramic media bulk density (ML^{-3}), θ_w is the dimensionless volumetric water content, t is time (T), v is the linear water velocity (LT^{-1}), S_1 and S_2 are the concentrations of the AgNPs associated with the ceramic (solid) phase (MM^{-1}) for kinetic sites 1 and 2, respectively, D is the coefficient of hydrodynamic dispersion (L^{2}T^{-1}), x is longitudinal distance (L), k_{att1} and K_{att2} are the AgNP attachment coefficients for kinetic sites 1 and 2, respectively, and k_{det} is the AgNP detachment coefficient.

Equation (4-1) with S=0 was used to simulate the tracer transport using D and v as fitting parameters. Then, AgNP transport was simulated with equations (4-1 to 4-3) using k_{att1}, k_{att2}, and k_{det} as fitting parameters along with the previously determined values of D and v. This model assumes that transfer of AgNPs from water to the ceramic matrix is kinetic and can be approximated by two first-order attachment rate coefficients and one

detachment rate coefficient. The values of these parameters for all experiments that had

AgNPs in the inflow solution are summarized in Table 4-S1. In general, the model was

able to reasonably simulate the observed effluent silver concentrations as shown in

Figures 4-1, Figure 4-2, Figure 4-3 and Figure 4-S1.

For experiments wherein the Ag was incorporated into the ceramic disks during

fabrication, the inflow solution did not contain any AgNPs and the release of Ag^0 from

the disks into solution was monitored over time. These data were fit to the following

simple first-order model:

$$C = C_0 e^{-kt} \tag{4-4}$$

Table 4-S1. Summary of experimental conditions, percentage of influent silver retained, and simulation parameters for silver-nanoparticle transport experiments through ceramic disk with nanoparticles present in the inflow solution to the ceramic porous media.

No.	Silver nanoparticle	Ionic strength cm/min	Flow rate mL/min	Percent silver retained	Rate coefficient, min^{-1}		
					k_{att1}	k_{det}	k_{att2}
1	Argenol	1	0.6	16	0.141	0.236	0.015
2	Argenol	10	0.6	27	0.220	0.239	0.023
3	Argenol	50	0.6	71	0.461	1.240	0.085
4	NanoXact-10	1	0.6	20	0.053	0.065	0.017
5	NanoXact-10	10	0.6	45	0.035	0.017	0.032
6	NanoXact-10	50	0.6	59	0.079	0.563	0.099
7	NanoXact-50	1	0.6	21	0.172	0.340	0.018
8	NanoXact-50	10	0.6	49	0.277	0.842	0.038
9	NanoXact-50	50	0.6	76	2.615	6.613	0.069
10	NanoXact-100	1	0.6	16	0.089	0.094	0.013
11	NanoXact-100	10	0.6	70	0.290	0.453	0.080
12	NanoXact-100	50	0.6	100	-	-	-
13	NanoXact-50	1	3	13	1.317	2.352	0.048
14	NanoXact-50	1	0.2	30	0.052	0.031	0.008

* where C_0 is the initial effluent concentration measured in the experiment (ML^{-3}) and k is a first-order rate coefficient (T^{-1}). Parameter values for the experiments shown in Figures 4-5 and 4-7 are summarized below in Table 4-S2.

Table 4-S2. Initial effluent silver nanoparticle concentrations, C_0, and first-order rate coefficients for the model fits to the experimental data depicted in Figures 4-5 and Figure 4-7 for different flow rates and solution ionic strengths.

		Dipping		Paint-on	
		C_0, mg/L	k, min^{-1}	C_0, mg/L	k, min^{-1}
Flow Rate	0.6	13.2	-0.0174	14.8	-0.0202
(mL/min)	1.2	1200	-0.0335	690	-0.0329
Ionic Strength	11	2.54	-0.0198	1.33	-0.0138
(mM)	0	3.49	-0.0142	1.08	-0.00868
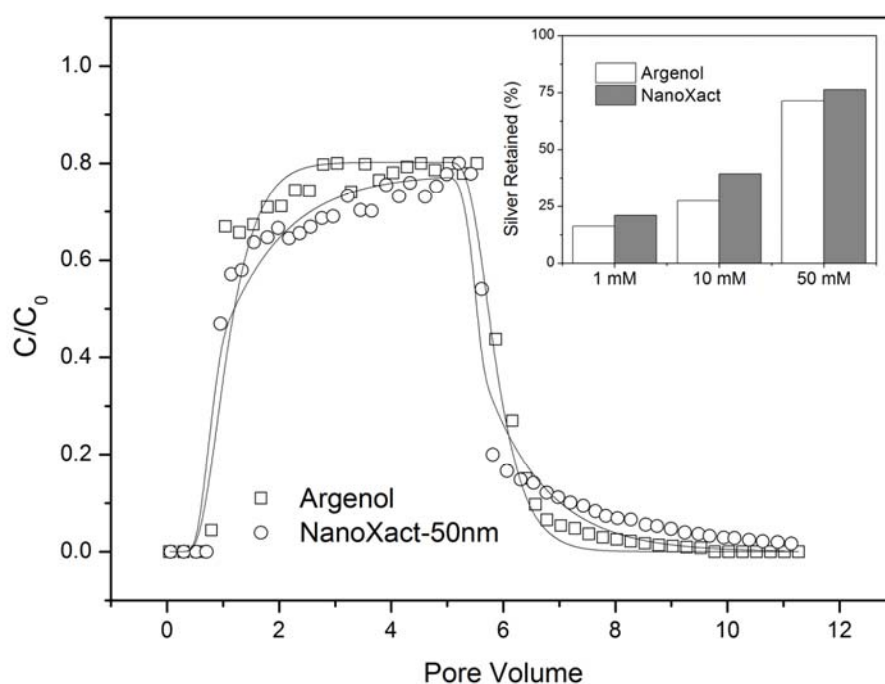
Figure 4-S1. Plots of effluent total silver concentration from ceramic disks (*C*) normalized to the influent total silver concentration (*C₀*) as a function of pore volumes of flow for Argenol and NanoXact 50-nm silver nanoparticles at a solution ionic strength of 1 mM and a flow rate of 0.6 mL/min. Inset: Percent silver retained in the ceramic disk at each ionic strength (1 mM, 10 mM, and 50 mM) and for both types of silver nanoparticles.

4.5.2 Ceramic/AgNP Interaction Energies

Classical DLVO theory can be modified to account for AgNP interaction with ceramic surfaces. As mentioned in the main text, the combined attractive force, Φ_T, between the AgNP and the ceramic surface is the summation of the van der Waals (VDW) attraction and electrostatic double layer repulsion (EDL).

$$\Phi_T(h) = \Phi_{SwS}^{vdW}(h) + \Phi_{SwS}^{EDL}(h) \tag{4-5}$$

This combined force determines the stability of nanoparticles in the aqueous phase. In this study, we simplified the interaction between nanoparticle and ceramic surface to that between nanoparticle and an infinite flat surface. The attraction from van der Waals forces, Φ_{SwS}^{vdW}, is expressed as (Elimelech, 1995):

$$\Phi_{SwS}^{vdW}(h) = -\frac{A_{123}}{6}\left[\frac{a}{h} + \frac{a}{h+2a} + \ln\left(\frac{a}{h+2a}\right)\right] \tag{4-6}$$

where, h is the separation distance and a is the particle radius ($d_p/2$). A_{123} refers to the overall Hamaker interaction constant for the deposition of nanoparticle "1" onto a surface of collector "3" when suspended in the medium of water "2". The individual Hamaker constants for mediums 1, 2, and 3 in a vacuum are denoted as A_{11}, A_{22}, and A_{33} (Table S3) and are used to calculate A_{123} through the following relation:

$$A_{123} = (A_{33}^{0.5} - A_{22}^{0.5})(A_{11}^{0.5} - A_{22}^{0.5}) \tag{4-7}$$

Repulsion from the electrostatic double layer is given as (Gregory, 1975; Petosa, Jaisi, Quevedo, Elimelech, & Tufenkji, 2010):

$$\Phi_{SwS}^{EDL}(h) = 64\pi\varepsilon_0\varepsilon_r a\left(\frac{k_B T}{ze}\right)^2 \Gamma_1\Gamma_2 e^{-\kappa h} \tag{4-8}$$

73

where, ε_0 is vacuum permittivity, ε_r is the dielectric constant of the medium (in this case, water), z is the valence of electrolyte, e is electron charge, k_B is the Boltzmann's constant, Γ_1 and Γ_2 are the surface potentials for the AgNP and sand surfaces, respectively, and κ is the reciprocal of the Debye length. The inverse of the Debye length is given as follows:

$$\kappa^{-1} = \frac{\varepsilon_r \varepsilon_0 k_B T}{2000 N_A I e^2}$$

(4-9)

where N_A is Avogadro's number and I is the ionic strength.

Table 4-S3. Hamaker constant for silver nanoparticles, water and ceramic disk

Material	Hamaker Constant (10^{-20} J)	Reference
Silver Nanoparticles	38.5	(Bargeman & Vanvoors.F, 1972; Butt, Cappella, & Kappl, 2005)
Water	3.7	(de Mesquita, Lins, & Torem, 2003)
Ceramic (derived from clay)	4.89	(Anderson & Lu, 2001; Bergstrom, 1997; Novich & Ring, 1984)

* Figure 4-S2 to 4-S5 present the calculated interaction energies between each type of AgNP as a function of separation distance at each solution ionic strength.
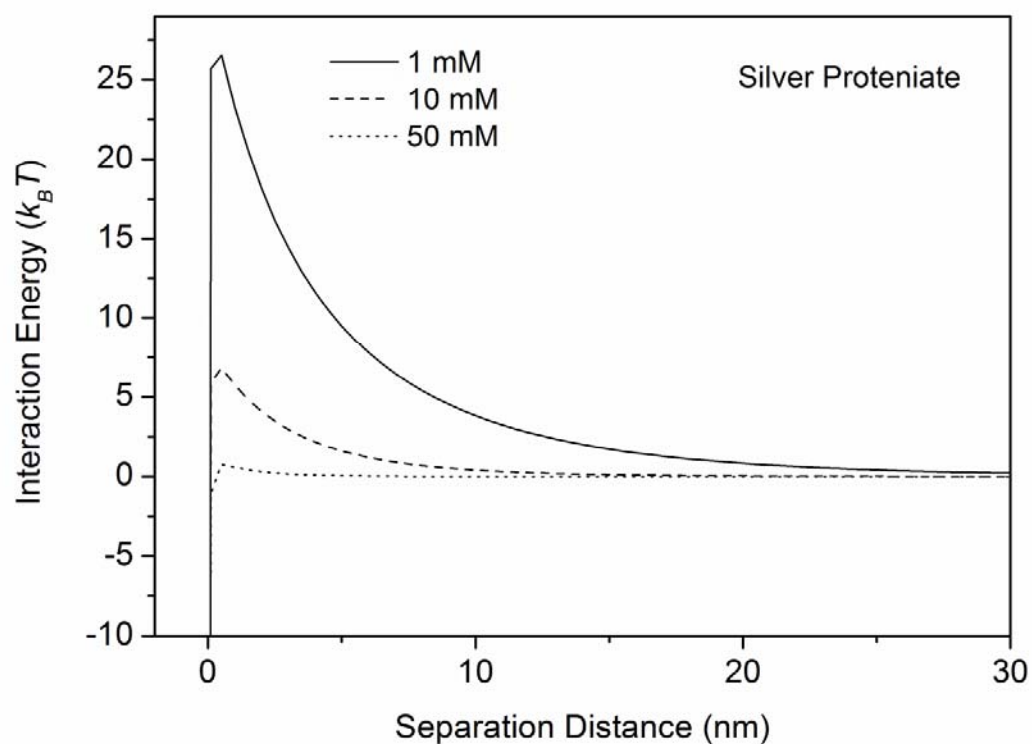
Figure 4-S2. Interaction energy profile between silver proteinate nanoparticles and the ceramic collector surface as a function of separation distance.
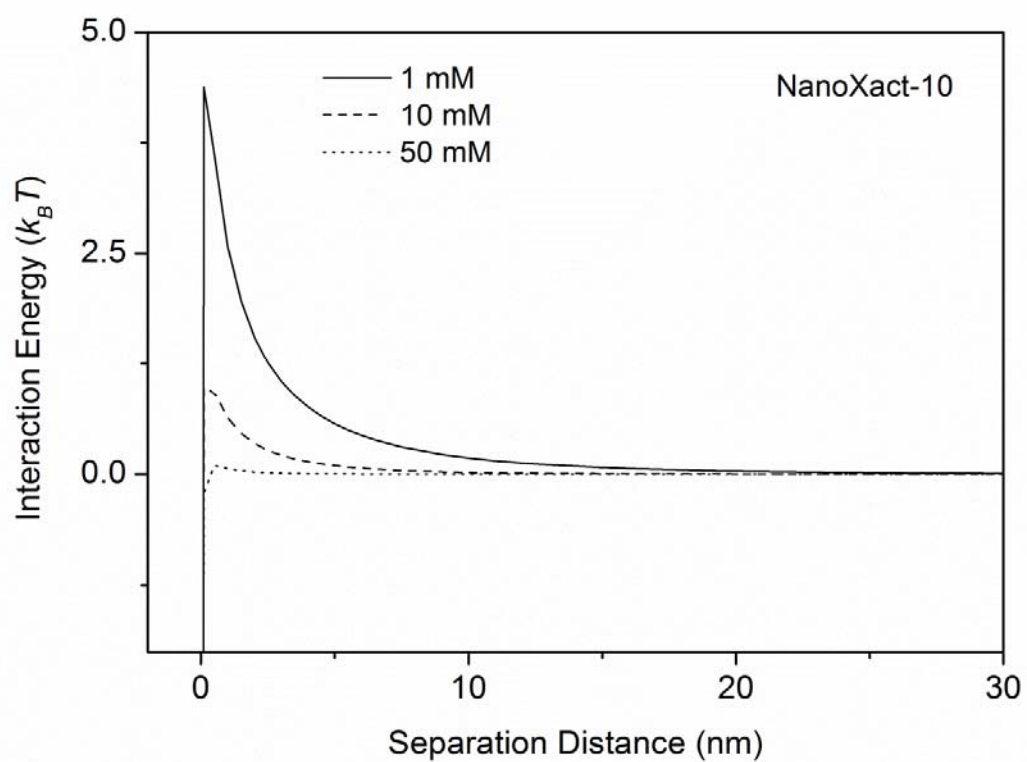
Figure 4-S3. Interaction energy profile between NanoXact-10 nanoparticles and the ceramic collector surface as a function of separation distance.
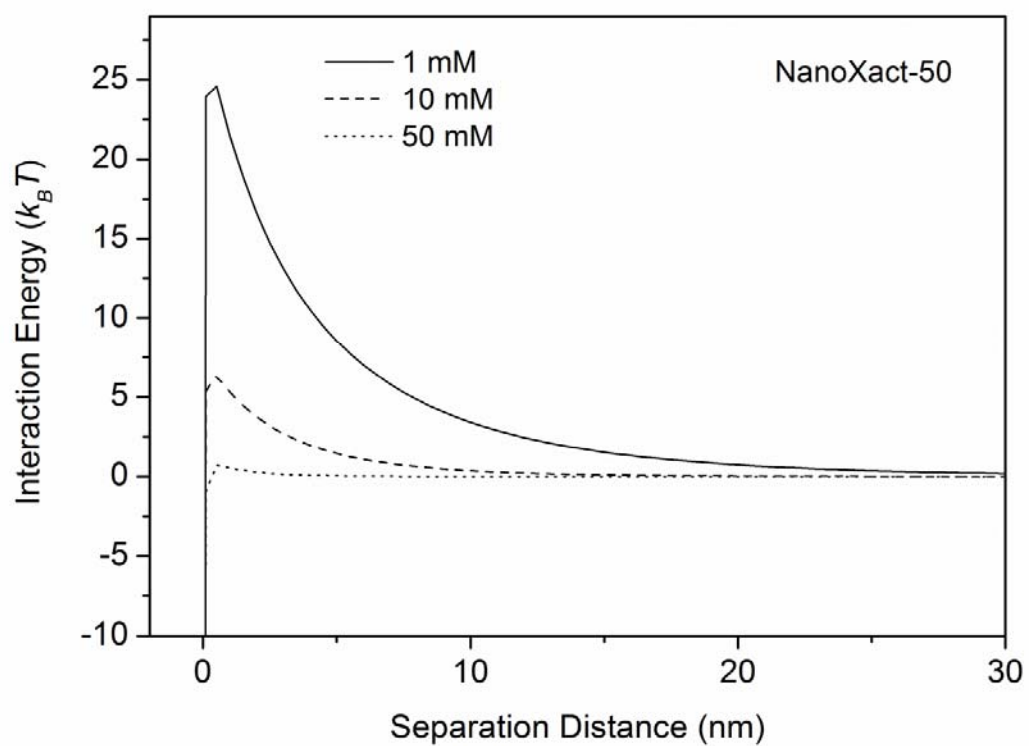
Figure 4-S4. Interaction energy profile between NanoXact-50 nanoparticles and the ceramic collector surface as a function of separation distance.
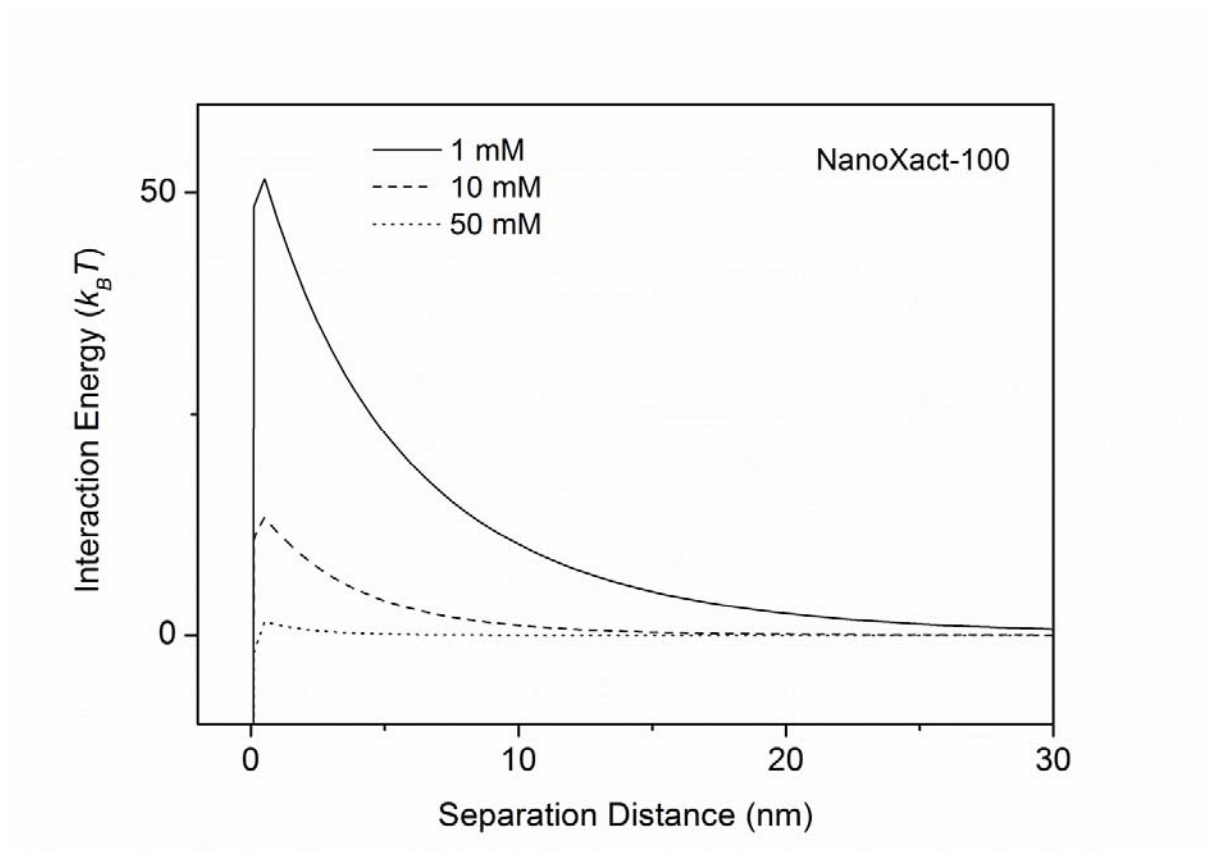
Figure 4-S5. Interaction energy profile between NanoXact-100 nanoparticles and the ceramic collector surface as a function of separation distance.

Reference

Anderson, M. T., & Lu, N. (2001). Role of Microscopic Physicochemical Forces in Large Volumetric Strains for Clay Sediments. *Journal of Engineering Mechanics-Asce, 127*(7), 710-719

Bargeman, D., & Vanvoors.F. (1972). Van-Der-Waals Forces between Immersed Particles. *Journal of Electroanalytical Chemistry, 37*(Jun), 45-&

Bergstrom, L. (1997). Hamaker Constants of Inorganic Materials. *Advances in Colloid and Interface Science, 70*, 125-169

Bielefeldt, A. R., Kowalski, K., Schilling, C., Schreier, S., Kohler, A., & Summers, R. S. (2010). Removal of Virus to Protozoan Sized Particles in Point-of-Use Ceramic Water Filters. *Water research, 44*(5), 1482-1488

Bradford, S. A., & Kim, H. (2010). Implications of Cation Exchange on Clay Release and Colloid-Facilitated Transport in Porous Media. *Journal of Environmental Quality, 39*(6), 2040-2046

Bradford, S. A., Simunek, J., Bettahar, M., Van Genuchten, M. T., & Yates, S. R. (2003). Modeling Colloid Attachment, Straining, and Exclusion in Saturated Porous Media. *Environmental Science & Technology, 37*(10), 2242-2250

Brown, J., Sobsey, M. D., & Loomis, D. (2008). Local Drinking Water Filters Reduce Diarrheal Disease in Cambodia: A Randomized, Controlled Trial of the Ceramic Water Purifier. *American Journal of Tropical Medicine and Hygiene, 79*(3), 394-400

Butt, H. J., Cappella, B., & Kappl, M. (2005). Force Measurements with the Atomic Force Microscope: Technique, Interpretation and Applications. *Surface Science Reports, 59*(1-6), 1-152

Chen, K. L., Mylon, S. E., & Elimelech, M. (2006). Aggregation Kinetics of Alginate-Coated Hematite Nanoparticles in Monovalent and Divalent Electrolytes. *Environmental Science & Technology, 40*(5), 1516-1523

Choi, O., & Hu, Z. (2008). Size Dependent and Reactive Oxygen Species Related Nanosilver Toxicity to Nitrifying Bacteria. *Environmental Science & Technology, 42*, 4583-4588

Choi, O., & Hu, Z. (2009a). Nitrification Inhibition by Silver Nanoparticles. *Water Science and Technology, 59*, 1699-1702

Choi, O., & Hu, Z. (2009b). Role of Reactive Oxygen Species in Determining Nitrification Inhibition by Metallic/Oxide Nanoparticles. *Journal of Environmental Engineering, 135*(12), 1365-1370

Clasen, T., Nadakatti, S., & Menon, S. (2006). Microbiological Performance of a Water Treatment Unit Designed for Household Use in Developing Countries. *Tropical Medicine & International Health, 11*(9), 1399-1405

Clasen, T., Schmidt, W.-P., Rabie, T., Roberts, I., & Cairncross, S. (2007). Interventions to Improve Water Quality for Preventing Diarrhoea: Systematic Review and Meta-Analysis. *British Medical Journal, 334*(7597), 782-785

Dankovich, T. A., & Gray, D. G. (2011). Bactericidal Paper Impregnated with Silver Nanoparticles for Point-of-Use Water Treatment. *Environmental Science & Technology, 45*(5), 1992-1998

de Mesquita, L. M. S., Lins, F. F., & Torem, M. L. (2003). Interaction of a Hydrophobic Bacterium Strain in a Hematite-Quartz Flotation System. *International Journal of Mineral Processing, 71*(1-4), 31-44

Elechiguerra, J. L., Burt, J. L., Morones, J. R., Camacho-Bragado, A., Gao, X., Lara, H. H., & Yacaman, M. J. (2005). Interaction of Silver Nanoparticles with Hiv-I. *Journal of Nanobiotechnology, 3*(6), 1-10

Elimelech, M. (1995). *Particle Deposition and Aggregation: Measurement, Modelling, and Simulation*.

Gregory, J. (1975). Interaction of Unequal Double Layers at Constant Charge. *Journal of Colloid and Interface Science, 51*(1), 44-51

Jaisi, D. P., & Elimelech, M. (2009). Single-Walled Carbon Nanotubes Exhibit Limited Transport in Soil Columns. *Environmental Science Technology, 43*(24), 9161-9166

Kallman, E. N., Oyanedel-Craver, V. A., & Smith, J. A. (2011). Ceramic Filters Impregnated with Silver Nanoparticles for Point-of-Use Water Treatment in Rural Guatemala. *Journal of Environmental Engineering-Asce, 137*(6), 407-415

Lantagne, D. S. (2001). Investigation of the Potters for Peace Colloidal Silver Impregnated Ceramic Filte. Allston, MA.

Lok, C. N., Ho, C. M., Chen, R., He, Q. Y., Yu, W. Y., Sun, H., . . . Che, C. M. (2007). Silver Nanoparticles: Partial Oxidation and Antibacterial Activities. *Journal of Biological Inorganic Chemistry, 12*(4), 527-534

Lydia Shawel Abebe, James A. Smith, Sophia Narkiewicz, Vinka Oyanedel-Craver, Mark Conaway, Alukhethi Singo, . . . Dillingham, R. (2013). Ceramic Water Filters Impregnated with Silver Nanoparticles as a Point-of-Use Water-Treatment Intervention for Hiv-Positive Individuals in Limpopo Province, South Africa: A Pilot Study of Technological Performance and Human Health Benefits. *Journal of Water and Health, In review*

MacCuspie, R. I., Rogers, K., Patra, M., Suo, Z., Allen, A. J., Martin, M. N., & Hackley, V. A. (2011). Challenges for Physical Characterization of Silver Nanoparticles under Pristine and Environmentally Relevant Conditions. *J. Environ. Monit., 13*, 1212-1226

Morones, J. R., Elechiguerra, J. L., Camacho, A., Holt, K., Kouri, J. B., Ramirez, J. T., &
Yacaman, M. J. (2005). The Bactericidal Effect of Silver Nanoparticles.
Nanotechnology, 16(10), 2346-2353

Novich, B. E., & Ring, T. A. (1984). Colloid Stability of Clays Using Photon-Correlation
Spectroscopy. *Clays and Clay Minerals, 32*(5), 400-406

Oyanedel-Craver, V. A., & Smith, J. A. (2008). Sustainable Colloidal-Silver-Impregnated
Ceramic Filter for Point-of-Use Water Treatment. *Environmental Science &
Technology, 42*(3), 927-933

Petosa, A. R., Jaisi, D. P., Quevedo, I. R., Elimelech, M., & Tufenkji, N. (2010).
Aggregation and Deposition of Engineered Nanomaterials in Aquatic
Environments: Role of Physicochemical Interactions. *Environmental Science &
Technology, 44*(17), 6532-6549

Rayner, J. (2009). *Current Practices in Manufacturing of Ceramic Pot Filters for Water
Treatment.* (Master), Loughborough University, Leicestershire, UK.

Ren, D. J., & Smith, J. A. (2013). Proteinate-Capped Silver Nanoparticle Transport in
Water-Saturated Sand. *Journal of Environmental Engineering-Asce, 139*(6), 781-
787

Schijven, J. F., Hassanizadeh, S. M., & de Bruin, R. H. A. M. (2002). Two-Site Kinetic
Modeling of Bacteriophages Transport through Columns of Saturated Dune Sand.
Journal of Contaminant Hydrology, 57(3-4), 259-279

Schijven, J. F., & Simunek, J. (2002). Kinetic Modeling of Virus Transport at the Field
Scale. *Journal of Contaminant Hydrology, 55*(1-2), 113-135

Schweitzer, R. W., Cunningham, J. A., & Mihelcic, J. R. (2013). Hydraulic Modeling of Clay Ceramic Water Filters for Point-of-Use Water Treatment. *Environmental Science & Technology, 47*(1), 429-435

The Ceramics Manufacturing Working Group. (2011). Best Practice Recommendations for Local Manufacturing of Ceramic Pot Filters for Household Water Treatment. Atlanta, GA: Center for Disease Control and Prevention.

Theodore Peters, J. (1996). *All About Albumin: Biochemistry, Genetics, and Medical Applications*. San Diego: Academic Press.

Thio, B. J. R., Lee, J. H., Meredith, J. C., & Keller, A. A. (2010). Measuring the Influence of Solution Chemistry on the Adhesion of Au Nanoparticles to Mica Using Colloid Probe Atomic Force Microscopy. *Langmuir, 26*(17), 13995-14003

Thio, B. J. R., Zhou, D. X., & Keller, A. A. (2011). Influence of Natural Organic Matter on the Aggregation and Deposition of Titanium Dioxide Nanoparticles. *Journal of Hazardous Materials, 189*(1-2), 556-563

Tian, Y. A., Gao, B., Silvera-Batista, C., & Ziegler, K. J. (2010). Transport of Engineered Nanoparticles in Saturated Porous Media. *Journal of Nanoparticle Research, 12*(7), 2371-2380

Tosco, T., Bosch, J., Meckenstock, R. U., & Sethi, R. (2012). Transport of Ferrihydrite Nanoparticles in Saturated Porous Media: Role of Ionic Strength and Flow Rate. *Environmental Science & Technology, 46*(7), 4008-4015

U.S. Environmental Protection Agency. from http://water.epa.gov/scitech/methods/cwa/wet/upload/2007_07_10_methods_wet_disk2_atx7-10.pdf

Wang, C., Bobba, A. D., Attinti, R., Shen, C. Y., Lazouskaya, V., Wang, L. P., & Jin, Y. (2012). Retention and Transport of Silica Nanoparticles in Saturated Porous Media: Effect of Concentration and Particle Size. *Environmental Science & Technology, 46*(13), 7151-7158

Zhang, H. Y., & Oyanedel-Craver, V. (2012). Evaluation of the Disinfectant Performance of Silver Nanoparticles in Different Water Chemistry Conditions. *Journal of Environmental Engineering-Asce, 138*(1), 58-66

Zhang, H. Y., Smith, J. A., & Oyanedel-Craver, V. (2012). The Effect of Natural Water Conditions on the Anti-Bacterial Performance and Stability of Silver Nanoparticles Capped with Different Polymers. *Water research, 46*(3), 691-699

Zhang, L. L., Hou, L., Wang, L. L., Kan, A. T., Chen, W., & Tomson, M. B. (2012). Transport of Fullerene Nanoparticles (Nc60) in Saturated Sand and Sandy Soil: Controlling Factors and Modeling. *Environmental Science & Technology, 46*(13), 7230-7238

CHAPTER 5: TRANSPORT THROUGH GEOSYNTHETIC CLAY LINERS

5.1　Introduction

With the extensive use of silver nanoparticle-impregnated products, it is expected to have an increasing amount of nanoparticles entering landfill (Mueller & Nowack, 2008). Among various nanoparticles, silver nanoparticles are of particular interest as they account for approximately 20% of nanoparticle-imbedded consumer products. The disposed consumer products, leached silver nanoparticles from usage of consumer products, and disposal of sludge from wastewater treatment plant are three common pathways into landfill sites.

Waste disposed in landfills is usually contained by a low permeability composite layer ($<10^{-7}$ cm/s) of compacted clay placed underneath the waste to prevent the leachate from migrating downward and contaminating the groundwater system. To serve this purpose, a compacted clay liner is traditionally used because of its great durability and low permeability. Nevertheless, the difficulty in obtaining the raw clay for the liner may make it prohibitively expensive to obtain in some regions. As an alternative, several manufactures introduced a new type of liner: a geosynthetic clay liner (GCL). The GCL is sandwich shaped: a very thin layer of processed clay (usually bentonite, with a density of approximately 5 kg/m^2) is bounded between two sheets of geotextile fabric. A geotextile can either be woven or non-woven. The integrity of the structure is maintained by stitching or needle punching and/or by applying an adhesive layer between the bentonite and geotextile (Figure 5-1) (Estornell & Daniel, 1992). Compared to a traditional compacted clay liner, GCL is cheaper, yet has a comparable permeability.

Thus, GCL has gained wide popularity since 1990 and is used extensively in many landfill sites.
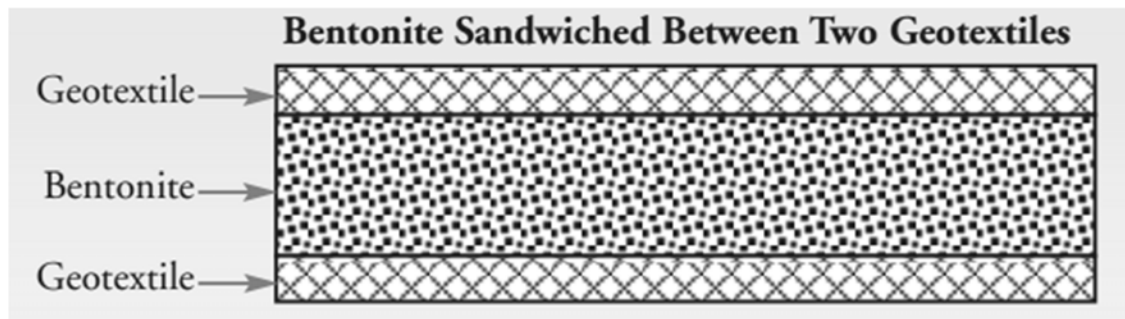
Figure 5-1. Schematic diagram of a typical geosynthetic clay liner configuration.

Although researchers found that the GCL was effective in attenuating metals from some mining leachates (Lange, Rowe, & Jamieson, 2007), it is uncertain whether the impermeability will hold true for nanoparticles, and silver nanoparticles in particular. The exposure to silver nanoparticles poses a new challenge to the retention capability of the GCL and eventually the safety of the groundwater system. Thus, it is necessary to evaluate the design of landfill sites to assess their robustness towards silver nanoparticles. The first logical step is to investigate the mobility of silver nanoparticles through the GCL under different water chemistry conditions.

To date, however, there is no single study that evaluates the risk of breakthrough through the GCL by any nanoparticle. Some earlier studies on the diffusion of volatile organic compounds (VOC) through the GCL were relevant but not immediately applicable to this study for two clear reasons: 1) diffusion is not equivalent to transport, and 2) there is a solid-liquid-air interface with VOCs, and a solid-liquid interface for silver nanoparticles.

Hence, the two main objectives of this section were to: 1) evaluate the transport characteristics of silver nanoparticles through the GCL, and 2) investigate the factors affecting the mobility of silver nanoparticles.

5.2 Material and methods

5.2.1 Materials

A couple of GCL specimens (Claymax 200R) were provided by Colloid Environmental Technologies Company (CETCO, Arlington Heights, Illinois, USA). The specimens provided were unreinforced, adhesive-bonded GCLs with granular bentonite in between the two geotextiles. The bentonite content is 3.5 kg/m^2. The initial water content of the bentonite is between 10% - 12%. The thickness of the dry specimen is about 6 mm. The silver proteinate nanoparticle was manufactured by Argenol Laboratories (Spain) and used as received. The characteristics of this type of nanoparticle have been described in Chapter 3 and in Ren (2013). Reagent-grade KNO_3 and $MgSO_4$ from Sigma-Aldrich (Milwaukee, WI) were used to prepare divalent and monovalent electrolyte solutions. A 0.45 μm PTFE on-syringe filter from Fisher Science was used to filter samples before analysis.
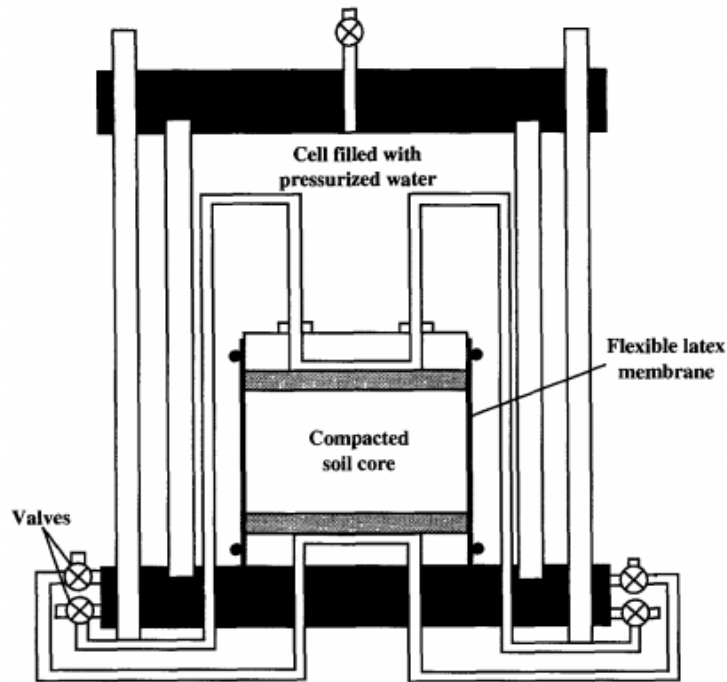
Figure 5-2 Schematic diagram of the flexible wall permeameter used in this study. (Smith & Jaffe, 1994)

The tests were carried out in a flexible wall permeameter in general accordance with ASTM D5084 and ASTM D6766 (Figure 5-2). It includes the outer chamber and inner specimen core. In response to a typical concern for many earlier research on GCL specimens, the specimen of GCL used in this study was cut slightly larger than the desired size and lightly hydrated around the rims with a few drops of deionized water to minimize the loss of bentonite (Daniel, Bowders, & Gilbert, 1997). After a few minutes, it was carefully trimmed into a circular shape with a nominal diameter of 60 mm. The specimen was then placed on a stainless steel base pedestal with an O-ring between the pedestal and ring. A stainless steel top cap was placed on the top of the specimen with

another O-ring between the specimen and top cap. The resulting sandwich-shaped cylinder was then wrapped with a flexible latex membrane. After the preparation of the specimen, the permeameter was assembled and filled with water. A pressure control board applied water pressure on the membrane-wrapped specimen cylinder in order to eliminate the side-flow. Once the setup was complete, an Acuflow series IV HPLC pump introduced permeate liquid into the specimen at a flow rate of 0.01 mL/min, with an initial back-pressure of 3 psi. The confining (cell-water) pressure applied to the specimen was gradually raised to 5 psi to overcome the back pressure. To maintain a positive net pressure, the continuous increment of back pressure was accounted for by increasing the confining pressure accordingly. The process took 48 hours before the back pressure and confining pressure reached equilibriums of 21 psi and 25 psi, respectively. The final configuration of both pressures was kept at these levels throughout the experiments. DI water with an electrical conductivity equal to 18 ohm per second and a pH of 6.8 was used as the permeant liquid and for filling the outer cell of the permeameter.

5.2.3   *Testing procedure*

The specimen inside the chamber was flushed continuously with DI water at a flow rate of 0.01 mL/min for seven days. This was done for two reasons: 1) to saturate the GCL (Petrov, Rowe, & Quigley, 1997; Ruhl & Daniel, 1997; Shan & Daniel, 1991), and 2) to remove excess immobilized bentonite particles from the specimen. After seven days, a pulse injection of tritiated water [^{3}H-H$_2$O] was introduced into the specimen as a conservative tracer to characterize the hydraulic characteristics of the specimen. The hydraulic properties of the GCL were evaluated based on the breakthrough curve of the conservative tracer. Upon the completion of tracer test, a solution of silver nanoparticles

(10 mg/L) suspended in water at a specific ionic strength was fed into the specimen for 24 hr. A AgNP-free background solution with the same ionic strength was applied to the specimen for the rest of experiment period.

Effluent was sampled every 3 hr for up to 120 hr. For each sample, it was first filtered through a disposable 0.45 μm PTFE on-syringe membrane filter to remove the fine bentonite particles mixed in the effluent. DI water was used to dilute the 1.5 mL filtered sample to 3 mL after acidifying the sample with a drop of 10% nitric acid to make up enough size of sample for follow up analysis. Finally, an atomic absorption spectrometer (AAS) AAnalyst 200 (Perkin-Elmer) was used to analyze the total silver concentration of the sample.

The quality control of sample preparation was performed with a series of known concentration standard samples of silver nanoparticles varying from 0.05 mg/L to 5 mg/L. Each sample underwent the same procedure as the effluent samples, and was analyzed by AAS to determine the concentration. The recovery rate was identified and the standard curves were adjusted accordingly.

5.2.4 Testing scenarios

As shown in Table 5-1, four scenarios were explored in this study: zero ionic strength, low ionic strength (with monovalent K^+), low ionic strength (with divalent Mg^{2+}), and high ionic strength. Between each test, the 1% nitric acid (HNO_3) solution was used to flush the specimen at a rate of 0.01 mL/min and thereby dissolve previously retained silver nanoparticles and recover available attachment sites. Each nitric acid flush lasted about 10 hours. In order to restore the specimen back to the initial state, DI water was used to flush the specimen for another 48 hours at the same rate.

Table 5-1. Four transport test scenarios for proteinate-capped silver nanoparticles

Time Point / Scenarios	Day 0 ~ 1	Day 1 ~ 2	Day 2 ~ 3
Zero Ionic strength	DI water	DI water	-END-
Low ionic strength (Mg^{2+})	1 mM	1 mM	DI water
Low ionic strength (K^+)	1 mM	1 mM	DI water
High ionic strength (Mg^{2+})	100 mM	100 mM	DI water

* 1 mM or 100 mM refers to the ionic strength in terms of either Mg^{2+} or K^+;

** The injection of AgNP solution (10 mg/L) happens at the first 60 seconds when the experiment starts.

5.3 Results

5.3.1 Pretreatment of silver nanoparticle effluent

The presence of fine bentonite particles in the effluent sample would congest the AAS if left untreated. Filtration with 0.45 μm PTFE membrane was therefore used to remove those particles. It was found that the PTFE membrane retained a small fraction of silver nanoparticles during filtration. A quality control test was performed to validate the pretreatment approach. The results showed that the average recovery rate was 89% (results ranged from 86% to 94% with a standard deviation 3.45%), which is acceptable. The standard curves were divided into two regions: low concentration (0.05 mg/L to 0.5 mg/L) and high concentration (0.5 mg/L to 5 mg/L), as shown in Figure 5-3. Overall, the R-squared values for filtered samples on both ranges were greater than 0.99, which confirmed the validity of the sample pretreatment.
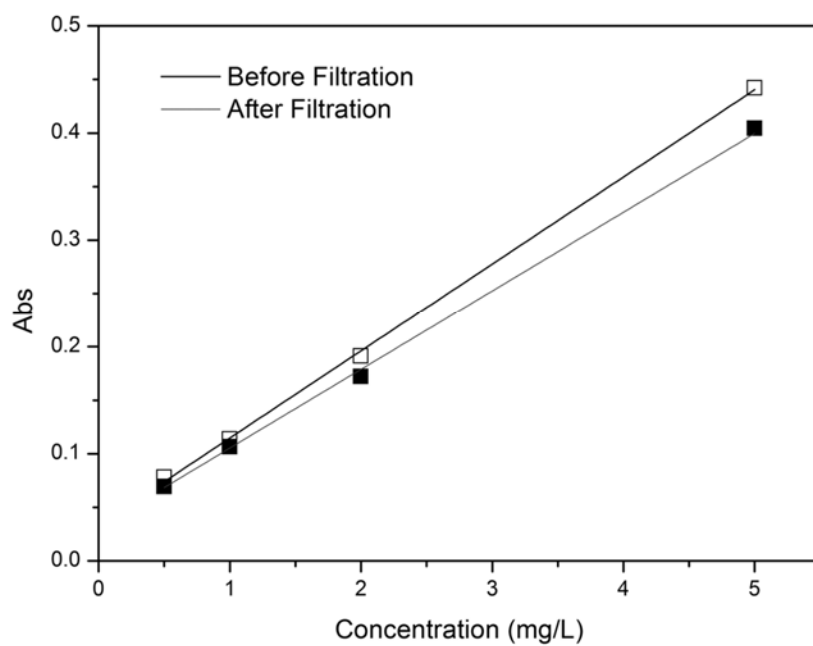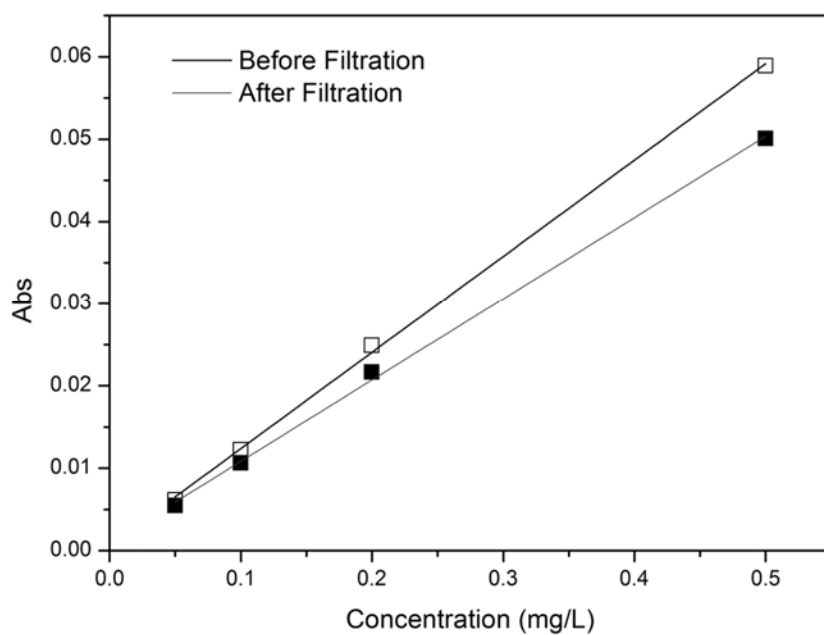
Figure 5-3: Standard curves for aqueous solutions of silver nanoparticles before filtration (black line with hollow symbol) and after filtration (gray line with solid symbol), for low (0.05 mg/L to 0.5 mg/L) and high (0.5 mg/L to 5 mg/L) concentration ranges.

5.3.2 Impact of ionic strength on transport behavior
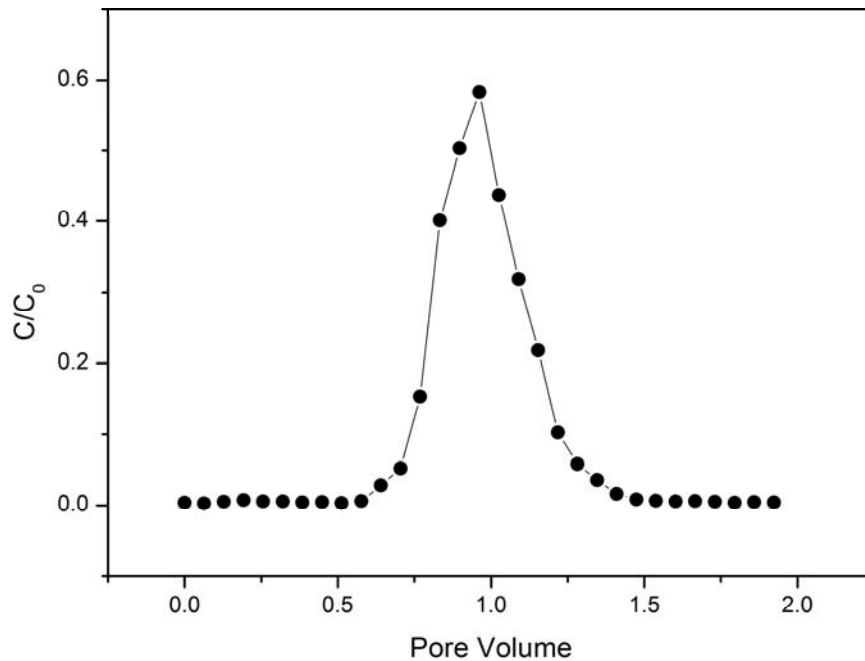
Figure 5-4. The tracer test result by tritium water (^{3}H-H$_2$O) with time as x-axis, relative concentration of tritium water as y-axis.

The breakthrough curve of the tracer test is given in Figure 5-4. The recovery rate of tritium tracer was around 97% (93%~ 110%). The peak was observed approximately 5 hours after the beginning of the test. A pore volume of 3.12 mL was mathematically determined by this test.

Following the tracer test, three silver nanoparticle transport scenarios were studied as listed in Table 5-1, with three corresponding breakthrough curves presented in Figure 5-5. Breakthrough of silver nanoparticles was observed for both DI water and low ionic strength water, yet no breakthrough was observed for the high ionic strength water.

Initial concentrations of silver in samples within the first 12 hours were too low to measure for all three scenarios. Breakthrough peaks were observed at 1.3 days and 1.5

days for the low ionic strength and zero ionic strength scenarios, respectively. The

breakthroughs of silver nanoparticles were all delayed by about 2 to 3 pore volumes

relative to the tracer for scenarios with observed breakthrough peaks.
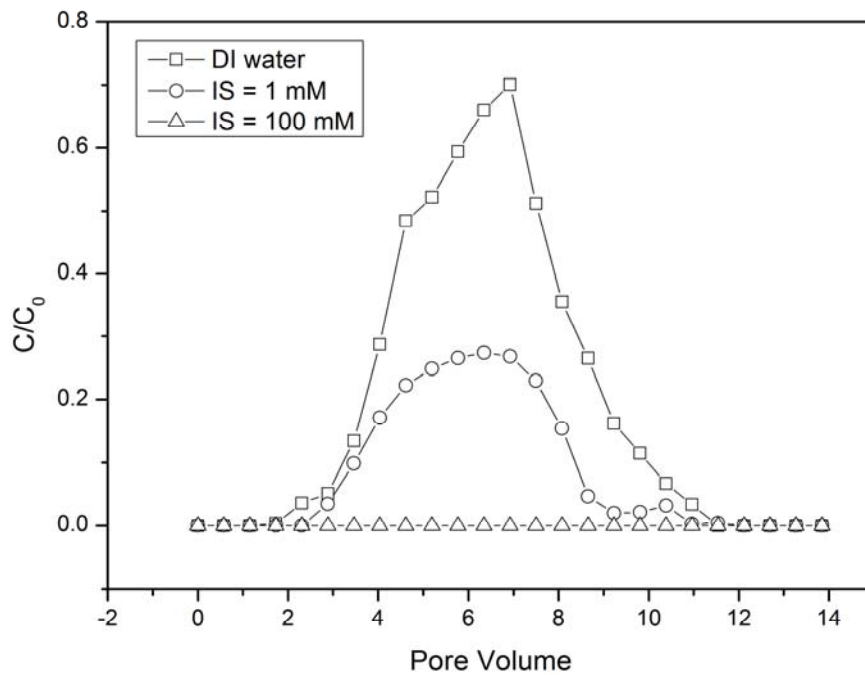
Figure 5-5. Normalized concentration of silver nanoparticles versus pore volume for three transport scenarios: DI water (hollow square), 1 mM ionic strength (hollow circle) and 100 mM ionic strength (hollow triangle). Solution ions are Mg^{2+} and SO_4^{2-}

To determine if the retention is reversible and what percentage of silver will be

washed out under lower ionic strength, the procedure for the two scenarios with some

ionic strength (1 mM and 100 mM) were further extended by one additional step:

introducing DI water into the specimens at the end of the 3-day transport experiment. The

normalized concentrations of silver nanoparticles with the addition of this extended flush

step were plotted against elapsed time in Figure 5-6.
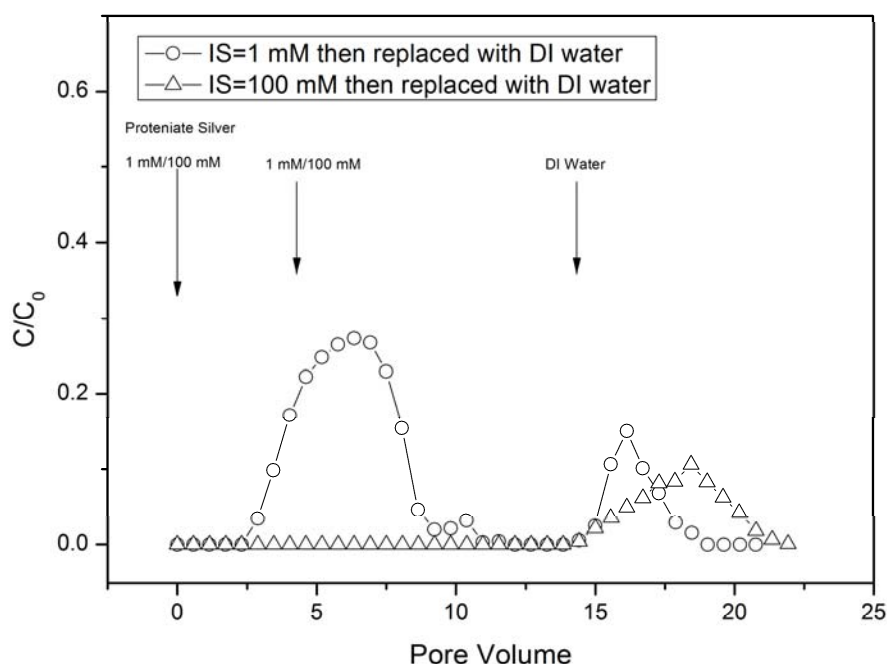
Figure 5-6. Breakthrough curves and following dislocation of AgNP with DI water. Time points when changes of solution were made are marked as arrows on the graph. Solution ions are Mg^{2+} and SO_4^{2-}

For both scenarios, the normalized concentration of silver nanoparticles had

achieved steady state by the end of the 3-day period, and no measurable silver was found

in all effluents. Upon the introduction of DI water, concentration spikes were observed

approximately half a day later following the introduction of DI water. This indicates that

the additional DI water flush did not further reduce the concentration of silver

nanoparticles in the effluent. The individual percentages of silver nanoparticles retained

and released from each step were calculated and listed in Table 5-2.

Table 5-2. Percentage of retained silver nanoparticles through different steps with MgSO₄ as electrolyte

Retention (%) / Scenario	Day 0 ~ 3	Day 3 ~ end
DI water	37.7	NA
IS = 1 mM	73.84	-6.28
IS = 100 mM	100	-8.24

Note: A negative number refers to the release of silver nanoparticles.

5.3.3 Impact of electrolyte

The influence of electrolyte was investigated by exploring K^+ and Mg^{2+} in the low ionic strength scenarios. The breakthrough curves are presented in Figure 5-7. The breakthrough peaks occurred at approximately the same time for both electrolytes, yet the retention rate was higher for the divalent Mg^{2+} than the monovalent K^+ electrolytes.
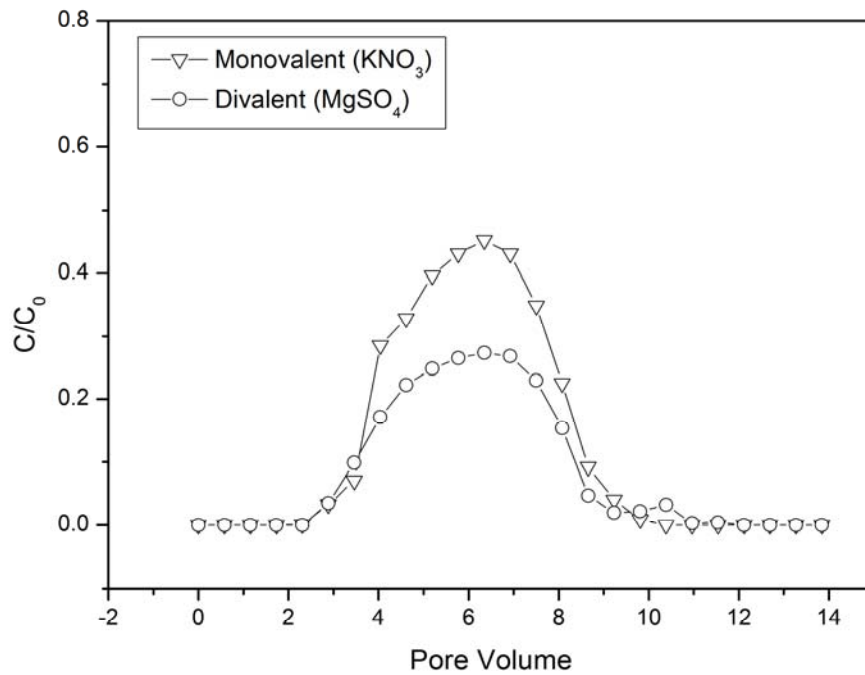
Figure 5-7. Breakthrough curves for silver nanoparticles with 1 mM monovalent (KNO₃) electrolytes and divalent (MgSO₄) solutions.

5.4   Discussions

5.4.1   *Mobility through the GCL*

The result from these breakthrough curves raised the concern that the silver

nanoparticles were quite mobile in most cases studied, despite the fact that GCL was

designed to stop leachate from migrating into the groundwater system. From the transport

breakthrough curves displayed in Figure 5-5, both the DI water and low ionic strength

scenarios failed to fully retain the silver nanoparticles. The retention rate with DI water

was 37.7%, while it was higher (60.7%) for silver nanoparticles owing to the increase of

the ionic strength to 1 mM. Only under highest ionic strength, complete retention was achieved.

Additionally, the environment under which the GCL was tested was slightly different from the environment in real circumstances. In order to reduce the experiment time period to a reasonable time range in this study, higher-than-normal confining pressure (25 psi) was applied to the GCL specimen. While two studies found a decrease in permeability of one order of magnitude from 2×10^{-9} cm/s to 3×10^{-10} cm/s when the confining pressure against the GCL was increased from 4 kPa to 140 kPa (Ruhl & Daniel, 1997; Shan & Daniel, 1991), other researchers believe that the impact on permeability is minimal (Petrov & Rowe, 1997; Petrov et al., 1997). In conclusion, the high pressure applied on the GCL would result in lower, if not the same, permeability.

5.4.2   *Ionic strength*

The impact of ionic strength (with the same electrolyte) on the retention of silver nanoparticles is presented in Figure 5-5. With an otherwise identical condition, the retention rate increased with the ionic strength.

An increase in ionic strength increases retention of silver nanoparticles through two mechanisms. First, it induces AgNP aggregation. Earlier studies have demonstrated that the stability of silver nanoparticles is sensitive to the ionic strength level, since ionic strength can effectively compromise the electronic double layer - which repels the aggregation - surrounding each nanoparticle to ensure stabilization. The proteinate diffusion layer is more durable and protective in terms of stabilizing the silver nanoparticle suspension; however, the gradual dissolution of proteinate weakens the stabilizing effect when it is over two or three hours (Ren & Smith, 2013). In this

investigation, however, the time scale of the whole transport experiment was approximately three hours, significantly longer than the critical time point. It is possible that the aggregation occurred and further contributed to the higher retention rate in the presence of ionic strength.

Similar to the compromised repulsion force between the nanoparticles, the ionic strength also reduced the repulsion force between the nanoparticle and bentonite particles. Higher ionic strength was found to be more effective in reducing the repulsion force, lowering the energy barrier that prevents the occurrence of deposition, and thus creating a higher retention rate of silver nanoparticles through the specimen.

5.4.3   Electrolyte type

In contrast to porous mediums composed of Ottawa sand or clay, the difference of electrolyte valence in the GCL not only affects the silver nanoparticles but also the porous medium itself.

The impacts from electrolytes on silver nanoparticles are related to two separate aspects, which is similar to the ionic strength influence previously discussed: the aggregation between nanoparticles, and the deposition of nanoparticles onto the bentonite surface. The divalent electrolyte has a stronger effect in both compressing the electronic double layer and reducing the deposition energy barrier than the monovalent electrolyte.

On the other hand, the influence on the porous medium by the electrolyte valence should not be ignored. Previous studies have shown that the cation exchange process can significant increase the hydraulic conductivity. The increase is more profound when divalent electrolyte is presented than the monovalent electrolyte. An increase of two orders of magnitude in valence was reported when calcium presents in the permeate

solution (Benson & Meer, 2009; Scalia & Benson, 2011). When James, Fullerton, and

Drake (1997) investigated the leakage through GCLs in a cover system protecting water

reservoirs, they found that the divalent electrolyte Ca^{2+} replaced the monovalent

electrolyte Na^+, resulting in subsequent shrinkage and cracking of bentonite. In the study

presented here, divalent ion Mg^{2+} produces additional adverse impacts on the swelling of

bentonite and thus increases the hydraulic conductivity of the GCL. The increase of

hydraulic conductivity was confirmed by the observation of a decrease in pump pressure

from 21 psi to 18 psi. Because the pump maintained a steady flow, no effect on

breakthrough curve was observed.

5.4.4   *Reversibility of retained silver nanoparticles*

As shown in Figure 5-6, when the specimen was rinsed with DI water, release or

immobilization of previously retained silver with ionic strength 1 mM and 100 mM as

$MgSO_4$ was observed for all three scenarios. According to the DLVO theory, there exists

two types of energy barriers: a primary energy barrier and a secondary energy barrier.

While the deposition of silver nanoparticles is permanent (irreversible) when overcoming

the primary energy barrier, the deposition by overcoming the secondary energy barrier is

temporary (reversible). The reintroduction of DI water into the specimen could possibly

minimize or even eliminate the secondary minimum, resulting in the release of silver

nanoparticles into the effluent again. Similar results were confirmed by earlier studies, as

well as on latex spheres (Franchi & O'Melia, 2003). Also it should be noted that the

higher the ionic strength, the greater the percentage of silver released when rinsing with

DI water: 8.24% of silver nanoparticles were released following deposition with 100 mM

ionic strength, which was greater than the 6.28% with 1 mM ionic strength.

5.4.5 Implication of AgNP transport through GCL

GCL serves a critical role in preventing the contamination of groundwater systems from leachate. The breakthrough of AgNP though the GCL under certain conditions has important implication to the study of GCLs. Prior to the widespread use of nano-materials, the design of a GCL would not factor in the existence of nanomaterial. It leaves the possibility that the GCL may not be able to effectively contain silver nanoparticles. Nevertheless, it shall be noted that the actual landfill environment exhibits much more complicated characteristics than in a lab-scale study. The leachate is typically characterized by high ionic strength, and is high in ions, metals, and dissolved organic matter. The aggregation and deposition of AgNP is expected to occur. This behavior would positively facilitate the GCL's retention of AgNP and reduce the risk AgNP may bring to the groundwater system.

Reference

Benson, C. H., & Meer, S. R. (2009). Relative Abundance of Monovalent and Divalent Cations and the Impact of Desiccation on Geosynthetic Clay Liners. *Journal of Geotechnical and Geoenvironmental Engineering, 135*(3), 349-358

Daniel, D. E., Bowders, J. J., & Gilbert, R. B. (1997). Laboratory Hydraulic Conductivity Testing of Gcls in Flexible-Wall Permeameters. *SAE Special Publications*(1308), 208-226

Estornell, P., & Daniel, D. E. (1992). Hydraulic Conductivity of 3 Geosynthetic Clay Liners. *Journal of Geotechnical Engineering-Asce, 118*(10), 1592-1606

Franchi, A., & O'Melia, C. R. (2003). Effects of Natural Organic Matter and Solution Chemistry on the Deposition and Reentrainment of Colloids in Porous Media. *Environmental Science & Technology, 37*(6), 1122-1129

James, A. N., Fullerton, D., & Drake, R. (1997). Field Performance of Gcl under Ion Exchange Conditions. *Journal of Geotechnical and Geoenvironmental Engineering, 123*(10), 897-901

Lange, K., Rowe, R. K., & Jamieson, H. (2007). Metal Retention in Geosynthetic Clay Liners Following Permeation by Different Mining Solutions. *Geosynthetics International, 14*(3), 178-187

Mueller, N. C., & Nowack, B. (2008). Exposure Modeling of Engineered Nanoparticles in the Environment. *Environmental Science & Technology, 42*(12), 4447-4453

Petrov, R. J., Rowe, R. K., & Quigley, R. M. (1997). Comparison of Laboratory-Measured Gcl Hydraulic Conductivity Based on Three Permeameter Types. *Geotechnical Testing Journal, 20*(1), 49-62

Ren, D. J., & Smith, J. A. (2013). Proteinate-Capped Silver Nanoparticle Transport in Water-Saturated Sand. *Journal of Environmental Engineering-Asce, 139*(6), 781-787

Ruhl, J. L., & Daniel, D. E. (1997). Geosynthetic Clay Liners Permeated with Chemical Solutions and Leachates. *Journal of Geotechnical and Geoenvironmental Engineering, 123*(4), 369-381

Scalia, J., & Benson, C. H. (2011). Hydraulic Conductivity of Geosynthetic Clay Liners Exhumed from Landfill Final Covers with Composite Barriers. *Journal of Geotechnical and Geoenvironmental Engineering, 137*(1), 1-13

Shan, H. Y., & Daniel, D. E. (1991). *Results of Laboratory Tests on a Geotextile/Bentonite Liner Material.* Paper presented at the Proc. Geosynthetics, St. Paul, MN.

Smith, J., & Jaffe, P. (1994). Benzene Transport through Landfill Liners Containing Organophilic Bentonite. *J Environ Eng-Asce, 120*(6), 1559-1577

CHAPTER 6: SUSTAINABILITY OF CERAMIC FILTERS FOR POINT-OF-USE DRINKING WATER TREATMENT

6.1   Introduction

Lack of access to safe, reliable water sources remains a critical problem for millions of people worldwide, especially in the developing world. The United Nations and the World Health Organization (WHO) estimate that 780 million people (roughly 11% of the world's population), were without access to improved water supply as of 2012(Joint United nations Program on HIV/AIDS (UNAIDS), 2012). As such, waterborne diseases such as diarrhea, cholera, enteric fever, and hepatitis cause 1.6 million deaths annually, and children under five years old are especially vulnerable(WHO/UNICEF Joint Water Supply and Sanitation Monitoring Programme., World Health Organization., & UNICEF., 2006). Thus, there is a great need for technology and infrastructure capable of providing clean drinking water in economically depressed regions.

Point-of-use water (POU) treatment devices are one appealing option for expanding access to clean water in developing countries via "decentralized" water treatment, whereby individual households treat their own drinking water before

consuming it. This is in contrast to "centralized" water treatment systems, wherein water is treated at one central location and then distributed via pipes to households for consumption without any additional treatment. In a recent review, the WHO concluded that point-of-use water treatment technologies constitute simple, socially acceptable, low-cost interventions with significant potential to reduce global waterborne disease and death (T. Clasen, Nadakatti, & Menon, 2006). In a follow-up meta-analysis, Clasen et al.(2007) found that water interventions at the individual household level are more effective in improving water quality, and by extension reducing diarrheal illness, than source-level interventions and that they may be more cost-effective over time than centralized systems. These findings are especially compelling given the dramatic growth in the accessibility of piped water within individual household premises, from 45% of the global population in 1990 to 54% in 2010(Joint United nations Program on HIV/AIDS (UNAIDS), 2012). Ready access to piped water, though not necessarily treated water, presumably increases the appeal of point-of-use water treatments. Thus, it is worthwhile to examine point-of-use treatment technologies in depth.

Silver-impregnated ceramic water filters are one particularly promising type of POU water treatment technology(van Halem, van der Laan, Heijman, van Dijk, & Amy, 2009). This technology has been shown to effectively remove microorganisms (e.g., *Escherichia coli*, total coliforms, protozoan oocysts) and turbidity from water during extensive laboratory testing and field testing with actual household consumers(Campbell, 2005; Kallman, Oyanedel-Craver, & Smith, 2011; Lantagne, 2001; Oyanedel-Craver & Smith, 2008; Simonis & Basson, 2012). Recent work has focused on assessing the cultural acceptability of this treatment among its intended users, understanding the

impacts of raw water quality on disinfection performance, and varying materials composition and/or manufacturing techniques to optimize disinfection (Kallman et al., 2011; Zhang, Smith, & Oyanedel-Craver, 2012). The results of these studies are generally positive; therefore, it is promising that nongovernmental agencies such as Potters for Peace, PureMadi, and FilterPure have successfully established more than 35 filter factories worldwide to produce the filters using local labor and predominantly local materials (i.e., clay and combustible matter such as sawdust or flour)(Rayner, 2009).

This study used the framework of the "triple bottom line" to assess the overall sustainability of silver-impregnated ceramic filters for POU water treatment in developing world communities. The three elements of the triple bottom line are social sustainability, environmental sustainability, and economic sustainability; thus we evaluated the ceramic filter technologies from each of these perspectives, using different metrics for each. We also evaluated a centralized water treatment and distribution system, to enable comparison between both treatment options. Because some inputs required for calculation of the selected metrics are location-dependent, we used data from Limpopo Province, South Africa for this analysis; however, it is expected that the results could be generalized for other developing world countries. To our knowledge, this is the first comprehensive sustainability assessment for the ceramic filter technology.

6.2   Methodology

We evaluated ceramic filter POU water treatment devices based on their social, economic, and environmental performances. A different metric was used to assess each criterion. All metrics for both systems, the ceramic filters and the benchmark, were calculated in spreadsheet format using Crystal Ball®. This software suite facilitates Monte

Carlo analyses by allowing users to define statistical distributions for input parameters and then automating a user-defined number of sampling trials (100,000 in this study). It then generates distributions of selected output parameters, for use in assessing uncertainty and sensitivity.

Both water systems were evaluated on the basis of their ability to deliver the so-called "functional unit" (FU), which was defined as the amount of water consumed for drinking by a "typical" developing-world household over ten years. The assumed household size was 5.2 persons, arising from the average of 5.6 persons per household in Near East/North Africa, 5.1 in Asia, 5.3 in sub-Saharan Africa, and 4.8 in Latin America(Bongaarts, 2001). Assuming 2 L/d per person for drinking water(Institute of Medicine (U.S.). Panel on Dietary Reference Intakes for Electrolytes and Water, 2005), the total amount of water consumed over 10 years is roughly 37,960 L.

6.2.1 *Evaluating Social Sustainability*

The key *social* metric was efficacy of reduction in waterborne diarrheal illness, based on previously published studies, as quantified using disability adjusted life years (DALYs). This is a commonly used metric that accounts for the amount of productive time (in years) lost due to illnesses or deaths associated with a particular disease. There are two components: years of life lost (YLL), and years of life lived with disability (YLD). These correspond to mortality and morbidity, respectively. Equations 1 and 2 summarize calculation of how many YLLs and YLDs, respectively, from diarrhea could be averted following implementation of the ceramic filters as a POU water treatment(Edejer, 2003).

$$YLD = (1 - CFR) \times \mathrm{N} \times E \times \mathit{Eff} \times \mathit{Weight} \qquad (6\text{-}1)$$

$$YLL = \frac{CFR \times Eff \times N}{r} \times (1 - e^{-r \times LE})$$ (6-2)

Where, *CFR* is case-fatality rate; i.e., the percentage of persons dying from diarrhea once they have contracted it. *CFR* values for the general population (0.04-0.12%) and children under five (0.15%) were collected from previously published literature (Kosek, Bern, & Guerrant, 2003; UNICEF & WHO, 2009; World Health Organization). A CFR value for individuals with human immunodeficiency virus (HIV) (7%) was taken from previously published literature (Brinkhof et al., 2009). *Eff* is the effectiveness of the selected intervention in mitigating diarrhea, as expressed using a percentage. This parameter was computed based on results from numerous field studies, as summarized in section 6.4.1 of supplemental information. *N* is the number of people in a typical household (5.2). *E* is the duration of illness per person per year: 0.077 year for the general population or 0.074 year for persons with HIV (du Preez et al., 2008; Mwachari et al., 2003; Schmidt et al., 2011). Weight is an empirical factor assigned to the days on which a person experiences diarrhea, as a way of accounting for impairment in quality of life. A value of 0.11 was used in this study (Murray, Lopez, Harvard School of Public Health., World Health Organization., & World Bank., 1996). *r* is an empirical parameter which assigns a quality of life premium for years lived at younger ages compared to years lived at older ages. A discount rate of 3% was used for this study (Edejer, 2003). Finally, *LE* is the typical life expectancy for the local population: 49.3 years for the general population or 34.0 years for individuals with HIV (Brinkhof et al., 2009).

The YLD and YLL quantities from Equations 6-1 and 6-2 are summed together to compute DALYs per year. This annual quantity is then integrated over some time

duration (t) of interest, as shown in Equation 6-3. The duration for this study was 10 years, based on the selected functional unit.

$$\text{Total DALYs} = \sum_{t=0}^{10\,years} \frac{(YLD + YLL)}{(1+r)^t} \qquad (6\text{-}3)$$

We computed the quantity of DALYs that could be averted for the general population, children under five, and adults with the human immunodeficiency virus (HIV). These groups have different vulnerabilities to diarrheal illness.

6.2.2 Evaluating Economic Sustainability

The key *economic* metric was cost-effectiveness, which combines the price per FU with the efficacy of diarrheal prevention metric referenced in Section 6.3.1. These two parameters are combined into a ratio, with price as numerator and efficacy as denominator, similar to "cost effectiveness" ratios described by the World Bank in 1993 and later revised by the World Health Organization(Edejer, 2003). The retail price per filter was based on data from a survey by Rayner et.al(Rayner, 2009), accounting for not only the cost of raw materials, but also for capital investment, maintenance and reinvestment, and marketing, all of which are essential to sustain a functioning ceramic filter factory. The time value of money over the 10-year span encompassed by the FU was accounted for with a 5% discount rate.

6.2.3 Evaluating Environmental Sustainability

There were five environmental metrics: net energy consumption per FU (in MJ), net global warming potential per FU (in Kg CO_2-equivalent), net water usage per FU (in

m^3), smog potential per FU (in g NO$_x$-equivalent), and particulate matter emissions per FU (in g PM10, comprising particles with diameters less than 10 μm). These quantities were computed using life cycle assessment (LCA). This a systematic accounting of all impacts associated with a process or product throughout all stages of its life cycle; from extraction of raw materials, through materials processing, manufacturing, distribution, use and maintenance, and ultimately disposal or recycle at the end of its useful life. Figure 1 shows the system boundaries for the ceramic filter LCA that were included in this study, identifying the necessary materials and energy inputs required to produce each filter and also identifying the sub-processes which make of the manufacturing (i.e., production) stage. Life cycle data for the materials and energy inputs were taken from the ecoinvent database(Weidema, 2007). Section 6.4.2 of the supplemental information provides additional details about the LCA procedures used for the ceramic filter.
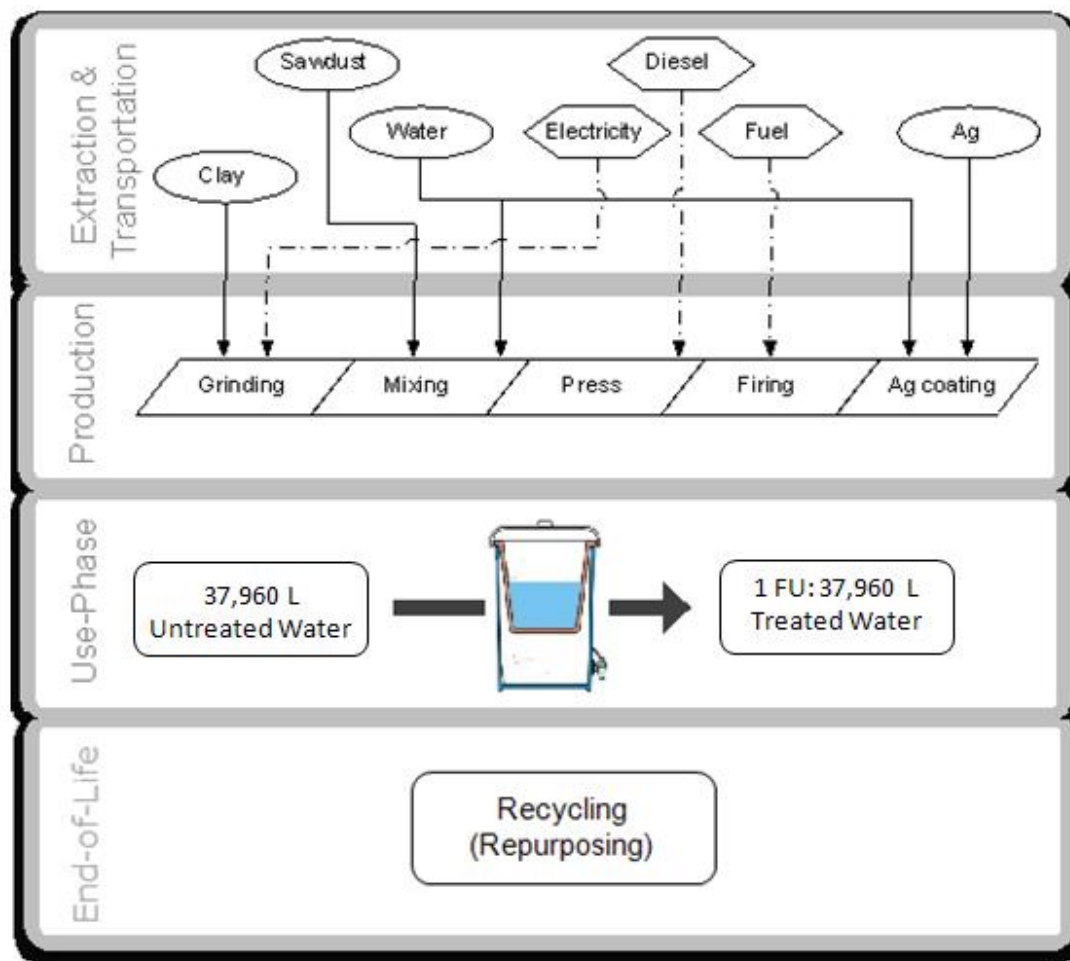
Figure 6-1. System boundaries for the ceramic filter POU LCA. Life cycle stages are shown from top to bottom. Ovals depict raw materials inputs, and hexagons depict energy inputs.

6.2.4   Benchmarking Analysis

The social, economic, and environmental metrics from Sections 6.3.1, 6.3.2, and

6.3.3, respectively, were also computed for a typical centralized water distribution system

in South Africa. This system performs the following functions: collection and

impoundment of raw water, treatment of raw water to potable quality, and distribution of

potable water. We assumed that surface water from an aboveground reservoir (i.e., dam)

111

is used as the raw water and that the treatment train consists of coagulation-flocculation-settling, gravity filtration, granular activated carbon (GAC) absorption, and chlorination for disinfection (Bonton, Bouchard, Barbeau, & Jedrzejak, 2012). Finally, because environmental burdens of a centralized water system are accrued mostly during the operation (use) phase (typically 60-70 years), construction and decommissioning burdens were excluded from the benchmark LCA analysis(Stokes & Horvath, 2006). Sections 6.5.2 and 6.5.3 of the supplemental information provide additional details about calculation of the social/economic and environmental (LCA) metrics, respectively, for the centralized water system.

6.3 Results and Discussion

6.3.1 Social Sustainability

With respect to social performance, the most desired outcome for any water treatment system is sustained prevention of waterborne illness. Thus, our first task was evaluating the ceramic filter's ability to reduce diarrheal illnesses and deaths in three groups of interest: the general population, children under five, and adults with HIV. The efficacy of the filters was quantified using DALYs, as summarized in Equations 6-1 to 6-3 and Section 6.4.1 of the supplemental information. The values of *CFR* and *weight* arose from selection of diarrhea as the target illness. Similarly, the values for *N* and *LE* arose from selection of the Limpopo Province as the location of interest. *r* was fixed by standard convention. Thus, *Eff* was the most informative parameter for calculating what reduction of DALYs could be achieved by the ceramic filter POU technology or the centralized system.

Eff values for the silver-impregnated ceramic filters were taken from previously published field tests. Clasen et al. (2004) reported that silver-impregnated ceramic filters reduced diarrheal incidence among the general population by 64% in a Bolivian community. The same study also reported a 71% reduction in diarrhea among children under five. A similar study in Cambodia reported 46% reduction for the general population and 48% reduction for children under five (Hagan et al., 2009). These data were assigned to input distributions for *Eff* in both populations. The resulting values for DALYs averted per FU by the use of the ceramic filter technology were 0.71 year for the general population and 0.14 for children under five. The breakdown of DALYs for the general population was 0.50 years of life lost (YLL; i.e., mortality) plus 0.21 years of life with disability (YLD; i.e., morbidity) for a typical household over ten years. Correspondingly, the DALY breakdown for children under five was 0.11 YLL plus 0.02 YLD.

The ceramic filters were also evaluated for their effectiveness in reducing waterborne diarrheal illness among adults with HIV. This is of great relevance because HIV-positive individuals make up an appreciable percentage of the population in many developing countries (e.g., roughly 30% in South Africa since 2008(Joint United nations Program on HIV/AIDS (UNAIDS), 2012)), and persons with HIV are especially vulnerable to waterborne illness(Mwachari et al., 2003; Serwadda et al., 1985). Diarrhea is one of the most frequent ailments of HIV-positive persons in resource-limited countries (Carr, Marriott, Field, Vasak, & Cooper, 1998; Maggi et al., 2000). Raw data for estimation of the *Eff* parameter were taken from a field study of persons with HIV receiving standard antiretroviral therapy (ART) in Limpopo Province and using ceramic

water filters(Abebe et al., 2013). The average value of *Eff* for the POU device was 79%. This translates to 15.5 DALYs averted (15.5 YLL and 0.02 YLD) over ten years.

Eff values for the centralized water treatment system were also taken from published studies on centralized water distribution in the developing world. Bahl et al.(1976) reported the risk of diarrhea contraction to be 63% for consumption of piped water in Zambia. Wang et al. (1989) reported a similar value of 62% for consumption of piped water in a Chinese community. These values were converted into effectiveness via subtraction from 100%, such that *Eff* for the general population was roughly 37.5%. A previously published review of 67 studies found that centralized water systems reduce childhood diarrhea by 21-30% (Esrey, Feachem, & Hughes, 1985), thus *Eff* was roughly 26% for children under five. These values are lower than *Eff* values for centralized water systems in the US or Europe; however, lack of proper management and recontamination during distribution are known to adversely impact water quality for systems in developing countries (Esrey et al., 1985; Ryder et al., 1985). The resulting DALY reductions for the benchmark system were 0.48 per household for the general population and 0.17 per household for children under five. The breakdown was 0.34 YLL plus 0.14 YLD for the general population and 0.14 YLL plus 0.03 YLD for children under five. These values are lower than what was reported for the ceramic filter POU technology, consistent with previous studies in which children with access to piped water were found to have higher diarrheal incidence than children without access to piped water(Ryder et al., 1985; Tonglet, Isu, Mpese, Dramaix, & Hennart, 1992).

The ceramic filter POU technology offers additional social sustainability benefits, compared to the centralized system, that are less easily quantified than DALY reduction.

For one, field testing indicates that the filters offer good cultural acceptance, by virtue of their convenience and health benefits (Kallman et al., 2011). They also offer good robustness and resiliency compared to the centralized system, because there is less likelihood of post-treatment recontamination during normal operation and the risk of widespread service disruption following natural disasters is significantly reduced. Finally, the use of local materials and labor to produce the filters gives the community a sense of ownership over the technology and also renders the filter factory enterprise a vehicle for stimulation of the local economy(The Ceramics Manufacturing Working Group, 2011). In contrast, centralized water treatment and distribution systems are so capital-intensive that their construction in developing countries must be financed or subsidized by outside entities, such as the World Bank (Gadgil, 1998).

Having quantified and/or articulated the possible social sustainability *benefits* associated with use of the ceramic filter POU and its benchmark system, it was then necessary to compute what economic and environmental *costs* could arise from use of either option. A *sustainable* water system should deliver safe water without engendering undue environmental burdens or economic costs. Thus, cost-benefits ratios were computed for both systems and compared to each other.

6.3.2 Economic Sustainability

The most immediate indicator of economic sustainability for each evaluated water treatment technology is the direct cost to the consumer for delivery of one FU. For the ceramic filter, it was first necessary to compute how many filters would be required to deliver the FU over 10 years. Taking into account filter lifetime (~3.5 years(Campbell, 2005; Lantagne, 2001; UNICEF & Waste Sanitation Project, 2007)), the likely number

of filters required per household at one time (1 (van Halem et al., 2009)), and the

expected factory yield (~88% (Rayner, 2009)), roughly 3.5 filters are required to deliver

1 FU over 10 years. Rayner (2009) reports that retail prices are $8-$35 per filter (average

$16.68); accounting for raw materials, capital investment, maintenance and reinvestment,

and marketing. Taking into account the time value of money over 10 years, the full

economic cost to deliver 1 FU via the ceramic filter POU technology is approximately

$63.

For the centralized water system, it has been estimated that the initial investment

for a system with 40 years of useful life is roughly $164 per person in South Africa and

nearby countries. Operational costs for treatment and distribution of the piped water to

individual households account for an additional $0.20-0.30 per m^3 delivered (World

Health Organization., UNICEF., Water Supply and Sanitation Collaborative Council., &

WHO/UNICEF Joint Water Supply and Sanitation Monitoring Programme., 2000).

Taking into account the time value of money, the full economic cost to deliver 1 FU via

the centralized water system is roughly $221. Thus, the ceramic filter POU technology is

less expensive than the benchmark. However, the costs alone fail to capture the full

complexity of this comparison, since both systems do not necessarily deliver the same

water quality. We therefore defined the cost-effectiveness ratio (CER) of each water

treatment system as the cost per FU in each system divided by the quantity of DALYs

averted by each system. The results of the cost and cost-effectiveness comparisons

between the ceramic filter POU and the centralized system are depicted in Figure 2.
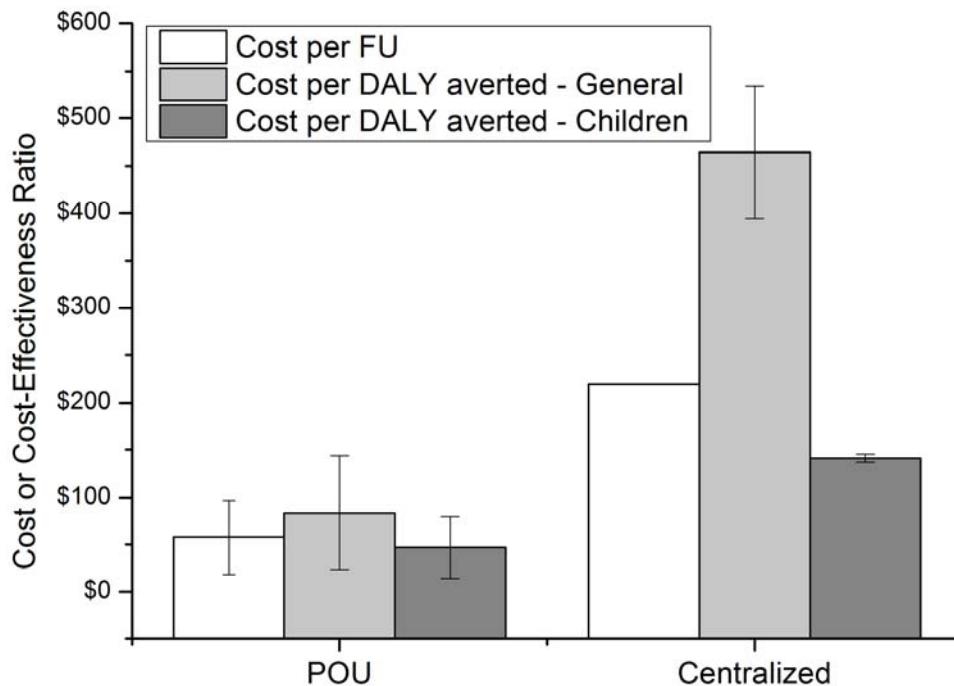
Figure 6-2. Cost per functional unit (FU) and cost per DALY averted for the general population ("general") and children under five years old ("children"). Data show the comparison between the ceramic filter ("POU") and the benchmark centralized system. White bars represent costs per FU. Gray bars represent cost-effectiveness. Error bars represent empirical standard deviations from Monte Carlo sampling; however, lack of data prevented computation of error bars for the cost per FU in the centralized system.

From Figure 6-2, the ceramic POU technology is not only less expensive per FU than the centralized system, but it also delivers better cost-effectiveness when accounting for reduction in diarrheal illness. When considering the general population, the filter POU ($84/DALY averted) is nearly six times more cost effective than the centralized system ($466/DALY averted). When considering only children under five, the filter POU ($47/DALY averted) is three times more cost effective than the centralized system ($141/DALY averted). This comparison cannot be performed for the population of individuals with HIV, because we were unable to find data for diarrheal reduction among

HIV-positive persons using a centralized water treatment system. Still, the ceramic filter exhibits excellent cost-effectiveness ($1.11/DALY averted) for this especially vulnerable population. For perspective, the World Bank estimates that standard ART treatment typically costs $6-12 per DALY averted; therefore, the additional cost for the filter should be both manageable and worthwhile as a secondary intervention(Jamison et al., 2006).

Beyond the comparisons in Figure 6-2, the ceramic filter POU also exhibits better cost-effectiveness than any of the technologies evaluated by Clasen et al.(Thomas F. Clasen & Haller, 2008) for the region including South Africa. Their range of reported cost-effectiveness values was $95-180 per DALY averted (for the general public). Interestingly, the Clasen (2008) study did include evaluation of ceramic filters POU devices; however, their filters were imported from developed countries, and they did not contain any silver to enhance the filter's disinfection capability. These changes resulted in significantly decreased cost-effectiveness compared to what is shown in Figure 2, because more expensive filters were used to deliver poorer-quality treated water. Finally, the WHO's Commission on Macroeconomics and Health (CMH) defines "cost-effective" interventions as those costing less than or equal to three times the gross domestic product (GDP) per capita. Similarly, "very cost-effective" interventions must cost less than one times the GDP per capita(Shillcutt, Walker, Goodman, & Mills, 2009). Based on these definitions, the ceramic filter constitutes a "very cost-effective" water treatment intervention(World Health Organization CHOosing Interventions that are Cost Effective (WHO-CHOICE)).

6.3.3 Environmental Sustainability

The third component of sustainability is environmental sustainability. Although the ceramic filter POU technology has been the subject of several studies regarding its social and economic performances (as noted in Sections 6.3.1 and 6.3.2), there has been virtually no assessment of its environmental impacts. Moreover, many published LCA studies have focused on elucidating the environmental impacts of products, processes, or services for industrialized processes in developed countries; whereas fewer have focused on less industrialized countries, almost completely overlooking opportunities for developing world countries to pursue truly sustainable development. This study evaluates the environmental sustainability of locally-produced ceramic filters, to understand how they perform compared to the centralized water treatment systems which have become the technology of choice in most industrialized nations.

As shown in Figure 6-1, the environmental LCA of the ceramic filter POU device accounted for extraction of mostly local raw materials, transportation of materials and energy to the factory, manufacturing of the filter, use phase, and end of life. Sections 6.5.2 outlines the LCA calculations for procurement and transportation of clay, combustible material, water, silver solution, and energy sources (e.g., wood, diesel, etc). Section 2.1.3 of the SI summarizes LCA calculations for filter production processes, highlighting the dramatic variability that currently exists among operating filter factories. We accounted for this variability using three different scenarios: high-tech, low-tech, and medium-tech. The "high-tech" scenario assumes that all production processes are carried out using electricity or other advanced fuels (i.e., propane). In contrast, the "low-tech" scenario assumes that all production processes are carried out using either manpower or primitive fuels (i.e., wood). The third scenario, "medium-tech" reflects the expectation

119

that most filter factories will use some combination of high-tech and low-tech processes; as such, this scenario is expected to be most representative of the filter factories currently in existence(The Ceramics Manufacturing Working Group, 2011). This scenario was parameterized via random selection of which production steps were completed using either high-tech or low-tech methods. The LCA impacts of all steps were then added together over the entire filter life cycle. Use of Monte Carlo sampling (i.e., 100,000 trials) ensured adequate coverage of all combinations for high-tech and low-tech options for the various steps. It was assumed that the manufacturing (production) stage is the only life cycle stage subject to such wide variability. Finally, Section 6.4.1 describes LCA modeling of the use phase and end-of-life. Both of these life cycle stages accounted for negligible LCA impacts, and it was assumed that the filters would be used for some other purpose (i.e., storage) once they were no longer suitable for water treatment.

Figure 6-3 summarizes the environmental performance of the ceramic filter POU technology relative to that of the centralized water system. Five key LCA impacts were evaluated for the production of 1 FU in each system: energy use (panel A), global warming potential (panel B), water use (panel C), particulate matter emissions (PM10) (panel D), and smog formation potential (panel E). In all panels, the life cycle impacts for the high tech, medium tech, and low tech ceramic filter scenarios are plotted using column graphs. For comparison, the corresponding performance for the centralized water system is shown using a dashed line. The numerical data corresponding to Figure 6-3 are also presented in Table 6-S11 of the SI. There are three important observations arising from Figure 3. These pertain to: 1) the relative performances of the high-tech, medium-tech, and low-tech ceramic filter scenarios; 2) the breakdown of each LCA impact by life

cycle stage; 3) and comparison between the ceramic filters and the centralized water system. These items are discussed in more detail in the following paragraphs.
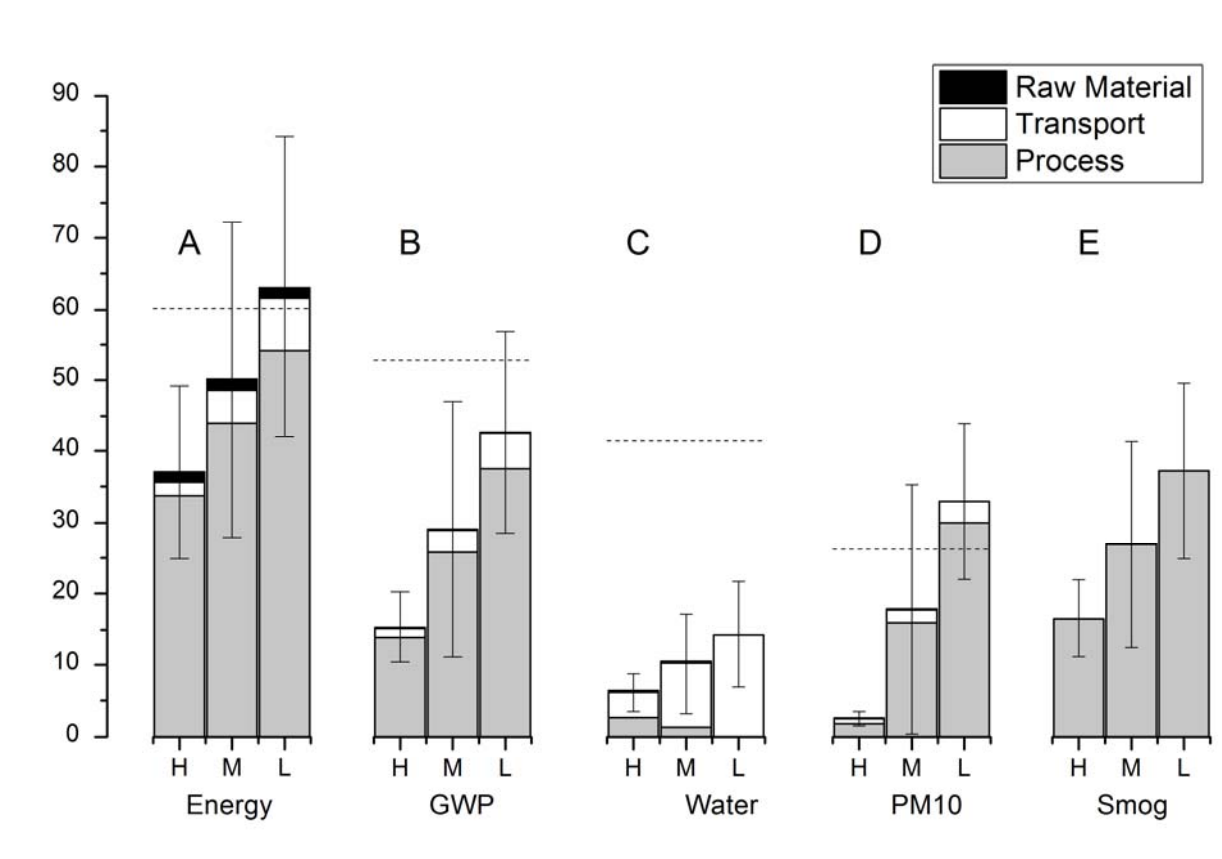
Figure 6-3. Environmental impacts per FU: (A) Total energy use (×10 MJ), (B) global warming potential (Kg CO_2-eq), (C) water use (m^3), (D) particulate matter emissions (PM10) (g) and (E) smog formation potential (g NO_x-eq) Error bar represents one standard deviation from iterative Monte Carlo simulation. Dashed horizontal lines represent corresponding environmental impacts from the benchmark centralized water system. The value of smog formation potential for the centralized system (0.1361 g) is too small to be depict on these axes in panel E. Column labels "H", "M", and "L" correspond to high-tech, medium-tech and low-tech scenarios, respectively.

First, for all LCA impacts, the performance of the medium-tech scenario is always between that of the high-tech and low-tech scenarios. This offers some validation for the randomization approach used to parameterize the medium-tech scenario. From a recent survey of existing filter factories (Rayner, 2009), it found that many factories use some

combination of high-tech and low-tech sub-processes. Thus, the medium-tech scenario likely captures "typical" filter factory performance even though it may not directly correspond to any specific, individual factory configuration. Further comparison of the three scenarios reveals, perhaps unexpectedly, that the high-tech scenario results in lower environmental burdens than the low-tech scenario for all evaluated LCA impacts. This suggests that adoption of appropriate advanced technologies improves the overall environmental performance of ceramic filter production. In particular, the use of propane-fueled kilns instead of wood-fueled kilns significantly improves both energy efficiency and particulate matter emissions (PM10). Thus, it is beneficial that the use of propane kilns appears to be on the rise among existing and new filter factories (The Ceramics Manufacturing Working Group, 2011).

Second, regarding the breakdown of each LCA impact by life cycle stage, the manufacturing stage is by far the largest contributor to all environmental burdens except water use. The sub-processes comprising this life cycle stage include: grinding the clay, mixing the clay with water and combustible material, pressing the clay into a pot-shaped filter, firing the filter to form the ceramic and burn off the combustible material, and coating the filter with a solution of silver nanoparticles. Many of these sub-processes can be achieved using either "high-tech" or "low-tech" procedures; therefore, the relative contribution of each sub-process to the overall impact varies by scenario and by LCA impact category. For the medium-tech scenario, the relative contribution of each sub-process is roughly as follows: firing >> grinding ≈ mixing ≈ pressing >> coating with silver. The transportation life cycle stage is the greatest contributor to overall water use and second largest contributor to all other environmental impacts. Less than 0.1% of each

122

transportation burden accounts for transport of the silver nanoparticles from Europe or China to Africa via airplane and diesel truck. This is somewhat surprising, given that this material must travel 3,000-9,000 km to arrive at a filter factor; however, the very large distance is evidently offset by the very small quantity of silver required to produce 1 FU (~225 mg). All other materials are locally produced, which gives them very low transportation burdens. Similarly, the use-phase and end-of-life burdens were essentially negligible.

The third and last observation from Figure 6-3 pertains to the LCA-based comparison between the ceramic filter POU technology and the centralized water system. LCA calculations for the centralized water system were summarized in Section 6.4.2. From Figure 3, the ceramic filter offers better environmental performance than the centralized water treatment system in all evaluated impact categories other than smog formation potential. This was an unanticipated result of this study, but breakeven analyses for the medium-tech scenario indicate that this trend holds true so long as the daily volume of water treated per household is greater than 8.6 L (See Table 6-S10). At daily treatment volumes less than this value, the ceramic water filters deliver larger environmental burdens per FU than the centralized water system; however, the WHO recommendation of 2 L of drinking water per day per individual requires that at least 10.4 L be treated daily for a household size of 5.2 persons(WHO/UNICEF Joint Water Supply and Sanitation Monitoring Programme. et al., 2006). Finally, the poor smog performance of the ceramic filter arises almost entirely (99%) from firing the filters. From panel E of Figure 6-3, use of high-tech equipment and/or procedures (e.g., high efficiency propane kiln) instead of low-tech options (e.g., wood kiln) significantly reduces smog formation

potential for the ceramic filter but does not make it less than that of the centralized water system. Thus, stakeholders will need to evaluate to what extent smog formation is a significant priority compared to all other environmental impacts.

To understand the "environmental cost-effectiveness" of the filters compared to the centralized system, it was necessary to normalize the environmental burdens from Figure 6-3 in a manner analogous to what was done for economic costs in Section 6.4.2. Each type of LCA impact was thus divided by the quantity of DALYs that could be averted using either technology. Data corresponding to the ceramic filter's medium-tech scenario were used for these calculations. Results are presented in Figure 6-4 (and Table 6-S12). These data closely mirror Figure 6-3; whereby, the ceramic filter offers better environmental cost-effectiveness than the centralized water system for all evaluated impacts except smog. The use of the DALY normalization appears to accentuate the differences between the POU technology and the benchmark, making it seem more preferable (compared to Figure 6-3) on the basis of energy, water, PM10, and GWP; but less preferable on the basis of smog formation potential.
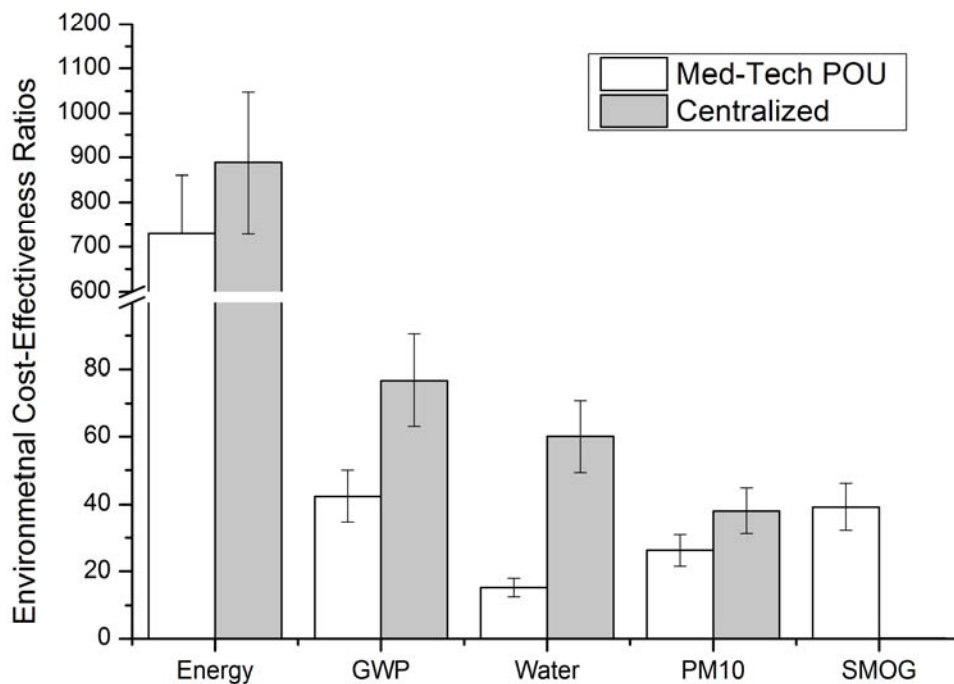
Figure 6-4. Environmental impacts per FU for the POU ceramic filter technology and the centralized water system, normalized using the quantity of DALYs averted. Evaluated impacts include: energy use ("energy") in MJ, global warming potential (GWP) in Kg CO_2-eq, total water consumption ("water") in m^3, particulate matter emissions ("PM10") in g, and smog formation potential ("smog") in g NO_x-eq. All ceramic filter POU data correspond to the medium-tech LCA scenario. DALYs correspond to the general population. Error bars represent empirical standard deviations derived from Monte Carlo sampling.

6.3.4 Implications

This study presents quantitative evidence that silver-impregnated ceramic filters deliver better quality of life improvements, better cost-effectiveness, and enhanced environmental performance compared to centralized water systems of the developing world. This convergence of social, economic, environmental criteria offers clear indication that the ceramic filter POU technology is a more *sustainable* choice for drinking water treatment in developing countries than the "one-size-fits-all" centralized

treatment approach that has been widely adopted in industrialized countries. The sustainability benefits of the ceramic filter POU technology are especially pronounced for vulnerable populations such as children under five and persons with HIV. Thus, this technology is a compelling option for delivery of safe drinking water in developing countries.

6.4 Supplemental information

6.4.1 *Social and Economic Performance Calculations*

6.4.1.1 *DALY Reduction*

Table 6-S1 summarizes the numerical parameters required for DALY calculations using Equations 6-1 to 6-3 in the text. Values of *CFR*, *weight*, *LE*, *E*, *r*, and *N*, were the same for both the ceramic filters and the centralized water system. In contrast, effectiveness (*Eff*) values were different between each system. Different values of *Eff* (and some other parameters) were also used to compute DALYs averted for the general population ("general"), children under five years old ("children"), and HIV-infected adults ("HIV").

Table 6-S1. Parameters used to compute DALYs averted via use of both treatment systems.

Parameter	Modeled Distribution	Min Value	Max Value	Likeliest Value	Sources
CFR (general)	Triangular	0.04%	0.12%	0.08%	(World Health Organization. et al., 2000)
CFR (children)	Single Value	-	-	0.15%	(Kosek et al., 2003; UNICEF & WHO, 2009)
CFR (HIV)	Single Value	-	-	7%	(Dillingham et al., 2009)
Weight	Single Value	-	-	0.15	(Lopez & Murray, 1998)
LE (general, children)	Single Value	-	-	49.3	(Central Intelligence Agency)
LE (HIV)	Single Value	-	-	34.0	(Brinkhof et al., 2009)
E (general, children)	Single Value	-	-	0.077	(du Preez et al., 2008)
E (HIV)	Single Value	-	-	0.074	(Mwachari et al., 2003)
r	Single Value	-	-	0.03	(Edejer, 2003)
N	Single Value	-	-	5.2	Functional unit
Eff (general, filters)	Uniform	0.46	0.64	-	(T. F. Clasen et al., 2004)
Eff (children, filters)	Uniform	0.48	0.71	-	(T. F. Clasen et al., 2004; Hagan et al., 2009)
Eff (HIV, filters)	Normal	Average = 79% St. Deviation = 2%			(Abebe et al., 2013)
Eff (general, centralized)	Uniform	0.37	0.38	-	(Bahl, 1976; Wang et al., 1989)
Eff (children, centralized)	Uniform	0.21	0.30	-	(Esrey et al., 1985)

6.4.1.2   Cost-Effectiveness

- *Delivery of the Functional Unit – Ceramic Filters*

The first stop in evaluating cost effectiveness of the ceramic filter POU technology is determining how many filters are required to deliver 1 FU over 10 years. Several factors were taken into consideration for this calculation, including: the average lifetime of one filter, the number of filters required per household at one time to meet daily drinking water needs, and the efficiency of filter production.

Filter Lifetime and Number of Filters per Household. Ceramic filters have a finite lifetime, because: 1) they are subject to cracking and breaking during improper handling, and 2) the quality/quantity of the output water is known to degrade slowly over time (van Halem et al., 2009). Filter lifetime also depends on various factors such as frequency of cleaning, the quality of water being treated, etc. But, even under the best of conditions, more than one filter is likely required for the ten-year duration specified by the FU. Several studies indicated the ceramic filter could have a potential service life above 5 years (Campbell, 2005; Lantagne, 2001), but most agencies recommend a service lifetime of about 2 years (UNICEF & Waste Sanitiation Project, 2007). These data were thus combined into a uniform distribution with minimum = 2 years and maximum = 5 years. The number of filters required per FU was then computed stochastically for each Monte Carlo trial, by dividing filter lifetime into the required duration.

Filters per Household For simplicity, it was assumed that each household would have only one filter at any given time. This was deemed acceptable, given that the amount of water required per household (5.2 persons × 2 L/d = 10.4 L/d) is less than the

128

expected daily output of one single filter (2 L/h $\times$ 12 waking hours per day 24 L/d (van Halem et al., 2009)).

Factory Yield. Not all of the ceramic filters produced at a given factory are suitable for consumer use. For example, some filters in a particular batch generally exhibit flow rates outside of that factory's acceptable range. These filters are then either discarded or ground-up and recycled. In either event, the factory's yield is less than 100%. This was accounted for using previously published failure rates fit to a normal distribution with average = 12% and standard deviation = 8%. The yield rate (as %) was then defined as 100% less the failure rate.

- *Cost of the Functional Unit – Ceramic Filters*

From a survey by Rayner (Rayner, 2009), retail prices are $8-$35 per filter, with an average value of $16.68. This data was assembled into the following triangular distribution for price per filter: minimum = $8, maximum = $35, and likeliest = $16.68. These prices account for raw materials, capital investment, maintenance and reinvestment, and marketing, all of which are essential to sustain a functioning ceramic filter factory. The time value of money over the 10-year span encompassed by the FU was accounted for using a 5% discount rate.

- *Cost of the Functional Unit – Centralized Water Treatment System*

The economic cost of a centralized water supply system for the WHO region containing South Africa was estimated based on previously published data (Haller, Hutton, & Bartram, 2007). The initial investment for a system with 40 years of useful life is roughly $164 per person. Operational costs for treatment and distribution of piped water to household users accounts for an additional $0.20-0.30 per m^3 delivered(World

Health Organization. et al., 2000). As for the ceramic filters, annual discount rate was 5%.

6.4.2 Environmental Performance Calculations

6.4.2.1 Calculation Details for Selected LCA Impacts

- *Global warming potential*

Global warming (GWP) potential was first quantified in terms of kilogram equivalents of CO_2 based on the IPCC (intergovernmental panel on climate change) protocol. The time horizon is chosen to be 100 years. The conversion factors between greenhouse gas emission and global warming potential were listed in the table as follows.

Table 6-S2 Global warming potential values for each greenhouse gas

Greenhouse gas	Global warming potential
CO_2	1
CH_4	25
N_2O	298

6.4.3 LCA Modeling for the Ceramic Filters

6.4.3.1 Extraction and Transport of Raw Materials and Other Inputs

Four main materials are required to make a ceramic filter: clay, combustible material, water, and silver solution. At some factories, sand, grog or laterite is also included in the mixture, but these have been excluded from this analysis because they are somewhat atypical. Electricity and/or other fuels are also required.

- *Clay*

The quality of clay strongly affects the quality of the resulting filter, since it impacts the filter's flow rate, durability, shrinkage and propensity towards cracking and

130

warping. Consistent with current practice, we assumed that filter factories are located

nearby to suitable clay deposits where the clay can be collected using manual labor. Thus,

there was no need to account for upstream or transportation burdens associated for the

clay input. Nevertheless, it was also assumed that, on average, 4.7 kg of clay is required

per filter (with standard deviation = 0.75 kg) (Rayner, 2009); therefore, 16.5 kg of clay is

required per FU.

- *Combustible Material*

Addition of a combustible material, which can be burned off during kiln firing,

results in the formation of porous filter media. Sawdust, rice husks, or peanut shells are

suitable for this purpose, and each is widely used for filter production depending on local

availability. As an added benefit, each of these materials comprises a "waste" by-product

arising from other industrial processes.

Because sawdust is the most widely used of all the typical combustible materials

(used in 50% of existing filter factories (Rayner, 2009)), it was used as representative

combustible material for this study. The ratio of sawdust to clay strongly affects the

performance of the finished filter (e.g., filtration rate, crack rate, etc.) and is highly

dependent on site-specific conditions (e.g., clay quality, firing technique, etc.)(Rayner,

2009). Based on current practice, it was assumed that the weight fraction of sawdust in

the pre-firing mixture takes the following triangular distribution: minimum = 5%,

maximum = 25%, and likeliest value = 20%. Thus, roughly 1.3 kg sawdust is required to

produce one filter, and 4.7 kg of sawdust is required to deliver one FU.

Environmental impacts of the sawdust input were assigned based on a weight

allocation procedure, consistent with typical LCA. Sawdust comprises roughly 0.06 kg of

the total mass of wood used to produce 1 kg of lumber from softwood lumber (Milota, West, & Hartley, 2005); therefore, 6% burdens associated with lumber production can be attributed to the sawdust if it is used for some beneficial purpose (i.e., for production of ceramic filters). As softwood is the major supply of commercial wood because of the ability to be dried and processed faster and more easily, hardwood was excluded as the source of sawdust production.

Table 6-S3 summarizes calculation of environmental impacts for sawdust, based on life cycle database entries for softwood timber. For simplicity, it was assumed that the sawdust used for filter production arises exclusively from softwood timber production. The density of softwood lumber was set to 525 kg/m^3. Thus, these values were multiplied by 6%.

Table 6-S3. Life cycle inventory of sawdust as by product of lumber production.

Burdens \ Item	Energy Use (MJ)	GWP (kg CO2 eq)	PM10 (g)	Smog (g NOx eq)	Water Use (m3)
Softwood timber / kg	19.62	1.11E-01	8.55E-02	7.58E-04	2.34E-03
Sawdust / kg	1.1772	6.66E-03	5.13E-03	4.55E-05	1.40E-04

It was assumed that filter factories are located within convenient driving distance of a lumber factory or some other site from which sawdust can be procured. Thus, this distance was somewhat arbitrarily assigned to a uniform distribution spanning 25-100 km (Mellor, Personal communication). It was also assumed that a small, diesel-powered truck (<3.5 t) would be used for transportation of the sawdust.

- *Water*

During filter production, water is used to wet the mixture of clay and combustible material so that the material will hold its shape during and after compression. The water typically makes up 25% of the mixture's total wet weight, which was, on average 2 kg per filter or 7.1 kg per FU. A small amount of water is also used to dissolve the nanoparticle solution required for silver coating; about 0.3 kg per filter based on a recent survey of operational filter factories (Rayner, 2009), corresponding to roughly 1.1 kg per FU.

Aside from net consumption, no other environmental burdens were assigned for the water, since it was assumed that the water would be procured from nearby underground or surface sources without pre-treatment or significant pumping.

- *Silver*

It has been widely demonstrated that impregnation of a clay filter with colloidal silver dramatically increases its efficacy as a POU water treatment device. This is because silver deactivates waterborne pathogens through some mechanism that is not well understood at present (Lantagne, 2001; Oyanedel-Craver & Smith, 2008). There are several ways by which the silver can be applied, but more than 50% of existing filter factories use the brushing method, whereby a solution of colloidal silver is brushed by hand onto the filter and then allowed to air dry (Rayner, 2009). The brushing method is the simplest method, and, conveniently, use of this method also enables easy quantification of how much silver is applied to each filter. For this study, the mass of silver per filter was set to the following triangular distribution: minimum = 32 mg, maximum = 96 mg, and likeliest value = 64 mg (Rayner, 2009).

Life cycle inventory data for a silver nanoparticle solution was adapted from previous work by Walser et al.(Walser, Demou, Lang, & Hellweg, 2011). Their data was modified using LCA database information (from EcoInvent version 2.0(Weidema, 2007)) for the raw materials and energy inputs they identified in their study (e.g., oxygen gas, silver-octanoate, tributylphosphate) as necessary inputs for production of silver nanoparticles.

Table 6-S4. Life cycle inventory data for production of 1 kg silver nanoparticle.

``	Energy Use (MJ)	GWP (kg CO_2 eq)	PM10 (g)	Smog (g NO_x eq)	Water Use (m^3)
Silver Nanoparticles/kg	3180	221	200	1.03	1170

Most, if not all, colloidal silver and silver nanoparticles used for POU filters are produced in developed countries. In fact, many factories worldwide obtain their silver from either Laboratories Argenol in Spain or several factories in China (The Ceramics Manufacturing Working Group, 2011). As such, transport of silver generally consists of two parts: a long-distance international transport via commercial aircraft, followed by a short-distance ground transport from the airport to the factory. For this study, international travel distance was set to a triangular distribution: min = 3,000 km, max = 9,000 km, and likeliest value = 5,457 km. These distances are based roughly on Google-Earth estimated distances between factories in either Spain or China and several existing filter factories in Africa (Tanzania, South Africa, Nigeria), Latin America (Dominican Republic, Peru, Haiti), or Asia (Indonesian, Thailand, Cambodia). Local transport distance (via small truck) was likewise set to a triangular distribution: minimum = 200 km, maximum = 800 km, and likeliest value = 400 km, based on the distances from the main airports to the factory sites.

6.4.3.2   Electricity, Other Fuels, and Transportation Life Cycle Impacts

Many of the processes required for production of ceramic filters are powered by electricity and/or other fuels (propane, diesel, or wood). Environmental impacts associated with each fuel and the various modes of transport modeled within this study are outlined in the following paragraphs.

- *Electricity*

Electricity use comprises a significant contributor to environmental burdens associated with water treatment and distribution systems (Friedrich, Pillay, & Buckley, 2007). In this study, life cycle inventory data for electricity from the South African grid was assumed to be representative of power production in other developing countries. Their grid profile is as follows: 88.6% coal, 6.7% nuclear, 0.7% hydropower, 1.3% pump storage, and 2.7% imports (Friedrich, Pillay, & Buckley, 2009). Life cycle inventory data for South African electricity production (including transmission) is summarized in Table 6-S6. Electricity consumption for production of ceramic filters was estimated to be 0.0324 MJ per filter, which corresponds to roughly 1.15 MJ per FU.

- *Propane*

Some propane use is required for filter production under the high-tech production scenario. Life cycle inventory data for propane production is summarized in Table S4. Propane demand was 0.84 kg per filter, or 2.97 kg per FU. It was assumed that propane transport occurs over a distance of 100 km, in a small diesel truck. Calculations pertaining to the heat content of the propane used and the emissions generated when it is combusted are summarized in Section   .

- *Wood*

Wood is the sole fuel used under the low-tech scenario. Consistent with current practice, it was assumed that wood could be procured from one of two sources, either: 1) natural, untended forest growth; or 2) managed tree plantations, wherein nursing, tending, thinning, and harvesting are optimized for fast-growth(Jungmeier, Werner, Jarnehammar, Hohenthal, & Richter, 2002). For simplicity, it was assumed that equal amounts of wood from natural and managed forest sources are used for filter production. Thus, the life cycle impacts for "harvested" wood (Table 6-S5) were divided by two to account for both wood types. It was also assumed that both types of wood would require transportation over a 100-km distance, in a small diesel truck (<3.5 t) (Mellor, personal communication, 2012). Finally, calculations pertaining to the energy content of the wood used and the emissions generated when it is combusted are summarized in next section.

Table 6-S5. Life cycle inventory of wood from two sources.

Burdens Item	Energy Use (MJ)	GWP (kg CO_2 eq)	PM10 (g)	Smog (g NO_x eq)	Water Use (m³)
Natural Wood / m3	1500	0	0	0	0
Harvested Wood / m3	10300	15.5	18.5	0.124	0.202
Wood / m3	5900	7.75	9.25	0.062	0.101

- *Diesel*

Diesel is required for operation of ground transportation equipment (small trucks) and also the hydraulic press required for filter pressing under the high-tech scenario. Diesel consumption for ground transport was accounted for using the "small truck" transportation impact factor, as outlined as following section and Table 6-S6. For the hydraulic press, it was assumed that this equipment is powered using a modified

automobile engine, which consumes roughly 0.042 kg of diesel per filter (Lisa Ballantine, personal communication, July 2011). This corresponds to 0.15 kg of diesel per FU. Life cycle data for diesel production is included in Table 6-S6.

- *Transportation*

As referenced in previous sections, two types of transportation were accounted for in this study: short-distance transport in diesel-powered small trucks, and intercontinental transport via commercial aircraft. Life cycle impacts for both modes are summarized in Table 6-S6.

Table 6-S6. Life cycle inventory of electricity, fuel and transportation.

Burdens / Item	Energy Use (MJ)	GWP1 (kg CO_2 eq)	PM10 (g)	Smog (g NO_x eq)	Water Use (m^3)
Electricity/ MJ	3.14	0.36	0.24	1.01E-03	0.07
Propane / kg	55.00	0.60	0.25	1.96E-03	0.76
Wood / m3	5900.00	7.75	9.25	6.20E-02	0.10
Diesel / kg	53.90	0.51	0.18	1.89E-03	0.68
Small truck (<3.5 t) /tKm	29.00	1.96	1.14	8.61E-03	5.52
Aircraft, /tKm	15.80	1.08	0.08	4.72E-03	0.59

[1] *GWP accounts only for procurement of the various fuels, not for emissions arising during their combustion.*

6.4.3.3 Production of Filters

From Figure 6-1, the second stage of a filter's life cycle is production (manufacturing) of the filter itself. This stage comprises five steps: grinding, mixing, pressing, firing, and coating with silver. These processes can be achieved with various levels of technological sophistication. High-tech and low-tech options for each step are therefore discussed in the following paragraphs. Medium-tech estimates were computed

based on randomized combinations of the high-tech and low-tech inputs during Monte Carlo trials.

- *Grinding*

Local clay is transported to the filter factory, where it is generally dried using sunlight and air. It is then cleaned by hand (to remove particles and debris), ground, and sieved (The Ceramics Manufacturing Working Group, 2011). Grinding can be done using manual labor (as in the low-tech scenario) or with an electricity-powered hammer mill (high-tech scenario). The power requirement for operation of the hammer mill is roughly 5.0-7.5 kW (Hagan et al., 2009). Based on personal communication with *FilterPure* personnel (Lisa Ballantine, personal communication, July 2011) from their filter factory in the Dominican Republic, one hammer mill generally produces enough clay for 25 filters in about 40 minutes. Thus, the amount of electricity required for grinding under the high-tech scenario is roughly 11.9-18 MJ per filter. These values were assigned to a uniform distribution for input into the LCA model.

- *Mixing*

After the clay has been ground, sawdust and water are added and the materials are mixed to achieve a homogeneous combination. For the low-tech scenario, either hand mixing or a rotating drum mixer can be used; although the latter generally achieves better consistency. In either instance, no external power is required. For the high-tech scenario, an electric mortar mixer can be used. In this study, the MM60 mixer from MBW Inc. was used to represent a "typical" mixer. This piece of equipment has a loading capacity of 0.17 m^3, which holds enough material to produce approximately 12.3 filters. Its power rating is 1.1. KW. Multiplying this value by the distribution of typical mixing times

(minimum = 10 min, maximum = 50 min, and likeliest value = 20 min) (Rayner, 2009), the resulting distribution of electricity consumption per filter is as follows: minimum = 0.05 MJ, maximum = 0.27 MJ, and likeliest value = 0.11 MJ. This range is consistent with previously reported mixing electricity requirements (0.21 MJ per filter) at the *FilterPure* filter factory in the Dominican Republic (Lisa Ballantine, personal communication, July 2011).

- *Pressing*

Once the mixture of clay, sawdust, and water has been completely homogenized, it is transferred into a mold to be pressed into shape. Past experience at the filter factories included in a recent survey (Hagan et al., 2009) indicated that hand pressing results in inconsistent filter quality; therefore, it is generally desirable to use a hydraulic press for this step. For the low-tech scenario, it is assumed that the hydraulic press can be operated using man-power alone. For the high-tech scenario, a diesel engine can be used. This provides more accurate control over the pressure applied to the wet mixture in the hydraulic press. Although the advantages of a diesel-powered press have been recognized in practice, these benefits cannot be quantified in this study because there is not enough data to parameterize the extent of improvement. Based on current practice at the *FilterPure* filter factory in the Dominican Republic, 0.046 L of diesel is consumed per filter during pressing. See previous section (diesel in Section 6.4.3.2) for a recap of the environmental impacts arising from diesel consumption for high-tech pressing.

- *Firing*

Firing is required to harden the pressed clay mixture and also to combust the sawdust (or other friable material). This can be done using various types of kilns, which

may differ in firing efficiency, temperature control, fuel type, loading capacity, level of production, etc. In this study, the low-tech scenario for filter firing is based on wood-fired kilns, since this is presently the most widely-used fuel (Nardo). The amount of wood required per filter was estimated based on three different sources: a factory in Cambodia uses 1.5 m^3 (~900 kg) of rubber tree wood to fire one batch of 96 filters (Hagan et al., 2009); a filter factory in Columbia consumes, on average, 600 kg of wood to fire 125 filters (Rayner, 2009); and a filter factory in Nicaragua consumes roughly 200 kg of wood to produce 50 filters (Rayner, 2009). These quantities correspond to 9.4, 4.8, and 4.0 kg of wood per filter, respectively. Based on these data, the wood requirement for kiln-firing of one filter was set to the following triangular distribution: minimum = 4.0 kg, maximum = 9.4 kg, and likeliest value = 6.1 kg.

The high-tech firing scenario is based on propane-powered kilns, since these are in use at several existing filter factories and are expected to become even more prevalent in the future (Nardo; Rayner, 2009). The growing popularity of propane-fueled kilns reflects the increasing scarcity of wood in many locations and the improved temperature control afforded by propane-firing compared to wood. Nevertheless, the absence of solid data on the extent to which propane-firing improves filter yield rate or overall filter quality makes it impossible for this benefit to be accounted for quantitatively in this study. Additionally, there is currently no available data on how much propane is consumed per filter in a propane-fired kiln. Therefore, this quantity was computed based on the assumption that the energy requirement for firing is independent of the type of fuel used. In other words, it was assumed that the amount of heat generated from wood during

filter firing is the same amount that must be generated from propane firing for an equivalent number of filters per batch.

Equation 6-S8 summarizes a methodology for determining how much propane ($M_{Propane}$) is required for firing one ceramic filter, given the wood requirements (M_{Wood}) referenced in Section 6.4.3.2. This equation accounts for differences in both energy density ($E_{Propane}$ versus E_{Wood}) and effective heating efficiency ($\eta_{Propane}$ versus η_{Wood}) between the two fuels.

$$M_{Wood} = M_{Propane} \times \frac{E_{Propane}}{E_{Wood}} \times \frac{\eta_{Propane}}{\eta_{Wood}} \qquad (6\text{-}S8)$$

Parameter values are as follows: $E_{Propane}$ is 43.2 MJ/kg, E_{Wood} is 16.3 MJ/kg, $\eta_{Propane}$ is 58% and η_{Wood} is 23% (Jungbluth, 1997b). Base on this calculation,

1 kg of propane delivers the same amount of kiln heat as 6.68 kg of wood. Dividing this into the triangular distribution for wood requirements per filter, a triangular distribution for the amount of propane required to fire one filter is as follows: min = 0.55 kg, max = 1.3 kg, and likeliest value = 0.90 kg.

The use of either wood or propane for filter firing gives rise to GWP, PM10, and smog. These impacts are summarized in Table 6-S7 based on literature sources for each fuel (Combustion Portal; Jungbluth, 1997a).

Table 6-S7 Life cycle inventory of combustion process of fuel (wood and propane)

Burdens Item	Energy Use (MJ)	GWP (kg CO_2 eq)	PM10 (g)	Smog (g NO_x eq)	Water Use (m^3)
Combustion of Propane / kg	0	3.35	0.16	4.98	0
Combustion of Wood / kg	0	1.62	1.30	1.62	0

- *Silver Coating*

After firing, the ceramic filters are tested for flow rate. Those exhibiting an acceptable flow rate are then coated with silver to improve disinfection performance. Reiterating from silver section from Section 6.4.3.1, silver is applied primarily via brushing, dipping or "firing in" (whereby the silver material is added to the wet clay mixture before firing). For this study, it was assumed that all silver addition operations are performed using manual labor, such that this step does not incur any environmental impacts beyond what is required to produce and transport the silver solution to the filter factory. For this reason, low-tech and high-tech scenarios are not defined for this step of the filter production stage. Finally, in determining how much silver is required per FU, the factory yield rate (%) was not applied. This is because silver is not added to filters which cannot deliver an acceptable flow rate.

6.4.3.4   Use Phase and End-of-Life

This study did not explicitly account for environmental impacts accruing during the use phase or at end-of-life (disposition). Regarding use phase, it was assumed that raw water is fetched manually from a nearby source and filtered via gravity without input of additional materials or energy sources. Regarding end of life, filters are generally repurposed for household storage or other uses or discarded to a landfill (or trash heap) once they are no longer useful as a POU water treatment device. In any event, solid waste generation was not accounted for as an environmental impact of concern in this study; as such, end of life impacts were not explicitly quantified.

6.4.4   LCA Modeling for the Centralized Water System

6.4.4.1   Materials Inputs

Materials usage for the collection, treatment, and distribution scheme in
centralized water system were based on previously published work by Bonton et
al(2012). Table 6-S8 summarizes the quantities of various materials required to produce 1
FU. Life cycle data for the materials were then collected from the ecoinvent database
(Weidema, 2007). These are summarized in Table 6-S9. Transportation burdens for these
materials were excluded from the analysis.

Table 6-S8. Material inputs required for production of 1 FU in the centralized water system.

Material	Amount Required per 1 FU (kg)
Phosphoric acid	0.04
CO_2	0.53
$Ca(OH)_2$	0.27
NaOH	2.28
Chlorine	0.02
Granular activated carbon	2.88
Alum	3.04
Polymer	0.01

Table 6-S9. Life cycle impacts for material inputs required in the centralized water system.

Item \ Burdens	Energy Use (MJ)	GWP (kg CO_2 eq)	PM10 (g)	Smog (g NO_x eq)	Water Use (m^3)
Phosphoric acid/ kg	18.60	1.46	2.07	3.87E-03	4.45
CO_2 / kg	9.19	0.82	0.22	7.95E-04	2.14
$Ca(OH)_2$ / kg	4.18	0.77	0.13	5.73E-04	2.47
NaOH / kg	14.20	1.12	0.45	1.98E-03	7.93
Chlorine / kg	13.70	1.08	0.45	1.91E-04	7.60
Granular activated carbon / kg	124.00	9.33	3.98	2.31E-02	4.65
Alum / kg	3.75	0.26	0.12	7.12E-04	1.16
Polymer (Acrylonitrile) / kg	87.50	3.21	0.61	4.52E-03	0.15

6.4.4.2 Energy Inputs

Electricity is the sole source of energy consumed in the centralized water system as modeled in this study. It is required for all three stages of the modeled system (i.e., impoundment, treatment and distribution), and it accounts for the majority of the overall operational burdens reported in previously published studies (Barrios, Siebel, van der Helm, Bosklopper, & Gijzen, 2008; Bonton et al., 2012; Friedrich et al., 2007, 2009; Lundie & Peters, 2004; Tripathi, 2007). From these published sources, electricity consumption per 1 m^3 water delivered ranges from 0.36 MJ to 2.74 MJ. The average value is roughly 1.73 MJ/m^3. These values were assigned to the following triangular distribution for electricity consumption per FU: minimum = 13.67 MJ/ m^3, maximum = 104.01 MJ/m^3, and likeliest = 65.67 MJ/m^3.

6.4.5 Selected Results

6.4.5.1 Comparison of environmental burdens between POU and centralized system

The environmental burdens of POU ceramic filters for delivering 1 FU, measured as energy, global warming potential, water, PM10 and smog, are compared to the centralized water system. Only med-tech scenario was selected for comparison considering its representative in most developing countries. The breakeven points for each burdens between POU and centralized system were summarized in Table 6-S10. All environmental burdens except smog from POU are fewer than those from centralized water system when water treated exceeds the breakeven point. The smog from centralized water system is always lower than that from POU filters until the water treated is more than 2050L per day.

Table 6-S10 Break-even point for environmental burdens between POU and centralized system

Impact	Energy	GWP	Water	Smog	PM10
Breakeven point	8.64 L	5.69 L	2.62 L	2050 L	6.99 L

6.4.5.2   Environmental burdens for three constructed scenarios

The numerical results for Figure 6-3 in manuscript were presented in Table 6-S11 with both its mean value and one standard deviation, which are obtained from 100,000 Monte Carlo simulations. Each environmental burden was broke down into three parts: raw material, process and transport.

Table 6-S11. Environmental burdens for ceramic filters delivering 1 FU over 10 years. Mean values are standard deviations (SD) from n = 100,000 Monte Carlo trials are presented.

Environmental Impact	Energy Use (MJ)		GWP (kg CO_2 eq)		Water Use (m^3)		PM10 (g)		Smog (g NO_x eq)	
	Mean	SD	Mean	SD	Mean	SD	Mean	SD	Mean	SD
High-tech	370.91	120.69	15.35	4.87	6.41	2.55	2.67	1.01	16.59	5.36
Raw Material	14.65	21.83	1.28E-01	5.74E-02	2.75E-01	9.77E-02	1.07E-01	6.41E-02	8.00E-04	4.50E-04
Process	338.08	109.83	13.99	4.47	2.69	1.05	1.84	0.75	16.58	5.36
Transport	18.18	8.74	1.23	0.60	3.44	1.88	7.14E-01	0.41	5.40E-03	2.85E-03
Med-tech	499.43	217.48	28.88	17.72	10.41	6.78	17.69	17.22	26.78	14.12
Raw Material	14.65	21.83	1.28E-01	5.74E-02	2.75E-01	9.77E-02	1.10E-01	6.41E-02	8.00E-04	4.50E-04
Process	438.53	183.24	25.61	15.43	1.36	1.41	15.77	15.91	26.77	14.11
Transport	46.25	36.90	3.14	2.54	8.78	7.45	1.82	1.61	0.01	0.01
Low-tech	631.48	209.18	42.76	14.02	14.51	7.24	33.11	10.85	37.25	12.19
Raw Material	14.51	21.72	1.28E-01	5.71E-02	2.74E-01	9.88E-02	1.07E-01	6.50E-02	8.00E-04	4.49E-04
Process	541.90	179.92	37.54	12.29	2.90E-03	1.23E-03	30.05	9.84	37.23	12.19
Transport	75.07	33.12	5.09	2.28	14.24	7.19	2.95	1.61	0.02	0.01

6.4.5.3 Environmental cost-effectiveness

We used environmental cost-effectiveness as the index number to compare the

POU ceramic filter system to centralized system. It was done through normalizing five

environmental burdens by DALYs averted for general population. While the figure is

shown in Figure 6-4, the data is presented here in Table 6-S12.

Table 6-S12. Environmental burdens for ceramic filters delivering 1 FU over 10 years

Environmental Impact	Med-Tech POU		Centralized	
	Mean	SD	Mean	SD
Energy	724.32	128.71	874.37	155.37
Global warming potential	41.95	7.45	76.62	13.62
Water	15.20	2.70	60.07	10.67
PM10	25.81	4.59	38.13	6.78
Smog	38.87	6.91	0.20	0.04

Reference

Bahl, M. R. (1976). Impact of Piped Water Supply on the Incidence of Typhoid Fever

and Diarrhoeal Diseases in Lusaka. *Med J Zambia, 10*(4), 98-99

Barrios, R., Siebel, M., van der Helm, A., Bosklopper, K., & Gijzen, H. (2008).

Environmental and Financial Life Cycle Impact Assessment of Drinking Water

Production at Waternet. *Journal Of Cleaner Production, 16*(4), 471-476

Bongaarts, J. (2001). Household Size and Composition in the Developing World in the

1990s. *Population Studies, 55*(3), 263-279

Bonton, A., Bouchard, C., Barbeau, B., & Jedrzejak, S. (2012). Comparative Life Cycle

Assessment of Water Treatment Plants. *Desalination, 284*, 42-54

Brinkhof, M. W. G., Boulle, A., Weigel, R., Messou, E., Mathers, C., Orrell, C., . . . Egger, M. (2009). Mortality of Hiv-Infected Patients Starting Antiretroviral Therapy in Sub-Saharan Africa: Comparison with Hiv-Unrelated Mortality. *Plos Medicine, 6*(4)

Campbell, E. (2005). Study on Life Span of Ceramic Filter Colloidal Silver Pot Shaped (Csp) Model. Managua, Nicaragua

Carr, A., Marriott, D., Field, A., Vasak, E., & Cooper, D. A. (1998). Treatment of Hiv-1-Associated Microsporidiosis and Cryptosporidiosis with Combination Antiretroviral Therapy. *Lancet, 351*(9098), 256-261

Central Intelligence Agency. South Africa - the World Factbook.   Retrieved July, 2012, from https://www.cia.gov/library/publications/the-world-factbook/geos/sf.html

Clasen, T., Nadakatti, S., & Menon, S. (2006). Microbiological Performance of a Water Treatment Unit Designed for Household Use in Developing Countries. *Tropical Medicine & International Health, 11*(9), 1399-1405

Clasen, T., Schmidt, W.-P., Rabie, T., Roberts, I., & Cairncross, S. (2007). Interventions to Improve Water Quality for Preventing Diarrhoea: Systematic Review and Meta-Analysis. *British Medical Journal, 334*(7597), 782-785

Clasen, T. F., Brown, J., Collin, S., Suntura, O., & Cairncross, S. (2004). Reducing Diarrhea through the Use of Household-Based Ceramic Water Filters: A Randomized, Controlled Trial in Rural Bolivia. *American Journal of Tropical Medicine and Hygiene, 70*(6), 651-657

Clasen, T. F., & Haller, L. (2008). Water Quality Interventions to Prevent Diarrhoea: Cost and Cost-Effectiveness. Geneva: World Health Organization.

Combustion Portal. Emissions Calculator for Propane-Fired Boilers.   Retrieved Aug,
2012, from http://www.combustionportal.org/bcalc2.cfm

Dillingham, R. A., Pinkerton, R., Leger, P., Severe, P., Guerrant, R. L., Pape, J. W., &
Fitzgerald, D. W. (2009). High Early Mortality in Patients with Chronic Acquired
Immunodeficiency Syndrome Diarrhea Initiating Antiretroviral Therapy in Haiti:
A Case-Control Study. *American Journal of Tropical Medicine and Hygiene,
80*(6), 1060-1064

du Preez, M., Conroy, R. M., Wright, J. A., Moyo, S., Potgieter, N., & Gundry, S. W.
(2008). Use of Ceramic Water Filtration in the Prevention of Diarrheal Disease: A
Randomized Controlled Trial in Rural South Africa and Zimbabwe. *American
Journal of Tropical Medicine and Hygiene, 79*(5), 696-701

Edejer, T. T.-T. (2003). *Making Choices in Health : Who Guide to Cost-Effectiveness
Analysis*. Geneva: World Health Organization.

Esrey, S. A., Feachem, R. G., & Hughes, J. M. (1985). Interventions for the Control of
Diarrhoeal Diseases among Young Children: Improving Water Supplies and
Excreta Disposal Facilities. *Bull World Health Organ, 63*(4), 757-772

Friedrich, E., Pillay, S., & Buckley, C. A. (2007). The Use of Lca in the Water Industry
and the Case for an Environmental Performance Indicator. *Water Sa, 33*(4), 443-
451

Friedrich, E., Pillay, S., & Buckley, C. A. (2009). Carbon Footprint Analysis for
Increasing Water Supply and Sanitation in South Africa: A Case Study. *Journal
Of Cleaner Production, 17*(1), 1-12

Gadgil, A. (1998). Drinking Water in Developing Countries. *Annual Review of Energy and the Environment, 23*, 253-286

Hagan, J., Harley, N., Pointing, D., Sampson, M., Saom, V., & Smith, K. (2009). *Resource Development International - Cambodia Ceramic Water Filter Handbook*. Phnom Penh, Cambodia.

Haller, L., Hutton, G., & Bartram, J. (2007). Estimating the Costs and Health Benefits of Water and Sanitation Improvements at Global Level. *Journal of Water and Health, 5*(4), 467-480

Institute of Medicine (U.S.). Panel on Dietary Reference Intakes for Electrolytes and Water. (2005). *Dri, Dietary Reference Intakes for Water, Potassium, Sodium, Chloride, and Sulfate*. Washington, D.C.: National Academies Press.

Jamison, D. T., Breman, J. G., Measham, A. R., Alleyne, G., Claeson, M., Evans, D. B., . . . Musgrove, P. (2006). *Disease Control Priorities in Developing Countries (2nd Edition)*. New York: Oxford University Press.

Joint United nations Program on HIV/AIDS (UNAIDS). (2012). Global Aids Response Progress Report 2012.   Retrieved Sep 22, 2012, from http://www.unaids.org/en/dataanalysis/knowyourresponse/countryprogressreports/2012countries/ce_ZA_Narrative_Report.pdf

Jungbluth, N. (1997a). Life-Cycle-Assessment for Stoves and Ovens. Uns-Working Paper No. 16. Eidgenössische Technische Hochschule, Zürich: Umweltnatur- und Umweltsozialwissenschaften (UNS).

Jungbluth, N. (1997b). Life Cycle Assessment for Stoves and Ovens *UNS-Working Paper No. 16*. Zürich.

Jungmeier, G., Werner, F., Jarnehammar, A., Hohenthal, C., & Richter, K. (2002). Allocation in Lca of Wood-Based Products - Experiences of Cost Action E9 Part I. Methodology. *International Journal Of Life Cycle Assessment, 7*(5), 290-294

Kallman, E. N., Oyanedel-Craver, V. A., & Smith, J. A. (2011). Ceramic Filters Impregnated with Silver Nanoparticles for Point-of-Use Water Treatment in Rural Guatemala. *Journal of Environmental Engineering-Asce, 137*(6), 407-415

Kosek, M., Bern, C., & Guerrant, R. L. (2003). The Global Burden of Diarrhoeal Disease, as Estimated from Studies Published between 1992 and 2000. *Bulletin of the World Health Organization, 81*(3), 197-204

Lantagne, D. S. (2001). Investigation of the Potters for Peace Colloidal Silver Impregnated Ceramic Filte. Allston, MA.

Lopez, A. D., & Murray, C. (1998). The Global Burden of Disease, 1990-2020. *Nature Medicine, 4*(11), 1241-1243

Lundie, S., & Peters, G. (2004). Life Cycle Assessment for Sustainable Metropolitan Water Systems Planning. *Environ Sci Technol*

Lydia Shawel Abebe, James A. Smith, Sophia Narkiewicz, Vinka Oyanedel-Craver, Mark Conaway, Alukhethi Singo, . . . Dillingham, R. (2013). Ceramic Water Filters Impregnated with Silver Nanoparticles as a Point-of-Use Water-Treatment Intervention for Hiv-Positive Individuals in Limpopo Province, South Africa: A Pilot Study of Technological Performance and Human Health Benefits. *Journal of Water and Health, In review*

Maggi, P., Larocca, A. M. V., Quarto, M., Serio, G., Brandonisio, O., Angarano, G., & Pastore, G. (2000). Effect of Antiretroviral Therapy on Cryptosporidiosis and

Microsporidiosis in Patients Infected with Human Immunodeficiency Virus Type 1. *European Journal of Clinical Microbiology & Infectious Diseases, 19*(3), 213-217

Milota, M. R., West, C. D., & Hartley, I. D. (2005). Gate-to-Gate Life-Cycle Inventory of Softwood Lumber Production. *Wood and Fiber Science, 37*, 47-57

Murray, C. J. L., Lopez, A. D., Harvard School of Public Health., World Health Organization., & World Bank. (1996). *The Global Burden of Disease : A Comprehensive Assessment of Mortality and Disability from Diseases, Injuries, and Risk Factors in 1990 and Projected to 2020*. Cambridge, MA: Published by the Harvard School of Public Health on behalf of the World Health Organization and the World Bank ; Distributed by Harvard University Press.

Mwachari, C. W., Meier, A. S., Muyodi, J., Gatei, W., Waiyaki, P., & Cohen, C. R. (2003). Chronic Diarrhoea in Hiv-1-Infected Adults in Nairobi, Kenya: Evaluation of Risk Factors and the Who Treatment Algorithm. *Aids, 17*(14), 2124-2126

Nardo, R. Factory Startup Manual: For the Production of Ceramic Water Filter.

Oyanedel-Craver, V. A., & Smith, J. A. (2008). Sustainable Colloidal-Silver-Impregnated Ceramic Filter for Point-of-Use Water Treatment. *Environmental Science & Technology, 42*(3), 927-933

Rayner, J. (2009). *Current Practices in Manufacturing of Ceramic Pot Filters for Water Treatment.* (Master), Loughborough University, Leicestershire, UK.

Ryder, R. W., Reeves, W. C., Singh, N., Hall, C. B., Kapikian, A. Z., Gomez, B., & Sack, R. B. (1985). The Childhood Health-Effects of an Improved Water-Supply

System on a Remote Panamanian Island. *American Journal of Tropical Medicine and Hygiene, 34*(5), 921-924

Schmidt, W. P., Arnold, B. F., Boisson, S., Genser, B., Luby, S. P., Barreto, M. L., . . . Cairncross, S. (2011). Epidemiological Methods in Diarrhoea Studies--an Update. *Int J Epidemiol, 40*(6), 1678-1692

Serwadda, D., Sewankambo, N. K., Carswell, J. W., Bayley, A. C., Tedder, R. S., Weiss, R. A., . . . Dalgleish, A. G. (1985). Slim Disease - a New Disease in Uganda and Its Association with Htlv-Iii Infection. *Lancet, 2*(8460), 849-852

Shillcutt, S., Walker, D., Goodman, C., & Mills, A. (2009). Cost Effectiveness in Low- and Middle-Income Countries. *PharmacoEconomics, 27*(11), 903-917

Simonis, J. J., & Basson, A. K. (2012). Manufacturing a Low-Cost Ceramic Water Filter and Filter System for the Elimination of Common Pathogenic Bacteria. *Physics and Chemistry of the Earth, Parts A/B/C*(0)

Stokes, J., & Horvath, A. (2006). Life Cycle Energy Assessment of Alternative Water Supply Systems. *International Journal Of Life Cycle Assessment, 11*(5), 335-343

The Ceramics Manufacturing Working Group. (2011). Best Practice Recommendations for Local Manufacturing of Ceramic Pot Filters for Household Water Treatment. Atlanta, GA: Center for Disease Control and Prevention.

Tonglet, R., Isu, K., Mpese, M., Dramaix, M., & Hennart, P. (1992). Can Improvements in Water-Supply Reduce Childhood Diarrhea. *Health Policy and Planning, 7*(3), 260-268

Tripathi, M. (2007). *Life Cycle Energy and Emissions for Municipal Water and Wastewater Services: Case-Studies of Treatment Plants in the U.S.* (Master of Science), University of Michigan, Ann Arbor, MI.

UNICEF, & Waste Sanitiation Project. (2007). Improving Household Drinking Water Quality: Use of Ceramic Water Filters in Cambodia: UNICEF/WSP.

UNICEF, & WHO. (2009). Diarrhoea: Why Children Are Still Dying and What Can Be Done. New York: United Nations Children's Fund.

van Halem, D., van der Laan, H., Heijman, S. G. J., van Dijk, J. C., & Amy, G. L. (2009). Assessing the Sustainability of the Silver-Impregnated Ceramic Pot Filter for Low-Cost Household Drinking Water Treatment. *Physics and Chemistry of the Earth, 34*(1-2), 36-42

Walser, T., Demou, E., Lang, D. J., & Hellweg, S. (2011). Prospective Environmental Life Cycle Assessment of Nanosilver T-Shirts. *Environ Sci Technol, 45*(10), 4570-4578

Wang, Z. S., Shepard, D. S., Zhu, Y. C., Cash, R. A., Zhao, R. J., Zhu, Z. X., & Shen, F. M. (1989). Reduction of Enteric Infectious-Disease in Rural China by Providing Deep-Well Tap Water. *Bulletin of the World Health Organization, 67*(2), 171-180

Weidema, B. (2007). Ecoinvent Data V2.0. 2008, from http://www.ecoinvent.org/

WHO/UNICEF Joint Water Supply and Sanitation Monitoring Programme., World Health Organization., & UNICEF. (2006). *Meeting the Mdg Drinking Water and Sanitation Target : The Urban and Rural Challenge of the Decade*. Geneva, Switzerland

New York: World Health Organization ;

United Nations Children's Fund.

World Health Organization. Revised Global Burden of Disease (Gbd) 2002 Estimates.
Retrieved July 19, 2012, from
http://www.who.int/healthinfo/global_burden_disease/estimates_regional_2002_r
evised/en/

World Health Organization CHOosing Interventions that are Cost Effective (WHO-
CHOICE). Threshold Values for Intervention Cost-Effectiveness by Region.
Retrieved May 15, 2013, from
http://www.who.int/choice/costs/CER_levels/en/index.html

World Health Organization., UNICEF., Water Supply and Sanitation Collaborative
Council., & WHO/UNICEF Joint Water Supply and Sanitation Monitoring
Programme. (2000). *Global Water Supply and Sanitation Assessment 2000
Report*. Geneva; New York: World Health Organization; UNICEF.

Zhang, H. Y., Smith, J. A., & Oyanedel-Craver, V. (2012). The Effect of Natural Water
Conditions on the Anti-Bacterial Performance and Stability of Silver
Nanoparticles Capped with Different Polymers. *Water research, 46*(3), 691-699

CHAPTER 7: CONCLUSIONS AND KNOWLEDGE GAPS

7.1 Conclusions

As stated in the objective section of Chapter One, a series of systematic investigations was performed to fill a knowledge gap related to the transport behavior of silver nanoparticles with distinct coatings in various porous media under relevant environmental physicochemical conditions. The investigations have revealed important observations. The conclusions derived from these observations are summarized as follows:

1) AgNPs transport through Ottawa sand

- The transport of silver nanoparticles depends on the ionic strength and the average sand particle diameter. Full retention was achieved under high ionic strength (50 mM) and the finest average sand-grain diameter.

- With an otherwise identical condition, an increase in ionic strength results in higher retention of silver nanoparticles. This is caused by the compression of the diffuse double layer surrounding AgNPs and the enhanced sorption of the AgNPs to sand surfaces.

- Fine sand particles retain more AgNPs than coarse sand particles. However, the removal mechanism varies with ionic strength: the straining effect plays the largest role under low ionic strength (≤10 mM); the sorption of AgNPs to sand surfaces is more important under high ionic strengths (50 mM).

2) Transport of AgNPs through porous ceramic media

- AgNPs are found to be relatively mobile through porous ceramic media. Under certain conditions, AgNP retention was as low as 13%.

- Retention rate is closely related to solution ionic strength due to the increased particle-particle interaction resulting in aggregation and straining, as well as a reduced repulsive force between the AgNP and the ceramic porous media surfaces.

- Retention rate is related to AgNP particle size, and to a lesser extent, the ionic strength. Physical filtration, as well as DLVO theory, both play a role in the retention rate.

- Compared to a dip-in and paint-on method, a fire-in method for immobilizing AgNPs in ceramic filters is a much more effective at retaining zero-valent silver in the porous ceramic media.

- Under a typical usage scenario, zero-valent silver applied using the fire-in method with 2.76 mg Ag will last 2.2 years and fire-in method with 27.6 mg Ag will last 9.7 years. In comparison, the life spans of silver applied using dip-in and paint-on methods with 2.76 mg Ag are expected to be shorter than 2.2 years.

3) AgNPs through the GCL

- GCLs could not effectively retain 100% of AgNPs under most of the experimental scenarios. Full retention was only achieved under at the highest ionic strength (100 mM).

- Ionic strength has a strong impact on AgNP retention. The impact from variations in the valence of the solution cation is less significant.

- The reversibility of AgNP retention in the GCL indicates that there are two energy minimums: a primary one, which causes irreversible deposition, and a secondary one, which could be reduced or even eliminated, leading to release of AgNPs with the reintroduction of DI water.

4) Sustainability evaluation of a AgNP-impregnated ceramic filter

- The function unit is defined as 37,960 L water, processed by a ceramic filter, which is the amount consumed by a typical household in a developing country over a 10-year span.

- Social sustainability is measured by DALYs reduced in terms of diarrhea or HIV. A function unit would save 0.71 lives per year for the general public and 0.14 lives per year for children under five for deaths caused by diarrhea. The numbers are 15.5 lives per year for the general public for deaths caused by HIV. Field tests also show that the ceramic filter has the flexibility to be used in a communities of varying economic conditions, thus having a higher social acceptance compared to a centralized water system.

- Ranging from $8 to $35 per ceramic filter, the total cost for a functional unit is roughly $63, which translates into $84/DALY averted for the general population and $46/DALY averted for children under five, which is far less than that for a centralized water system ($466/DALY and $141/DALY, respectively).

- Out of all the stages of production for a ceramic filter, firing is the main contributor to the environmental burden of a functional unit. Considering all environmental impacts, the ceramic filter outperforms a centralized water system in energy, GWP, water, and PM10, but not in SMOG.

- Conclusively, a one-size-fits-all centralized water system has less flexibility and is inferior to ceramic filter POU technology in terms of social, economic, and environmental sustainability.

7.2   Area of opportunities

The following four areas of research were identified as important for future study.

7.2.1   *Various manufacturing methods of AgNP*

Couple of silver nanoparticles fabricated with distinct method were investigated in this study. They were found to perform differently in the transport experiment despite the same water chemistry. It is recommended to examine more types of silver nanoparticles and better characterize their size, morphology and surface characteristics that could affect their behavior in ecosystem. This information would allow researchers to better evaluate the transport and retention capabilities of silver nanoparticles in a porous medium, through a porous ceramic filter as well as in a natural ecosystem. The variables in the manufacturing process cast a strong impact on the physiochemical characteristics of the resulting silver nanoparticles (such as shapes, size, and surface chemistry).

7.2.2   *Transport in a higher dimensional system*

The studies presented herein are limited to one dimension. A complex environmental system can often be simplified into lower dimensions by its homogenous characteristics, yet this is not the case when we are interested in a localized area with heterogeneous characteristics. That being said, it would be beneficial if future studies could integrate higher-dimensional investigations into silver nanoparticle transport with consideration of heterogeneous formations. For example, macro-pores may cause significantly greater transport of AgNPs than reported here.

7.2.3 Toxicity and disinfection mechanism

Being used mainly for the purpose of disinfection, silver nanoparticles' effectiveness should also be evaluated in terms of the disinfection capability.

In chapter five when we studied the silver release rate from three different immobilization methods, the fire-in method (either 1X or 10X) was found to better retain metallic silver in the ceramic porous medium than the 'paint-on' or 'dip-in' method. However, it is uncertain which silver application method will provide the best disinfection. Therefore, studies should be performed to compare microbe removal by each type of application method but for identical amounts of silver.

7.2.4 Mechanisms of silver ion release in the transport process

Silver ions released from silver nanoparticles are primarily responsible for microbe disinfection. In this study, as no measurable silver ions were detected, it was excluded from the scope of this study. Nevertheless, beyond the settings of this study, understanding the release rate of silver ions is important for predicting disinfection kinetics. This understanding is expected to shed light on the design of various silver-impregnated products, such as the silver-impregnated ceramic filter which was studied in

160

this dissertation. With the proper control of environmental chemistry and the characteristics of silver nanoparticles, a controlled release of silver ions could be achieved to minimize the release rate while not compromising the disinfection capability.